The Term Structure of Interest Rates in a Heterogeneous Monetary Union*

James Costain, Galo Nuño, and Carlos Thomas
Banco de España

June 2024

Abstract

We build an arbitrage-based model of the yield curves in a heterogeneous monetary union with sovereign default risk, which can account for the asymmetric shifts in euro area yields during the Covid-19 pandemic. We derive an affine term structure solution, and decompose yields into an expectations component, a term premium, an expected default loss, and a credit risk premium. In an extension, we endogenize the peripheral default probability, showing that it decreases with central bank bond-holdings. Calibrating the model to Germany and Italy, we show that both the level and the shifts in the sovereign spread are mainly attributable to the credit risk premium.

Keywords: sovereign default, quantitative easing, yield curve, affine model, Covid-19 crisis, ECB, pandemic emergency purchase programme.

JEL classification: E5, G12, F45.

*The views expressed in this manuscript are those of the authors and do not necessarily represent the views of Banco de España or the Eurosystem. The authors are grateful for helpful comments from Marcin Bielecki, Valery Charnavoki, Ricardo Gimeno, Ruggero Jappelli, Iryna Kaminska, Thomas King, Wolfgang Lemke, Bartosz Mackowiak, Dimitros Malliaropulos, Stephen Millard, Paolo Santos Monteiro, Ken Nyholm, Olaf Posch, Walker Ray, Ricardo Reis, Jean-Paul Renne, Dominik Thaler, Dmitry Vayanos, Andrea Vladu, and several anonymous referees, and also from participants in many seminars and workshops. We thank Ana Arencibia and Rubén Fernández Fuertes for substantial assistance with data, computations, and graphics. All remaining errors are ours.

Disclosure statements

Disclosure statement of James Costain.
I have no conflicts of interest to disclose.

Disclosure statement of Galo Nuño.
I have no conflicts of interest to disclose.

Disclosure statement of Carlos Thomas.
I have no conflicts of interest to disclose.

1 Introduction

Following the Great Financial Crisis of 2008-09, as policy rates in advanced economies approached their effective lower bounds, central banks relied on unconventional tools, such as large-scale asset purchases, to flatten the yield curve and thus provide further policy stimulus. In this context, models of the term structure have become important analytical tools for central bankers and for scholars of monetary policy. In particular, they underlie the prevailing view of the effects of asset purchase programmes, which revolves around the *duration risk extraction channel* (*e.g.* Greenwood and Vayanos, 2014; Hamilton and Wu, 2012; or Krishnamurthy, 2022). Under this mechanism, net purchases of long-maturity bonds flatten the yield curve by reducing the term premium that private markets demand to compensate for duration risk, while the short end of the curve is anchored by the risk-free short rate.

However, the movements of euro area yield curves (see Figure 1) following the pandemic outbreak of early 2020 and the ECB's subsequent monetary policy response seem inconsistent with this mechanism. While duration extraction might explain the flattening of the German yield curve after the pandemic emergency purchase programme (PEPP) announcement on March 18, 2020, it offers no explanation of the much larger movements in the Italian and Spanish yield curves. A key feature of these movements is the large shift in the short end of the peripheral curves, which cannot be explained by term premium considerations. The same is true for the large upward shift in peripheral yield curves as the pandemic shock unfolded (before PEPP was announced), which cannot be explained by invoking the pandemic's impact on the expected amount of duration risk to be absorbed by the market.

It is not hard to see why the mainstream view of term structure dynamics fails to explain yields in southern Europe, when we consider that today's workhorse models, such as the influential Vayanos and Vila (2021) framework, abstract from sovereign default risk. While this may be a reasonable abstraction when analyzing the safest issuers, such as the US Treasury, it is less suitable for the euro area, where sovereign issuers that are viewed as safe coexist – and share a common monetary policy – with others that face high and volatile sovereign spreads. Motivated by these observations, this paper extends the Vayanos and Vila (2021) term structure model to a multi-country setting with sovereign default risk. Concretely, we consider a monetary union with two member states: Core, which issues default-free bonds, and Periphery, which is subject

Figure 1: Effects of the pandemic and the PEPP announcement on German, Spanish, and Italian yields

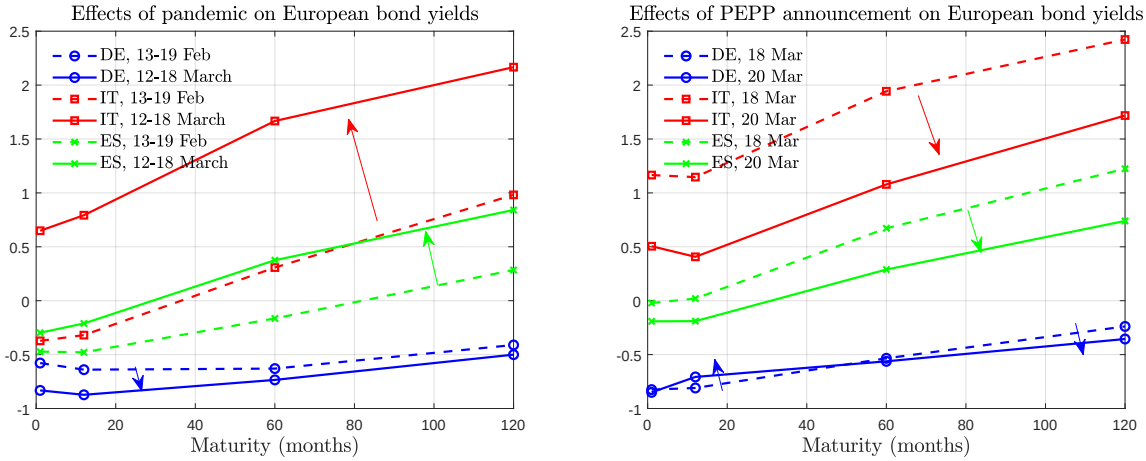

Notes. Data source: Datastream.
Left panel. Shifts in German, Spanish, and Italian zero-coupon yields (annual percentage points) from the weekly average of 13-19 Feb. 2020 (dashes), to that of 12-18 Mar. 2020 (solid).
Right panel. Shifts in German, Spanish, and Italian zero-coupon yields (annual percentage points) from 18 March 2020 (dashes, before PEPP announcement) to 20 March 2020 (solid, after).

to default risk. The model is populated by risk-averse arbitrageurs, who trade bonds across both countries and all maturities, and preferred-habitat investors, who demand bonds of a specific maturity from a specific jurisdiction. Bond yields in the model are driven by one or more stochastic factors, including the short-term riskless rate. Yields also depend on the *net* supply of bonds of each maturity and jurisdiction, that is, bond supply from the governments minus the bonds held by the common monetary authority.

The model permits an analytical decomposition of yields (see Prop. 1) into four components: (i) an *expectations* term that represents the expected future path of the risk-free rate; (ii) a *term premium* representing the risk-averse compensation for bearing duration risk; (iii) an *expected default loss*, which captures the compensation that a risk-neutral investor would require for holding defaultable bonds; and (iv) a *credit risk premium* that represents the risk-averse compensation for absorbing default risk (over and above expected default losses).[1] Thus, our framework complements the duration

[1]The expected default loss is the compensation for default under the physical measure; the sum of the expected default loss and the credit risk premium is the compensation for default under the equivalent martingale measure.

extraction channel with a *default risk extraction channel* that operates through the credit risk premium rather than the term premium: risk-averse investors demand less compensation to hold a defaultable bond when there is less default risk outstanding in the market. Changes in default risk can then shift the front end of the yield curve without affecting short-term riskless rates (Prop. 3).

We consider two ways of modelling default. First, in Sec. 2, we impose an exogenous but time-varying default probability, which permits a simple exposition of key analytical results that are independent of how one models sovereign default. But in Sec. 3 we develop a more realistic setup in which the default probability varies with events that shift net bond supply, such as the pandemic outbreak and the PEPP announcement. To this end, we assume that the peripheral bond market is subject to rollover crises in the spirit of Calvo (1988) and Cole and Kehoe (2000). When a rollover crisis arrives, the peripheral fiscal authority decides whether to continue servicing its debts or else to partially default by applying a haircut to bonds of all maturities. We show that, under certain conditions, central bank bond purchases ease the fiscal pressure that the peripheral government will face if a rollover crisis arrives, and thus reduce its incentives to default.[2] Importantly, our key analytical findings – including the yield decomposition – apply to both model versions. However, endogenizing default reinforces the impact of asset purchases on yields, both because purchases decrease the expected default loss and because the default risk extraction channel is stronger when asset purchases *both* reduce the net supply of defaultable bonds *and* reduce the default risk on each bond.

We calibrate a quantitative version of our endogenous default model to Germany and Italy.[3] We use ECB, Eurosystem, and Banco de España projections of bond supply and Eurosystem purchases, together with estimates of preferred-habitat demand from earlier studies, to calculate the amount of sovereign bonds to be absorbed by arbitrageurs.[4] We fit the model to data on yields from the euro period (1999-2022), and also from

[2]This is because redemptions of bonds held by the central bank (and interest payments on those bonds) are payments from the treasury to the central bank which may be rebated back to the treasury through central bank dividends. Therefore, by expanding the monetary base to purchase sovereign bonds, the central bank reduces the fiscal pressure that the peripheral government will face if a rollover crisis arrives, and thus reduces its incentives to default, a point made by Corsetti and Dedola (2016). This implicitly supposes that national central banks conduct asset purchases on behalf of the union-wide central bank, which is typically the case in the Eurosystem.

[3]For the empirical analysis in Secs. 4-5, we extend the one-factor model of Sec. 2, which features short-rate shocks only, to a multi-factor framework with preferred-habitat demand shocks.

[4]Our calibration of preferred-habitat demand uses information from Eser et al. (2023).

the two-day window around the ECB's initial PEPP announcement on March 18, 2020, when an aggregate purchase envelope of 750 billion euros was declared. Parameter identification is closely guided by our decomposition of yields. Assuming that German sovereign default risk is negligible, arbitrageurs' risk aversion can be inferred by fitting the German term premium.[5] The expectations components and term premia are tightly linked across the two countries (Prop. 2), so the spread between Italian and German yields represents (approximately) the total compensation for Italian default risk, i.e. the expected default loss plus the credit risk premium. Both components increase with the default probability, while the second one also increases with arbitrageurs' risk aversion. Thus, given the level of risk aversion consistent with long-run German term premia, fitting the sovereign spread identifies the long-run probability of default. We then have enough information to quantify both components of the Italy-Germany spread.

Our main quantitative finding is that both the mean level and the fluctuations of the sovereign spread are mainly attributable to the credit risk premium. In our model, the relative sizes of the credit risk premium and the expected default loss hinge critically on (i) arbitrageurs' risk aversion and (ii) the amount of defaultable bonds they must absorb. When we back out the degree of risk aversion that explains German term premia (e.g., 146 bp on ten-year bonds) and apply it to the quantity of Italian bonds arbitrageurs must absorb, we find that the credit risk premium is on average around three times as large as the expected default loss, accounting for roughly 3/4 of the sovereign spread. Similarly, default risk extraction is the main channel driving the reaction of Italian yields to the PEPP announcement.[6] The downward shift in the Italy-Germany spread, across all maturities, is mostly explained by a lower credit risk premium, caused both by a small decline in the Italian default probability and by a reduction in the quantity of defaultable assets that the market would have to hold from then on. In contrast, the decrease in the expected default loss, by itself, causes only a small change in the sovereign spread. Likewise, the reduction in the term premium had a fairly small effect on yields. The relative strength of the default risk channel,

[5]The German term premium also depends on the volatility of preferred habitat demand. We discipline the preferred habitat process by fitting the standard deviation of German yields together with the German term premium.

[6]These results are in line with the empirical study of Corradin and Schwaab (2023) for the same episode, which concludes that a reduction in default risk was the dominant channel through which the PEPP announcement affected Italian yields; likewise they are consistent with findings of Krishnamurthy et al. (2018) and Demir et al. (2021) regarding earlier asset purchase programs in Europe.

compared with the duration risk channel, explains the asymmetry of the responses of German and Italian yields. These results are robust across a wide range of alternative parameterizations. Credit risk premia always dominate expected default losses unless risk aversion or default haircuts take implausibly low values that are inconsistent with the observed level, slope, and responsiveness of yields.

We provide additional support for the model by discussing its fit to untargeted moments, including long-run Sharpe ratios and the impact of the pandemic outbreak. We show that a large credit risk premium on Italian bonds is consistent with a moderate Sharpe ratio on Italian default risk. We also inspect the mechanisms by which shocks to future net bond supply can immediately shift both long and short yields. The forward-looking nature of the default decision is crucial for shifting the sovereign spread on impact. The impact of projected asset purchases on future central bank remittances is particularly important for the fall in the yields on the shortest peripheral bonds in response to the PEPP announcement.

Our sharp analytical results, and hence our identification strategy, rely on the fact that our model, like that of Vayanos and Vila (2021), admits an explicit solution of affine form. To obtain this solution, we must assume that the probability of default is a *deterministic* function of time; otherwise, numerical solution methods would be required. In the endogenous default specification, this requires that the governments' bond supply and the central bank's bond demand are deterministic sequences.[7] This crucial simplifying assumption comes at a cost: in a steady state with a constant default rate, the sovereign spread is independent of maturity (Prop. 3). This contrasts with data on peripheral euro area yields, which show that the sovereign spread typically increases with maturity. Extending this framework to allow for a stochastically time-varying default rate is an important task that we leave for future research.

Related literature. This paper links two different strands of literature. First, we contribute to the finance literature on term structure models. In liquid markets, arbitrage links bond returns tightly across maturities and issuers. Duffie and Kan (1996) and Ang and Piazzesi (2003) developed an analytical solution for the yield curve consistent with arbitrage, when all yields are affine functions of a set of autoregressive Gaussian factors. Vayanos and Vila (2021) derived an affine term structure model (ATSM) of this type from a microfounded setting featuring arbitrageurs with mean-variance utility

[7] This may be interpreted as a scenario in which the public sector commits to a particular time path for the net supply of bonds in the market.

functions and "preferred-habitat" investors whose net demand for bonds of specific maturities is linear in those bonds' yields. This market structure makes it possible to model complex bond market interactions and policy interventions. For example, Greenwood and Vayanos (2014) showed empirically that the price of risk increases with arbitrageurs' maturity-weighted positions; therefore quantitative easing can reduce yields, even if the face value of debt outstanding is unchanged. Other applications include quantitative easing at the effective lower bound (Hamilton and Wu, 2012; King, 2019), corporate bond purchases (Gilchrist et al., 2024), repo market dynamics (He et al., 2023, Jappelli et al., 2023), and exchange rates (Greenwood et al., 2023; Gourinchas et al., 2022).[8] The ATSM structure has also been embedded into a New Keynesian model to analyze its monetary policy implications (Ray 2019). Motivated by the this literature, various papers have incorporated net supply factors into otherwise standard ATSMs, including Li and Wei (2013) and Eser et al. (2023); the latter paper uses security-level data on sectoral bond holdings to measure the duration risk held by arbitrageurs and to analyze the impact of the ECB's Asset Purchase Program (APP).

While they have been widely applied, much of the literature on ATSMs has studied US markets, under the assumption that Treasury securities are nominally riskless. Applications to fixed exchange rate environments – including monetary unions – or to commercial debt make it necessary to consider default risk. Hamilton and Wu (2012) construct an ATSM that includes one-period defaultable non-Treasury debt. A key insight about defaultable bond prices comes from Duffie and Singleton (1999), who show that if the loss caused by default is a fixed fraction of the bond's value, then the pricing formulas for default-free and defaultable bonds are formally identical, with an adjustment to the discount factor to account for expected losses due to default. Borgy et al. (2012) price defaultable euro-area debt under the assumption that the Duffie and Singleton (1999) condition holds. Altavilla et al. (2021) modelled euro area debt under the assumption that default risk can be priced like any other Gaussian factor.

We contribute to this literature in several ways. We show how the non-Gaussian risk of default – specifically, partial default on multi-period debt – can be incorporated into a microfounded ATSM in the Vayanos-Vila tradition. Crucially, we show that default risk opens up a novel *default risk extraction channel* of large-scale asset purchases, which enables the model to generate large, parallel yield curve shifts like those in Fig. 1. In

[8] See Greenwood et al. (2024) for a survey of this literature.

addition, we adapt the model to the context of a monetary union with heterogeneous default risk. The multicountry structure both sharpens the identification of model parameters and makes our model suitable for analyzing euro area monetary and fiscal policy interactions.[9] Finally, we model explicitly how central bank asset purchases affect the default probability by incorporating the possibility of rollover crises, showing how this reinforces the default risk extraction channel *vis-à-vis* the simpler case with exogenous default probability. This setup extends aspects of the two-period economy of Corsetti and Dedola (2016) to a fully dynamic environment.

This paper also relates to the literature on monetary-fiscal interactions in the presence of sovereign risk.[10] In contrast to previous related work, we study how central bank asset purchases can reduce the probability of default, and how they affect the whole term structure of interest rates. Linking the ATSM literature to that on sovereign risk is fruitful, because it clarifies that duration extraction is neither the only nor the primary channel by which asset purchases shift yields in the European context. Instead, default risk extraction is the predominant channel of asset purchases in the euro area. The quantitative discipline of the ATSM framework is crucial here, robustly showing that the sovereign spread on peripheral bonds is mostly a risk premium. This conclusion is consistent with evidence of De Grauwe and Ji (2013) showing that sovereign spreads are less stable in the euro area than in other open economies with independent monetary policies, and findings of Broeders et al. (2023) showing that ECB asset purchases reduced the impact of bond market volatility on euro area sovereign spreads.

2 Bond market equilibrium with default risk

We begin by building a model of bond market equilibrium that incorporates an exogenous but time-varying probability of partial default. This simple version of our model shows how introducing default risk in a Vayanos-Vila framework that is entirely standard – apart from its two-country monetary union structure – modifies the bond market

[9] As an application, in Online Appendix D, we quantify the increased effectiveness of the flexible purchase design of the PEPP, compared with the rigid design of the ECB's earlier asset purchase programme (APP).

[10] See Calvo (1988), Cole and Kehoe (2000), Aguiar et al. (2015), Reis (2013), Corsetti and Dedola (2016), Camous and Cooper (2019), Bacchetta et al. (2018), Nuño et al. (2023), Na et al. (2018), Arellano et al. (2020), or Bianchi and Mondragon (2022).

equilibrium and shapes the transmission of central bank asset purchases, without taking a stance on the modelling of sovereign default. Subsequently, we will extend the model to include a monetary/fiscal interactions block that endogenizes the default probability.

Time is continuous, with an infinite horizon. We consider a monetary union composed of two countries, Core and Periphery, with a single central bank. The key difference between the two governments is that Core issues risk-free debt whereas Periphery may default on its obligations. We denote Core variables with an asterisk, $'*'$. There exists a continuum of zero-coupon government bonds of different maturities. The time-t price of a bond with maturity τ is $P_t(\tau)$ for Peripheral bonds and $P_t^*(\tau)$ for Core bonds. The *yield* is the spot rate for maturity τ :

$$y_t(\tau) = -\frac{\log P_t(\tau)}{\tau}, \quad y_t^*(\tau) = -\frac{\log P_t^*(\tau)}{\tau} \ .$$

We assume that default follows a Poisson stochastic process, as in Duffie and Singleton (1999). Let ψ_t be the arrival rate of sovereign default by the government of Periphery. While it is easy to allow for default by both sovereigns, for clarity we focus on the case where the probability of Core default is zero. Peripheral default, when it occurs, consists of a restructuring in which the government reneges on fraction δ of each of its outstanding bonds. Default thus affects all maturities of Peripheral debt equally.

There exists a short-term (instantaneous) riskless interest rate which is exogenous and characterized by an Ornstein–Uhlenbeck process,

$$dr_t = \kappa(\bar{r} - r_t)\,dt + \sigma dB_t, \tag{1}$$

where B_t is a Brownian motion and κ, $\bar{r}$ and σ are constants. The short-term riskless rate and the default shock itself are the only stochastic processes in this economy. The Peripheral default arrival rate ψ_t is deterministic but may depend on time.[11] Allowing for time variation in the default rate allows us to model the impact of changes in fiscal conditions and changes in asset purchases on the default probability (see Sec. 3).

Net bond supply. The public sector of the monetary union determines the net supply of bonds, consisting of the gross supply issued by the Peripheral and Core governments minus the bonds held by the common central bank. Let $f_t(\tau)$ be the stock

[11] The assumption that ψ_t is deterministic is essential in order to obtain an affine solution, as we will see below.

of Peripheral sovereign debt of maturity τ outstanding at time t, and let $\iota_t(\tau)$ represent the rate of issuance of bonds of this type per unit of time. Then the law of motion of the stock of Peripheral debt is

$$\frac{\partial f_t(\tau)}{\partial t} = \iota_t(\tau) + \frac{\partial f_t(\tau)}{\partial \tau}, \tag{2}$$

which implies that the quantity of bonds of residual maturity τ outstanding at time t, $f_t(\tau)$, equals the current gross issuance of bonds of that maturity, $\iota_t(\tau)\,dt$, plus the stock of bonds of maturity $\tau + dt$ that was outstanding at time $t - dt$. The dynamics of the Core debt stock $f_t^*(\tau)$, given issuances $\iota_t^*(\tau)$, are formally identical to (2). Likewise, the central bank purchases $\iota_t^{CB}(\tau)$ bonds of maturity τ from Periphery per unit of time, resulting in a Peripheral portfolio $f_t^{CB}(\tau)$ that evolves as

$$\frac{\partial f_t^{CB}(\tau)}{\partial t} = \iota_t^{CB}(\tau) + \frac{\partial f_t^{CB}(\tau)}{\partial \tau}, \tag{3}$$

with analogous dynamics for its portfolio of Core bonds. We denote the net supplies of Periphery and Core bonds by

$$S_t(\tau) \equiv f_t(\tau) - f_t^{CB}(\tau), \quad S_t^*(\tau) \equiv f_t^*(\tau) - f_t^{CB*}(\tau),$$

respectively. For ease of exposition, but without loss of generality, we assume that net bond supplies are deterministic but possibly time-varying functions.

Bond demand. We consider two classes of private agents that demand bonds. *Preferred-habitat investors* demand bonds of a specific jurisdiction and specific maturity, as an increasing function of the bonds' yield. Market participants with these characteristics may include pension funds or insurance companies whose liability streams require them to hold assets paying off at specific times in the distant future, or money-market mutual funds that must hold assets that provide liquidity at short horizons. *Arbitrageurs* are willing to hold bonds of any maturity and jurisdiction, and may also invest in the riskless short rate, but their positions are limited by their risk aversion. These players represent liquid, well-informed market participants, such as hedge funds, which nonetheless are unwilling to take arbitrarily large risks.

As in Vayanos and Vila (2021) we assume that preferred-habitat investors' demand

for bonds of a given jurisdiction and maturity increases with the yield on those bonds:

$$\begin{aligned} Z_t(\tau) &= h(\tau) - \alpha(\tau)\,\mathbb{E}_t\left[\log P_t(\tau) + \tau\hat{\delta}dN_t\right] = h(\tau) + \tau\alpha(\tau)\left[y_t(\tau) - \hat{\delta}\psi_t\right] \quad (4) \\ Z_t^*(\tau) &= h^*(\tau) - \alpha^*(\tau)\log P_t^*(\tau) = h^*(\tau) + \tau\alpha^*(\tau)\, y_t^*(\tau) \end{aligned}$$

where $\alpha(\tau), \alpha^*(\tau) \geq 0$ and $h(\tau), h^*(\tau)$ are exogenous functions and dN_t is a Poisson process capturing the arrival of the default event. Note that the demand for peripheral bonds may depend on the probability of default. In particular, setting $\hat{\delta} = \delta$, the demand for peripheral bonds depends on their yield net of the expected default loss ($\psi_t\delta$). If instead we set $\hat{\delta} = 0$, then the demand for peripheral bonds, like that for core bonds, simply depends on their yield.[12]

The main focus of our analysis is the arbitrageurs, who maximize a mean-variance objective over instantaneous changes in wealth, as in Vayanos and Vila (2021),[13]

$$\max_{\{X_t(\tau), X_t^*(\tau)\}_{\tau\in(0,\infty)}} \mathbb{E}_t(dW_t) - \frac{\gamma}{2}\mathbb{V}ar_t(dW_t) \quad (5)$$

subject to the law of motion of wealth:

$$\begin{aligned} dW_t &= \left[W_t - \int_0^\infty \left(X_t(\tau) + X_t^*(\tau)\right)d\tau\right] r_t dt \\ &+ \int_0^\infty \left(X_t(\tau)\left(\frac{dP_t(\tau)}{P_t(\tau)} - \delta dN_t\right) + X_t^*(\tau)\frac{dP_t^*(\tau)}{P_t^*(\tau)}\right)d\tau, \quad (6) \end{aligned}$$

where $\gamma > 0$ is the representative arbitrageur's risk-aversion coefficient, and $X_t(\tau)$ and $X_t^*(\tau)$ are the nominal quantities of bonds of different maturities held in the arbitrageur's portfolio. The first term in (6) shows the income from investing in the short-term riskless rate, while the second term shows the capital gains from holding a portfolio of Peripheral bonds $X_t(\tau)$ and Core bonds $X_t^*(\tau)$, adjusted for the possible arrival of the default event. Note that arbitrageurs can operate in both markets (Core

[12] Later, in Sec. 4, we enhance the quantitative realism of the model by allowing for stochastic shifts in the preferred habitat demand equation (4), as in Vayanos and Vila (2021).

[13] Some papers have considered portfolio problems in mean-variance settings where asset returns are generated by jump processes, including Rachev and Han (2000), Ortobelli et al. (2003), Kallsen (2000), and Emmer and Kluppelberg (2004), among others. In the quantitative evaluation of the model presented in Sec. 4, we have verified that the variance of wealth due to diffusion (interest rate) risk is of the same order of magnitude as that associated to Poisson (default) risk.

and Periphery), similar to Gourinchas et al. (2022).

Bond market clearing. Bond market clearing requires consistency between supply and demand for bonds of each maturity and jurisdiction:

$$S_t(\tau) = Z_t(\tau) + X_t(\tau), \quad S_t^*(\tau) = Z_t^*(\tau) + X_t^*(\tau) \ . \tag{7}$$

That is, net supply by the public sector equals demand by preferred-habitat investors plus that of arbitrageurs.

Bond pricing. We assume that after default, the Peripheral government issues new bonds to replace the defaulted bonds, thus returning to its initial deterministic path of gross bond supply.[14] Thus, default leaves the state of the bond market unchanged, so we seek to construct an equilibrium in which bond prices do not depend on previous default events.[15] We conjecture that there exist two pairs of deterministic sequences of functions $(A_t(\tau), C_t(\tau))$ and $(A_t^*(\tau), C_t^*(\tau))$ such that the price of bonds can be expressed in log-affine form:

$$P_t(\tau) = e^{-[A_t(\tau) r_t + C_t(\tau)]}, \ P_t^*(\tau) = e^{-[A_t^*(\tau) r_t + C_t^*(\tau)]}. \tag{8}$$

Applying Itô's lemma to construct the expectation and variance terms in (5), the arbitrageurs' problem can be written as follows:

$$\begin{aligned} \max_{\{X_t(\tau), X_t^*(\tau)\}_{\tau\in(0,\infty)}} \quad & \int_0^\infty \left(X_t(\tau)\left(\mu_t(\tau) - r_t\right) + X_t^*(\tau)\left(\mu_t^*(\tau) - r_t\right)\right) d\tau \\ - \quad & \frac{\gamma\sigma^2}{2}\left[\int_0^\infty \left(X_t(\tau) A_t(\tau) + X_t^*(\tau) A_t^*(\tau)\right) d\tau\right]^2 \\ - \quad & \psi_t \delta \left[\int_0^\infty X_t(\tau)\, d\tau\right] \\ - \quad & \frac{\gamma\psi_t}{2}\delta^2 \left[\int_0^\infty X_t(\tau)\, d\tau\right]^2, \end{aligned} \tag{9}$$

[14] Perhaps surprisingly, it would be unrealistic to suppose that debt decreases when default occurs. On the contrary, Arellano et al. (2023) show that debt is more likely to *increase* following a restructuring. As in their paper, the model of monetary/fiscal interactions that we develop in Sec. 3 implies that default serves to alleviate short-term fiscal pressure, not to reduce the debt load permanently.

[15] Duffie and Singleton (1999) show that default risk is easier to price if default causes the bondholder to lose a fixed proportion of the market value of the bond. By assuming, first, that default amounts to reneging on the fixed quantity δ of each bond, and second, that default leaves the state of the bond market unchanged, we construct an equilibrium in which bondholders lose fraction δ of the market value of their holdings of Peripheral bonds. Hence we can price default risk as Duffie and Singleton (1999) do, reflected in the term δdN_t in (6).

where $\mu_t(\tau)$ and $\mu_t^*(\tau)$ are the expected returns on Peripheral and Core bonds, respectively. Here, wealth is affected by two different types of risk: Brownian variation in bond prices, together with a Poisson risk of losing a fraction δ of the investment in Peripheral bonds. The first two terms in (9) represent the expectation and variance of the price variation component, while the last two terms are derived from default risk, using $\mathbb{E}[\delta dN_t] = \delta\psi_t$ and $\mathbb{V}ar[\delta dN_t] = \delta^2\psi_t$.

The first-order conditions are

$$\mu_t(\tau) = r_t + A_t(\tau)\lambda_t + \psi_t\delta + \xi_t, \tag{10}$$

$$\mu_t^*(\tau) = r_t + A_t^*(\tau)\lambda_t, \tag{11}$$

where[16]

$$\lambda_t = \gamma\sigma^2 \int_0^\infty \left(X_t(\tau) A_t(\tau) + X_t^*(\tau) A_t^*(\tau)\right) d\tau \tag{12}$$

is the *market price of (interest rate) risk*, and

$$\xi_t = \gamma\psi_t\delta^2 \int_0^\infty X_t(\tau)\, d\tau \tag{13}$$

is the compensation required by risk-averse arbitrageurs for *default risk*. Equation (11) shows that the expected return on Core bonds equals the short-term riskless rate of return, r_t, plus the compensation $A_t^*(\tau)\lambda_t$ for the instantaneous price risk on a bond of a given maturity τ. Analogous terms apply to the expected growth of Peripheral bond prices, given by (10), plus the compensation $\psi_t\delta$ for the rate of expected loss due to default, together with the instantaneous default risk premium ξ_t.

Constructing an affine solution. Market clearing (7) requires that the positions of arbitrageurs equal those of the public sector minus those of the preferred-habitat investors. Hence equations (12) and (13) imply

$$\lambda_t = \gamma\sigma^2 \int_0^\infty \left[\left(S_t(\tau) - Z_t(\tau)\right) A_t(\tau) + \left(S_t^*(\tau) - Z_t^*(\tau)\right) A_t^*(\tau)\right] d\tau, \tag{14}$$

$$\xi_t = \gamma\psi_t\delta^2 \int_0^\infty \left(S_t(\tau) - Z_t(\tau)\right) d\tau. \tag{15}$$

[16] Our notation in this section follows Vayanos and Vila (2021), except that we have reversed the sign on the variables λ and h.

Equations (14)-(15) can be used to solve for the unknown coefficients $A_t(\tau)$, $A_t^*(\tau)$, $C_t(\tau)$, and $C_t^*(\tau)$ in the bond price functions. The solution hinges on the observation that if ψ_t is a deterministic function of time, then the left- and right-hand sides of (15) can both be affine functions of r_t (since preferred-habitat demand Z is affine in r).[17] In this case, we can construct a (potentially) time-varying affine solution (8) for prices and yields, in which the risk prices are also affine: $\lambda_t = \Lambda_t r_t + \bar{\lambda}_t$ and $\xi_t = \Xi_t r_t + \bar{\xi}_t$. Online App. B.1 spells out the affine solution in detail, stating the formulas for the factor loadings Λ_t and Ξ_t and intercept terms $\bar{\lambda}_t$ and $\bar{\xi}_t$ consistent with (14)-(15).

2.1 Equilibrium yield curves and monetary policy transmission: analytical results

Our model's explicit solution provides insight into yield curve dynamics and the transmission of conventional and unconventional monetary policy. Here we discuss four main findings. First, we decompose yields to distinguish the familiar *expectations* and *duration extraction* transmission channels of asset purchase policy from our model's novel *default risk extraction channel*, which arises when debt is defaultable. Second, we show that, if the default arrival rate is small, the Core and Peripheral term premia are approximately equal, and both depend on the *aggregate* net bond supply in the monetary union, irrespective of its distribution across countries. Third, we show that default risk allows for heterogeneous fluctuations in short-term sovereign rates in a monetary union, including shifts in the short end of the Peripheral yield curve even when the short-term riskless rate does not change. Finally, we show that conventional interest rate policy transmits homogeneously across a monetary union, limiting its scope for stabilizing asymmetric fluctuations.

Decomposing bond yields. In the absence of default risk, equations (10)-(11) imply identical yield curves for Core and Periphery. But when Peripheral bonds are defaultable, this opens up a spread relative to Core bonds. Using Ito's Lemma to calculate the expected capital gain $\mathbb{E}_t dP_t(\tau)/P_t(\tau)$, then using (10) and the fact that

[17] If instead ψ_t is a stochastic process that depends on r_t, then there are nonlinear terms on the right-hand side of (15), so the affine solution fails.

$P_t(0) = 1$, we can decompose the yield on a Peripheral bond of maturity τ as follows.[18]

Proposition 1 (Bond yield decomposition) *Peripheral yields* $y_t(\tau)$ *decompose as*

$$y_t(\tau) = \underbrace{\frac{1}{\tau}\mathbb{E}_t \int_0^\tau r_{t+s} ds}_{\text{Expected rates } y_t^{EX}(\tau)} + \underbrace{\frac{1}{\tau}\mathbb{E}_t \int_0^\tau \left\{ A_{t+s}(\tau - s)\lambda_{t+s} - \frac{\sigma^2}{2}\left[A_{t+s}(\tau - s)\right]^2 \right\} ds}_{\text{Term premium } y_t^{TP}(\tau)}$$
$$+ \underbrace{\frac{1}{\tau}\mathbb{E}_t \int_0^\tau \delta\psi_{t+s} ds}_{\text{Expected default loss } y_t^{DL}(\tau)} + \underbrace{\frac{1}{\tau}\mathbb{E}_t \int_0^\tau \xi_{t+s} ds}_{\text{Credit risk premium } y_t^{CR}(\tau)} . \quad (18)$$

For the proof, see Online App. B.2.1. Thus, Peripheral yields decompose into four affine components. The default-related components are zero for Core:

$$y_t(\tau) = y_t^{EX}(\tau) + y_t^{TP}(\tau) + y_t^{DL}(\tau) + y_t^{CR}(\tau), \quad (19)$$
$$y_t^*(\tau) = y_t^{EX*}(\tau) + y_t^{TP*}(\tau). \quad (20)$$

The first component, which is equalized across countries, $y_t^{EX}(\tau) = y_t^{EX*}(\tau)$, is the yield in a default-free economy where investors are risk neutral. This is often called the *expected rates term*, since it is the yield in a default-free economy where the "expectations hypothesis" is true: that is, the bond yield equals the expected value of the short rate over the life of the bond. The second component is the *term premium*, that is, the compensation required by a risk-averse arbitrageur for holding a bond with a risky price.[19] Since the price process of a defaultable bond differs from that of a default-free bond, the Core and Peripheral term premia, $y_t^{TP*}(\tau)$ and $y_t^{TP}(\tau)$, are not exactly equal. The third component, in the case of Peripheral bonds, is the *expected default loss* $y_t^{DL}(\tau)$, which requires compensation even for a risk-neutral investor. Fourth, the yield on Peripheral bonds also carries a *credit risk premium* $y_t^{CR}(\tau)$, which is the

[18] Equivalently, the bond price can be written as a product of log-affine factors:

$$P_t(\tau) = P_t^{EX}(\tau)P_t^{TP}(\tau)P_t^{DL}(\tau)P_t^{CR}(\tau) \quad (16)$$
$$P_t^*(\tau) = P_t^{EX*}(\tau)P_t^{TP*}(\tau) \quad (17)$$

where, for each $i \in \{EX, TP, DL, CR\}$, we have $P_t^i(\tau) = \exp\left(-\tau y_t^i(\tau)\right)$, and likewise for Core.

[19] To simplify the decomposition, we include the Itô adjustment term $-\frac{\sigma^2}{2}\left[A_{t+s}(\tau - s)\right]^2$ in the term premium, since it is related to price variability. Note, though, that a term of this form also exists in the case where arbitrageurs are risk-neutral.

additional return required, beyond the expected default loss, in order for a risk-averse arbitrageur to be willing to hold a defaultable bond. Together, the two components $y_t^{DL}(\tau) + y_t^{CR}(\tau)$, plus the cross-country difference in term premia $y_t^{TP}(\tau) - y_t^{TP*}(\tau)$, constitute the (sovereign) spread between Peripheral and Core debt.

This decomposition highlights four different channels of monetary policy transmission. First, policy transmits through anticipated changes in the future path of interest rates (e.g. due to forward guidance). Second, it operates through *duration extraction*, by which central bank bond purchases reduce the market price of interest rate risk, as in the one-factor version of Vayanos and Vila (2021). Third, policy transmits through changes in the expected default loss, as central bank purchases may reduce the likelihood of sovereign default, as explained in Sec. 3 below. Finally, it transmits through *default risk extraction*, as we can see by using (15) to write the credit risk premium as

$$y_t^{CR}(\tau) = \frac{\gamma\delta^2}{\tau}\mathbb{E}_t \int_0^\tau \left[\psi_{t+s} \int_0^\infty \left(S_{t+s}(\tau) - Z_{t+s}(\tau)\right) d\tau\right] ds \ .$$

This shows that central bank bond purchases reduce credit risk premia, both by extracting defaultable debt $S_{t+s}(\tau)$ from the market, and – once it is allowed to depend on central bank purchases – by lowering the probability of default ψ_{t+s} on that debt.

Term premium and sovereign spread in a monetary union. While our decomposition highlights a new transmission channel going through credit risk, our model also delivers basic insights about the transmission of asset purchases via term premia in a monetary union. For simplicity, but without loss of generality, we focus on the model's ergodic distribution, in which the short rate r_t is stochastic, but there is no further time variation in the model's parameters. We suppress time subscripts wherever possible when analyzing the ergodic distribution. As shown in Online App. B.2.2, in this case the coefficients $A_t(\tau)$ and $A_t^*(\tau)$ are given by

$$A^*(\tau) = \frac{1 - e^{-\hat{\kappa}\tau}}{\hat{\kappa}}, \ A(\tau) = \frac{(1+\Xi)\left(1 - e^{-\hat{\kappa}\tau}\right)}{\hat{\kappa}}, \tag{21}$$

where

$$\hat{\kappa} = \kappa - \Lambda = \kappa + \gamma\sigma^2 \int_0^\infty \left(\alpha(\tau)\left(\frac{(1+\Xi)\left(1 - e^{-\hat{\kappa}\tau}\right)}{\hat{\kappa}}\right)^2 + \alpha^*(\tau)\left(\frac{1 - e^{-\hat{\kappa}\tau}}{\hat{\kappa}}\right)^2\right) d\tau,$$

is the risk-neutral counterpart of κ, and $\Xi = -\gamma\psi\delta^2 \int_0^\infty \alpha(\tau) A(\tau) d\tau < 0$ is the steady-state value of the loading of the default risk price ξ_t on the short rate. We then obtain the following result:

Proposition 2 (Term premia in a monetary union with low default risk) *Let the default arrival rate ψ be arbitrarily close to zero, $\psi \to 0$, so that $\Xi \to 0$. In this limiting case, $A(\tau) = A^*(\tau)$. Term premia are then equalized across the two countries:*

$$y_t^{TP}(\tau) = \frac{1}{\tau}\mathbb{E}_t \int_0^\tau \left\{ A(\tau - s)\lambda_{t+s} - \frac{\sigma^2}{2}\left[A(\tau - s)\right]^2 \right\} ds = y_t^{TP*}(\tau),$$

and the market price of duration risk depends on the aggregate net bond supply in the monetary union:

$$\lambda_t = \gamma\sigma^2 \int_0^\infty \underbrace{\left[\left(S(\tau) + S^*(\tau)\right) - \left(Z_t(\tau) + Z_t^*(\tau)\right)\right]}_{\textit{aggregate net bond supply}} A(\tau) d\tau.$$

A policy implication of this result is that, when default risk is arbitrarily small, asset purchases affect Core and Peripheral term premia symmetrically, and this effect depends only on the *aggregate* amount of purchases and not on how they are distributed across jurisdictions. This benchmark will be helpful in interpreting our subsequent numerical results, since our calibrated default arrival rate turns out to be fairly small.

Notice that if the term premia roughly coincide, then the sovereign spread is approximately the expected default loss plus the credit risk premium: $y_t^*(\tau) - y_t(\tau) \approx y_t^{DL}(\tau) + y_t^{CR}(\tau)$. In the ergodic distribution, both objects are independent of maturity, and hence the spread is constant across τ and equals $y_t^*(\tau) - y_t(\tau) \approx \psi\delta + \left(\Xi\bar{r} + \bar{\xi}\right)$.

What drives the short end of the yield curve? For a country without default risk, the shortest maturity yield coincides with the short-term riskless rate:

$$\begin{aligned}
\lim_{\tau\to 0} y_t^*(\tau) &= \lim_{\tau\to 0}\left[\frac{1}{\tau}\mathbb{E}_t\int_0^\tau r_{t+s}ds + \frac{1}{\tau}\mathbb{E}_t\int_0^\tau A_{t+s}^*(\tau - s)\lambda_{t+s} - \frac{\sigma^2}{2}\left[A_{t+s}^*(\tau - s)\right]^2 ds\right] \\
&= r_t + A_t^*(0)\lambda_t - \frac{\sigma^2}{2}\left[A_{t+s}^*(0)\right]^2 = r_t,
\end{aligned}$$

where the second line applies L'Hôpital's rule and the Leibniz rule and the fact that $A_t^*(0) = 0$. Therefore, in the absence of default risk, changes in structural parameters can produce changes in the slope of the yield curve, but the short end of the curve is

pinned down to equal the short-term rate.[20]

Hence, if we abstract from default, our model cannot reproduce yield curve shifts like those observed in Europe in the context of Covid-19 and the PEPP announcement (see Fig. 1 above). But once we allow for default risk, parallel shifts are possible, even in the absence of changes in the short-term riskless rate.

Proposition 3 (Default risk-related shifts in the Peripheral yield curve) *In a country with default risk, the yield curve in the ergodic distribution is the sum of a constant term that depends on default* $\left(\psi\delta+\bar{\xi}\right)$ *and a maturity-dependent affine term:*

$$\begin{aligned} y_t(\tau) &= \frac{A(\tau)\, r_t + C(\tau)}{\tau} \\ &= \left(\psi\delta+\bar{\xi}\right) + \frac{(1+\Xi)\left(1-e^{-\hat{\kappa}\tau}\right)}{\tau\hat{\kappa}} r_t + \frac{\int_0^\tau \left[A(u)\left(\kappa\bar{r}+\bar{\lambda}\right) - \frac{1}{2}\sigma^2\left[A(u)\right]^2\right] du}{\tau}. \end{aligned}$$

Therefore, the short-term Peripheral yield is given by

$$\lim_{\tau\to 0} y_t(\tau) = (1+\Xi)\, r_t + \left(\psi\delta+\bar{\xi}\right).$$

For proof details, see Online App. B.2.2. Note that the default-related term $\psi\delta+\bar{\xi}$ is independent of maturity τ, so this term produces a parallel shift in the yield curve when any of its components change. Hence, the possibility of default affects even the shortest yields, generating a spread between the shortest-maturity Peripheral yield and the risk-free short rate. The spread includes the expected default loss $\psi\delta$. The second term is the intercept $\bar{\xi}$ of the credit risk premium ξ_t, which is

$$\bar{\xi} = \gamma\psi\delta^2 \int_0^\infty \left(S(\tau) - h(\tau) - \alpha(\tau)\, C(\tau)\right) d\tau. \tag{22}$$

Equation (22) shows that changes in the default arrival rate ψ, the haircut δ or the risk aversion parameter γ will, *ceteris paribus*, modify the credit risk premium and hence shift the Peripheral yield curve. Asset purchases will also shift Peripheral yields, including the shortest yields, by decreasing $\bar{\xi}$ through two channels. First, they extract default risk from arbitrageurs' balance sheets (reducing the quantity $S(\tau)$ that private

[20] This result generalizes beyond the one-factor model considered here. Even in a multi-factor context, an instantaneous bond without default risk satisfies $A^*(0)=0$ and $C^*(0)=0$, implying $y_t^*(0)=r_t$. See Vayanos and Vila (2021), Lemma 3.

markets must hold). Second, if asset purchases reduce the probability of default, this will amplify the decrease in $\bar{\xi}$. In the next section, we show how monetary and fiscal interactions like those in the euro area imply that central bank sovereign bond purchases reduce fiscal pressure, and thereby lower the probability of Peripheral default.

Conventional monetary policy transmission. Finally, we analyze how default risk shapes the transmission of conventional (interest rate) monetary policy across the monetary union. For the purpose of this particular discussion, we interpret r_t as representing the interest paid by the central bank on its deposit facility.[21] Concretely, as in Vayanos and Vila (2021), we may assume that arbitrageurs are actually commercial banks, with access to the central bank's deposit facility. With this interpretation, $\tau^{-1}A_t(\tau)$ represents the reaction of the Peripheral yield curve, on impact, to a monetary policy shock, and $A_t^{'}(\tau)$ represents the reaction of the instantaneous forward rate, $i_t(\tau) \equiv -\frac{\partial \log(P_t(\tau))}{\partial \tau}$. Therefore:

Proposition 4 (Response to short-term rates) *The yield curve and the instantaneous forward rate both react less to a monetary policy shock in Periphery, compared with Core:*

$$\frac{\partial y_t^*(\tau)}{\partial r_t} = \frac{1-e^{-\hat{\kappa}\tau}}{\tau\hat{\kappa}} > \frac{(1+\Xi)\left(1-e^{-\hat{\kappa}\tau}\right)}{\tau\hat{\kappa}} = \frac{\partial y_t(\tau)}{\partial r_t}.$$

$$\frac{\partial i_t^*(\tau)}{\partial r_t} = -\frac{\partial}{\partial r_t}\frac{\partial \log\left(P_t(\tau)\right)}{\partial \tau} = e^{-\hat{\kappa}\tau} > (1+\Xi)\,e^{-\hat{\kappa}\tau} = \frac{\partial i_t(\tau)}{\partial r_t}.$$

Since $\Xi < 0$ (see Online App. B.2.2), the reaction of Peripheral yields is damped relative to that of Core yields. But in practice, the difference is small: if the default arrival rate ψ is sufficiently close to zero, then $\Xi \approx 0$, so the responses of the two yield curves are approximately equal. In the quantitative section below we will see that the data call for a fairly small ψ. Therefore, in our calibrated model, the responses of Core and Peripheral yields to conventional monetary shocks are virtually indistinguishable.

[21] This implies that the short-term Core yield, $\lim_{\tau\to 0} y_t^*(\tau)$, coincides with the deposit facility rate. Of course, this is not precisely true in the euro area data, where the yield on short-term core (e.g. German) bonds typically exhibits a non-negligible and time-varying spread vis-à-vis the ECB's deposit facility rate, reflecting institutional features that fall outside the scope of our analysis.

3 A simple model of default risk

Thus far, we have treated the default arrival rate ψ_t as an arbitrary exogenous sequence. In practice, however, policy shocks like the PEPP announcement or the pandemic outbreak are likely to affect the probability of default perceived by the market. Therefore, we next build a minimalist model of monetary and fiscal interactions that endogenizes ψ_t in a way that suffices for our analysis of the yield curve. We assume at this point that the governments and the monetary authorities commit to fixed time paths for their respective issuances and purchases of bonds, as long as no rollover crisis occurs.[22] The one key policy choice that we will endogenize is Periphery's decision whether to repay or default in case of a rollover crisis.

Budget constraint of the government. The flow budget constraint of the Peripheral government can be written as

$$\overbrace{d_t}^{\text{Primary deficit (det.)}} + \overbrace{f_t(0)}^{\text{Bond redemptions}} = \overbrace{\int_0^\infty P_t(\tau)\,\iota_t(\tau)\,d\tau}^{\text{Bond issuance}} + \overbrace{\Gamma_t}^{\text{CB remittances}} + \overbrace{\Pi_t}^{\text{Emergency taxation}}, \tag{23}$$

where d_t is the deterministic part of the primary deficit[23] and $f_t(0)$ the amount of debt maturing, which must be financed with new bond issuances $\iota_t(\tau)$, income from central bank remittances Γ_t, or through adjustments in taxation (or reduced spending) Π_t. Our assumption that bond issuances $\iota_t(\tau)$ are deterministic implies that redemptions $f_t(0)$ are deterministic too. Since the government takes Γ_t as given, Π_t represents the part of primary deficit that must be adjusted to ensure that the budget constraint (23) is satisfied at all times. In the context of a rollover crisis, we may suppose that Π_t represents emergency taxation or, equivalently, emergency spending cuts.

Rollover crisis. Mirroring Corsetti and Dedola (2016), we focus on self-fulfilling debt crises *à la* Calvo (1988) or Cole and Kehoe (2000). We assume that investors sometimes, with a certain probability, coordinate on a pessimistic equilibrium in which they stop purchasing Periphery's debt, thus forcing its government to stop issuing bonds ($\iota_t(\tau) = 0$, for all τ).[24] The arrival of this rollover crisis is governed by a Poisson process

[22] This assumption is imposed in order to preserve the ATSM structure derived in Sec. 2.

[23] This may include spending or revenue items that are "hard" to change in the short run, such as pensions, benefits, the government wage bill, etc.

[24] We assume that the central bank cannot purchase new sovereign bonds at issuance, consistently

with rate parameter η. This random event is unrelated to the amount of a country's debt or its fiscal position.

At the onset of the crisis, the government must decide whether to default on its debts or to continue repaying bonds that mature. If it decides to repay, the duration of the crisis is stochastic, governed by a Poisson process with parameter ϕ, and the government will be forced to finance its deficits and debt repayments with revenues from emergency taxation and/or seigniorage as long as the crisis persists. Emergency taxes represent a utility loss for the government, which it seeks to minimize. Under these assumptions, the government's *cost of repayment* conditional on a rollover crisis at time 0, denoted by V_0^R, incorporates the present discounted value of emergency taxation incurred during the crisis, valued at a subjective discount rate $\hat{r}$, plus the continuation cost $V_t\left[f_t\left(\cdot\right), f_t^{CB}\left(\cdot\right)\right]$ after the crisis ends:

$$V_0^R\left[f_0\left(\cdot\right), f_0^{CB}\left(\cdot\right)\right] = \mathbb{E}_0\left\{\int_0^\infty e^{-(\hat{r}+\phi)t}\left(\underbrace{\Pi_t}_{\text{Flow of emergency taxes}} + \underbrace{\phi V_t\left[f_t\left(\cdot\right), f_t^{CB}\left(\cdot\right)\right]}_{\text{Loss after the crisis}}\right)dt\right\}. \tag{24}$$

If instead the government decides to *default*, it restructures by repudiating a fixed fraction δ of each outstanding bond. This restructuring ends the rollover crisis, but imposes a stochastic fixed cost χ on the government, with *c.d.f.* $\Phi(\chi)$. Thus, the loss due to default is the post-crisis continuation cost plus the fixed cost:

$$V_0^D\left[f_0\left(\cdot\right), f_0^{CB}\left(\cdot\right)\right] = V_0\left[f_0\left(\cdot\right), f_0^{CB}\left(\cdot\right)\right] + \chi. \tag{25}$$

Note that (25) says that default leaves the fiscal position of the government unchanged, with the same debts it faced before the crisis. While this may seem counterintuitive, we make this assumption for two reasons. First, it is empirically realistic: Arellano et al. (2023) show that debt is rarely decreased by a restructuring. Second, it simplifies our asset pricing analysis, keeping the outstanding bond supply fixed, allowing us to seek a bond price solution that is unchanged by default.[25] Thus, in our model, default

with actual restrictions on the ECB's asset purchase programs. Thus, the fact that private investors stop purchasing new bonds effectively prevents the Peripheral government from issuing new bonds.

[25] Our interpretation of (25) is that after default, the Peripheral government immediately issues bonds that return it to the previously anticipated path of debt. Bondholders lose a fraction δ of their holdings, while the proceeds from the sale of new bonds accrue to international organizations, such as the IMF, that may intervene in the case of a sovereign debt crisis.

serves only to relieve short-term fiscal pressure during a rollover crisis, not to improve the government's long-term fiscal standing.

Default decision. The government's decision to default at the beginning of a crisis will thus depend on $\min\left[V_0^R, V_0^D\right]$. The continuation cost is given by

$$V_0\left[f_0(\cdot), f_0^{CB}(\cdot)\right] = \mathbb{E}_0\left\{\int_0^\infty e^{-(\hat{r}+\eta)t}\ \eta \underbrace{\min\left[V_t^R, V_t^D\right]}_{\text{Loss at onset of next crisis}}\ dt\right\}. \tag{26}$$

Equations (24)-(26) jointly determine the loss functions V_t^R, V_t^D, and V_t. For simplicity, we focus on the limit where crises are low-probability events ($\eta \to 0$), which means that the continuation cost is approximately zero, $V_t \to 0$, so that $V_0^D \to \chi$. Intuitively, the country compares the fixed cost χ to the present value of the expected emergency-tax deadweight cost V_0^R. Then the probability of default, conditional on a rollover crisis at time 0, is the probability that the cost of repayment exceeds the fixed cost χ:

$$\mathbb{P}\left(\text{default at time } 0|\text{crisis}\right) = \mathbb{P}\left(V_0^R > V_0^D\right) \approx \mathbb{P}\left(V_0^R > \chi\right) = \Phi\left(V_0^R\right). \tag{27}$$

Equations (27), (24) and (23), and the fact that there are no issuances during the rollover crisis ($\iota_t(\tau) = 0$ for all τ), imply that the *unconditional* arrival rate of default is $\psi_t = \eta\Phi_t$, where

$$\Phi_t \equiv \mathbb{P}\left(\text{default at time } t|\text{crisis}\right) = \Phi\left(\int_0^\infty e^{-(\hat{r}+\phi)s}\left\{d_{t+s} + f_{t+s}(0) - \Gamma_{t+s}\right\} ds\right). \tag{28}$$

Therefore, conditional on a rollover crisis materializing at time t, the probability that the government chooses to default increases with the discounted stream of primary deficits and bond redemptions during the crisis (as they both imply higher liquidity needs), and decreases with the discounted stream of remittances from the central bank during the crisis (a source of government income that reduces liquidity needs).

Remittances rule. To evaluate expression (28), we must specify the central bank's remittances rule. More specifically, what matters is its remittances rule during a rollover crisis – its remittances policy under other circumstances is irrelevant for our analysis. It is plausible to conjecture that, should a full-blown rollover crisis hit a national government, the central bank would follow a rule under which *increased* central bank holdings of that government's bonds would *not reduce* resources for that government for the

duration of the crisis.[26] We call such a rule *sovereign-supportive*. Formally, we define a sovereign-supportive rule $\Gamma_t = \Gamma\left(\left\{f^{CB}_{t+u}(\tau)\right\}_{u\geq 0,\tau\geq 0}\right)$ as a rule that, in a rollover crisis, satisfies:

$$\frac{\partial}{\partial \varepsilon}\left[\int_0^\infty e^{-(\hat{r}+\phi)u}\Gamma\left(\left\{f^{CB}_{t+u}(\tau)+\varepsilon h_{t+u}(\tau)\right\}_{u\geq 0,\tau\geq 0}\right)du\right]\geq 0, \tag{29}$$

where $h_{t+u}(\tau)\geq 0$ is a non-negative perturbation to the time-$(t+u)$ central bank holdings of Periphery bonds with residual maturity τ. That is, under a sovereign-supportive remittance rule, a central bank's decision to increase its future holdings of peripheral debt would not decrease the discounted stream of dividend payments to the peripheral government in case of – and for the duration of – a rollover crisis. It trivially follows that, for any rule satisfying this property, increasing central bank purchases of peripheral bonds (weakly) *reduces* the endogenous default arrival rate.

Having established this general result, we still need to specify a particular crisis-time remittance rule to use in our numerical analysis. There is little guidance as to how Eurosystem national central banks (NCBs) would adapt their dividend policy should their country's government be hit by a rollover crisis. In practice, NCB dividend payments are typically based on their accounting profits, whereby a fraction of these is paid out as dividends to the respective government and the rest is retained as capital.[27] Thus, it seems plausible that crisis-time dividends would continue to be based on profits.

However, with a profit-based rule in our model, we would no longer be able to obtain an affine solution for bond yields. This is because the default probability (28) would depend on bond prices and therefore would no longer be deterministic, which as explained in Sec. 2 is essential for obtaining an affine solution.[28] With this limitation in mind, we assume the following remittance rule:

$$\Gamma_t = \zeta f^{CB}_t(0) - \bar{\Gamma}, \tag{30}$$

[26] The central bank is assumed to stick to its bond purchase commitments when the private bond market enters into a rollover crisis.

[27] That being said, dividend rules are *not* harmonized across the Eurosystem. Each NCB autonomously decides how much of its accounting profit to pay to its national government, with criteria that vary across NCBs and also change over time.

[28] Online App. A shows how to calculate the central bank's profits in our model, and explains why a remittance rule based on profits would render our affine solution inapplicable. In a nutshell: the interest income on the central bank's bond portfolio depends on the price paid for each bond. Moreover, profits depend on interest payments on reserves. Keeping track of the stock of reserves introduces another endogenous state variable, and the evolution of this stock also depends on bond prices.

such that the NCB rebates to the Peripheral government a fraction $\zeta \in [0,1]$ of the inflow from redemptions of Peripheral government bonds ($f_t^{CB}(0)$), minus a fixed amount $\bar{\Gamma}$ aimed at preemptively protecting its capital during the rollover crisis against a possible default.[29] Rule (30) is compatible with an affine solution for bond yields, as redemptions of central bank-held bonds are assumed to follow a deterministic path.[30] Also, it is "sovereign-supportive" as defined above.[31]

The parameter ζ allows us to vary the "generosity" of the Peripheral national central bank's dividend policy in case of a rollover crisis. At one extreme, $\zeta = 1$ represents a case in which the NCB transfers its entire inflow from Peripheral bond redemptions. This is (much) higher than the accounting profits earned by the central bank on those bonds – as one needs to deduct the cost of purchasing them.[32] Therefore, this can be seen as a very generous crisis-time dividend policy.[33] At the other extreme, $\zeta = 0$ represents a case in which the NCB stops all dividend payments to its government during a rollover crisis (over and above net transfers in the amount $-\bar{\Gamma}$), motivated e.g. by concerns about preserving its capital base. This case is particularly useful because it allows us to shut down the channel through which central bank asset purchases reduce the endogenous default probability.

[29] In the event of a default, we assume there is no discrimination between public and private bondholders. Therefore, upon default the NCB would take a hit to its capital, which depending on its pre-default value could become even negative. As discussed by Del Negro and Sims (2015), among others, central banks can operate with negative capital, within certain limits related to their future stream of seigniorage. Thus, Γ can be seen as reflecting these concerns about central bank capital during a rollover crisis. Of course, in the event of default and for sufficiently negative capital, the NCB may still require recapitalization ex post by the government, via negative dividends.

[30] Notice that central bank remittances to the Peripheral government depend on its portfolio of Peripheral bonds only, instead of its whole portfolio of Core and Peripheral bonds. This is consistent with the fact that, in the Eurosystem, most sovereign bonds are held by the NCBs of the sovereigns that issued them, with only a small fraction of holdings subject to "risk sharing" across NCBs.

[31] Under the given rule, $\Gamma\left(\left\{f_{t+u}^{CB}(\tau)+\varepsilon h_{t+u}(\tau)\right\}_{u\geq 0,\tau\geq 0}\right) = \zeta\left(f_{t+u}^{CB}(0)+\varepsilon h_{t+u}(0)\right)-\bar{\Gamma}$. Therefore, $\frac{\partial \Gamma}{\partial \varepsilon} = \{\zeta h_{t+u}(0)\}_{u\geq 0}$, and hence the condition (29) is just $\zeta \int_0^\infty e^{-(\hat{r}+\phi)u} h_{t+u}(0) du \geq 0$, which is true since the constant ζ and the perturbation h are both non-negative.

[32] The income earned on a zero-coupon bond is the difference between its payment at redemption (i.e. its face value) and the price paid for it. Thus, the total interest income from the central bank's bond portfolio at a given point in time equals bond redemptions, $f_t^{CB}(0)$, *minus* the total amount paid for those bonds by the central bank. See Online App. A for further details.

[33] Of course, such a dividend policy would erode the central bank's capital position. Online App. A derives the dynamics of central bank capital under our remittance rule.

Default rate. Under remittance rule (30), the default rate equals

$$\psi_t \;=\; \eta\Phi\left(\int_0^\infty e^{-(\hat{r}+\phi)s}\left\{d_{t+s}+f_{t+s}(0)-\zeta f^{CB}_{t+s}(0)+\bar{\Gamma}\right\}ds\right). \tag{31}$$

Equation (31) shows that the three factors affecting the default probability (primary deficits, total bond redemptions, and redemptions of central bank-held bonds) do so through a single sufficient statistic, which we may call *fiscal pressure*, F_t:

$$F_t \equiv \int_0^\infty e^{-(\hat{r}+\phi)s}\left(d_{t+s}+f_{t+s}(0)-\zeta f^{CB}_{t+s}(0)\right)ds. \tag{32}$$

Hence, as long as $\zeta > 0$, central bank asset purchases affect the default probability, which is $\psi_t = \eta\Phi\left(F_t + \frac{\bar{\Gamma}}{\hat{r}+\phi}\right)$. Bond purchases imply higher future redemption payments from the government to the central bank ($\{f^{CB}_{t+s}(0)\}_{s\geq 0}$) conditional on, and during, a rollover crisis. But a fraction ζ of those repayments is rebated back to the government as dividends, partly alleviating the liquidity stress on the government from its total redemptions ($\{f_{t+s}(0)\}_{s\geq 0}$). This reduces the cost of emergency taxation during a crisis, making the government less likely to choose default once a rollover crisis arrives. Underlying this mechanism is the central bank's (unique) ability to finance bond purchases by expanding the monetary base (see Online App. A.1 for explicit modelling of the central bank's accounts). This ability, together with the links between the central bank and government budget constraints via dividends, explains why central bank asset purchases can reduce sovereign default risk in our model.

This framework makes several stark assumptions which, together, deliver tractability. On one hand, we focus on perfect-foresight scenarios for fiscal policy and central bank purchases, assuming that the government returns to its previous path of debt after default occurs. Moreover, our remittance rule (30) ensures that the default probability depends only on deficits and bond redemption flows. Together, these assumptions imply that fiscal pressure is foreseeable, so default is an event that arrives at a known, deterministic Poisson rate $\psi_t = \eta\Phi_t$. This preserves our ability to combine the default-pricing framework of Duffie and Singleton (1999) with an ATSM solution, maintaining the analytical results derived in Sec. 2.1. But now, unanticipated changes in fiscal conditions will shift the default probability, with potential to explain the yield curve dynamics seen over the course of the Covid-19 crisis. We next explore these issues in a quantitative version of our model.

4 Calibration

4.1 Quantitative model

To calibrate the model, we interpret the two countries in the union, Core and Periphery, as Germany (DE) and Italy (IT), respectively.[34] Since inflation and growth were relatively low in much of the euro period, especially as policy rates approached their effective lower bound (ELB), we calibrate the model in nominal terms, without adjusting for real GDP growth or inflation.

Multifactor model. For quantitative realism, we enhance the previous one-factor model with additional shocks. While a model where the risk-free rate r_t is the only stochastic factor can fit the level of the yield curve and its responsiveness to the pandemic and the PEPP announcement, the implied yields are much less variable than those observed in the data.[35] To better fit the variance of yields, we now allow for two mean-zero factors, ε_t^h and ε_t^{h*}, that shift preferred-habitat demand for Periphery and Core bonds as follows:

$$\begin{aligned} Z_t(\tau) &= h(\tau) - \varsigma(\tau)\varepsilon_t^h + \tau\alpha(\tau)\left(y_t(\tau) - \hat{\delta}\psi_t\right), \\ Z_t^*(\tau) &= h^*(\tau) - \varsigma^*(\tau)\varepsilon_t^{h*} + \tau\alpha^*(\tau)y_t^*(\tau), \end{aligned} \tag{33}$$

where the functions $\varsigma(\tau) \geq 0$ and $\varsigma^*(\tau) \geq 0$ represent the impacts of ε_t^h and ε_t^{h*} on demand for each maturity τ, respectively. We group the risk-free rate and the demand shifters into a vector of factors $q_t \equiv [r_t, \varepsilon_t^h, \varepsilon_t^{h*}]^\top$ that follows the process

$$dq_t = -K(q_t - \bar{r}\mathcal{E}_1)dt + \Sigma dB_t, \tag{34}$$

where K and Σ are 3×3 matrices, $\mathcal{E}_1 = (1,0,0)^\top$, and B_t is a 3×1 vector of independent standard Brownian motions.

We conjecture that there exist deterministic sequences of functions $(A_t(\tau), C_t(\tau))$ and $(A_t^*(\tau), C_t^*(\tau))$, where $A_t(\tau)$ and $A_t^*(\tau)$ are 3×1 vectors, such that bond prices

[34] Taken literally, this means that arbitrageurs hold bonds of only one country with default risk, thus limiting the scope for diversification across issuers. An alternative interpretation is to assume that an Italian default would lead to a collapse of the monetary union and the default of other peripheral countries. This assumption may be relevant for our results, as otherwise arbitrageurs would be able to diversify, reducing the exposure of their portfolios to the default of any particular country.

[35] The one-factor version of our model is analyzed in our earlier working paper, Costain et al. (2022).

are log-affine in q_t:

$$P_t(\tau) = e^{-\left[A_t(\tau)^\top q_t + C_t(\tau)\right]},\ P_t^*(\tau) = e^{-\left[A_t^*(\tau)^\top q_t + C_t^*(\tau)\right]}. \tag{35}$$

The solution procedure from our earlier one-factor model generalizes to this multi-factor framework. For details, see Online App. B.3.

Calibration strategy. To calibrate this multifactor model, we proceed in two steps. First, we calibrate a set of parameters that can be directly inferred from the data, including some monetary and fiscal variables that affect the bond market in a time-varying way. Using this information, we can construct a distance metric to evaluate the model's quantitative performance relative to yields data. Hence, in a second step, we estimate the remaining parameters by minimizing this metric.

Numerical method. The numerical method is described in Online App. C.2.[36] It requires first solving the stationary model under constant fiscal pressure, and then computing the transitional dynamics under alternative paths for fiscal pressure. Both cases can be characterized as systems of partial differential equations, which can be solved by the finite differences method.

As Hayashi (2018) has shown, there may be multiple equilibria in the Vayanos and Vila (2021) model. In this respect, we have tried different initial guesses when solving the stationary model, and our algorithm always converged to the same solution.

4.2 Observables

We extract data on one-month, one-year, five-year, ten-year, and twenty-year zero coupon yields on German and Italian sovereign bonds, and also the one-month euro overnight interest swap (OIS) rate from Datastream. We consider a sample stretching from the establishment of the euro in January 1999 up to December 2022.

Short-term rates. We first calibrate the risk-free short rate process, r_t.[37] We interpret this rate as the yield on one-month zero-coupon German sovereign bonds. The German one-month rate is only available back to 2011; therefore we splice it to the cor-

[36] The actual numerical implementation is programmed both as a discrete-time system of difference equations, and as a finite-difference approximation to the original continuous time problem. Both implementations give the same results. Online App. C.3 describes the discrete-time method.

[37] The time unit in our numerical model is one month. However, in the main body of the text we report yields and describe the parameters in annualized terms, for ease of interpretation.

responding one-month OIS rate for dates prior to 2011.[38] The spliced series has a mean of 122 basis points (bp) *per annum*, and its standard deviation is 179 bp. Running an AR(1) estimate on the monthly spliced series, we find that the monthly autocorrelation is 0.9948. We parameterize the Ornstein-Uhlenbeck process that governs the risk-free rate in our model for consistency with these statistics. In annualized terms, this implies $\bar{r} = 1.22\%$, $\kappa = 0.062$, and $\sigma = 63$ bp.

Fiscal variables and asset purchases. Solving our model also requires forecasts of fiscal variables and of Eurosystem asset purchases. We need these both because the bond price solution (Sec. 2) depends on arbitrageurs' current and future net bond-holdings, and because the default arrival rate (Sec. 3) depends on the Peripheral government's current and future liquidity needs. We take forecasts from several different sources and vintages. We employ two-years-ahead Eurosystem forecasts, and extend them using a Banco de España in-house debt sustainability model to produce long-term projections of fiscal trends at annual frequency for Germany and Italy, including the total face value of sovereign debt, primary deficits, and interest charges.[39] We interpolate these data to monthly frequency for use in our simulations.

Regarding Eurosystem bond absorption under the APP, we construct long-term projections of total Eurosystem holdings of German and Italian sovereign bonds, based on ECB announcements. Similarly, we derive a forecast for Eurosystem bond absorption under the PEPP, for forecast vintage March 2020, from the ECB's initial PEPP announcement at that time. Thus, subtracting predicted Eurosystem bond absorption from predicted bond supply, for each country, we can infer the total debt of each sovereign to be absorbed by the private sector at any future time, looking forward from any available forecast date.

Maturity distributions. The data discussed so far only address total quantitites of debt issued and absorbed. To calculate yields, we must also specify how bonds are distributed across maturities. We make several assumptions to characterize debt maturity distributions in a tractable way. We assume a maximum maturity τ^{max} of 20 years. From the ECB, we obtained data on the maturity distribution of Eurosystem holdings

[38] Alternatively, we could calibrate the risk-free rate process directly to OIS rates over the whole sample. However, this would oblige us to model the differences between OIS rates and German rates. Therefore, to simplify our model of sovereign yields, we interpret short rates as sovereign rates too, as far as data availability permits.

[39] In particular, we employ an extension of the model introduced by Burriel et al. (2022).

Figure 2: Cross-sectional asset distributions

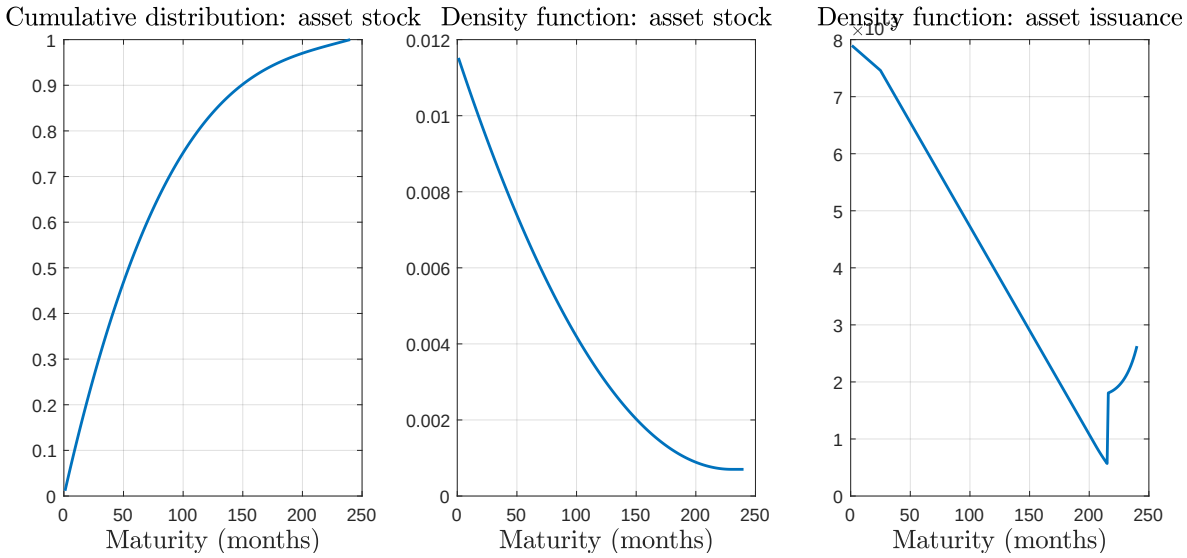

Data source: ECB data, smoothed by the authors.
Left panel: Cumulative distribution function, across maturities, of ECB holdings of German and Italian bonds, after smoothing.
Middle panel: Density, across maturities, of German and Italian bonds, approximated by a quadratic function. Called $g(\tau)$ in the text.
Right panel: Density of issuances, across maturities, that generates the PDF of the middle panel as the asset distribution in the long run. Called $\bar{\iota}(\tau)$ in the text.

of German and Italian debt of up to 20 years' maturity, as of July 2021. We assume for simplicity that the maturity distribution of these holdings replicates the distribution of debt in the market.[40] We then construct the density of these ECB holdings across maturities τ, at face value, smoothing it by computing its moving average over windows of 25 months and then fitting a quadratic polynomial. We call this smoothed density function $g(\tau)$, shown in the middle panel of Fig. 2. The corresponding cumulative distribution of bond holdings is shown in the left panel of the figure. In our simulations, we suppose that the initial density of gross bonds outstanding is proportional to $g(\tau)$. Thus, given the debt levels D_t^* and D_t of Germany and Italy at some initial time t, the initial bond densities are set to $f_t^*(\tau) = D_t^* g(\tau)$ and $f_t(\tau) = D_t g(\tau)$, respectively. Similarly, we set the initial density of Eurosystem bond holdings (if nonzero) in proportion to $g(\tau)$ in both countries.

[40] In practice, the maturity distribution of Eurosystem bond holdings broadly replicates that of the eligible universe, reflecting the "market neutrality" principle of Eurosystem asset purchases.

The time path of the distribution of net bond supply also depends on how issuances and central bank purchases are distributed across maturities. We calculate the density of issuances $\bar{\iota}(\tau)$ that, if maintained at a constant rate, would generate the observed maturity distribution $g(\tau)$.[41] We assume that new bond issuances $\iota_t(\tau)$ are always distributed proportionally to $\bar{\iota}(\tau)$, which is shown in the right panel of Fig. 2. To reflect the "market neutrality" of Eurosystem purchase design – that purchases should reflect available supply to avoid distorting relative prices – we assume that asset purchases are always distributed proportionally to $g(\tau)$. Given these assumptions about the initial distributions and the distributions of issuances and purchases, together with forecasts of total face value at each point in time, we can trace forward the distributions $f^*_{t+s}(\tau)$, $f_{t+s}(\tau)$, $f^{CB,*}_{t+s}(\tau)$, and $f^{CB}_{t+s}(\tau)$ from any forecast date t to any future time $t+s$.

Anticipated net debt and default. We will consider equilibria that take as given a deterministic time profile of net bond supply. Concretely, given forecasts of fiscal variables and Eurosystem asset purchases from a given forecast date t, we can calculate the net debt $f_{t+s}(\tau) - f^{CB}_{t+s}(\tau)$ of maturity τ that must be absorbed by the market at each future time $t+s$, for $s \geq 0$. Agents in the model regard this time path of net bond supply as a commitment of the public sector.

The data discussed above also give us sufficient information to calculate the default rate at any time t. First, we calculate the Italian deficit d_{t+s} as the sum of its forecasted primary deficit and interest charges. Then, given $f_{t+s}(\tau)$ and $f^{CB}_{t+s}(\tau)$ for each τ, we can calculate the net bond redemptions paid by the Italian government, $f_{t+s}(0) - \zeta f^{CB}_{t+s}(0)$. Thus, given forecasts of a particular vintage t, we have all the data needed to calculate fiscal pressure F_t from (32) and the default rate ψ_t from (31). The impact of default also depends on the haircut parameter δ, which we set at 25 percent ($\delta = 0.25$) in light of international evidence.[42]

We will compare equilibria looking forward from three key points in time. First, we construct a pre-pandemic forecast $\{d_{t+s}, f_{t+s}(\tau), f^*_{t+s}(\tau)\}^{pre-pan}_{\tau\geq 0, s\geq 0}$ using the last vintage of fiscal forecasts we have available prior to the pandemic (December, 2019). We assume that the anticipated Eurosystem portfolio $\{f^{CB}_{t+s}(\tau), f^{CB*}_{t+s}(\tau)\}^{pre-pan}_{\tau\geq 0, s\geq 0}$ is deter-

[41] The constant distribution of issuances $\iota(\tau)$ that generates maturity distribution $g(\tau)$ as a fixed point is simply $\iota(\tau) = -\frac{dg(\tau)}{d\tau}$ for $\tau < \tau^{max}$, with a point mass at $\tau = \tau^{max}$. We have smoothed $\iota(\tau)$ with a moving window of 49 months, and rescaled it to obtain $\bar{\iota}(\tau) \equiv \left(\int_0^{\tau^{max}} \iota(s)ds\right)^{-1} \iota(\tau)$.

[42] Cruces and Trebesch (2013) find haircuts on the order of 50% in evidence drawn mostly from emerging markets; for advanced economies we consider a smaller haircut more plausible.

mined by the announced trajectory of the APP as of end-2019. Second, we construct a pre-PEPP (or post-outbreak) forecast $\{d_{t+s}, f_{t+s}(\tau), f^*_{t+s}(\tau)\}^{pre-PEPP}_{\tau\geq 0, s\geq 0}$, which takes account of increased deficits and debt implied by the pandemic, by averaging forecast vintages from December, 2019 and June, 2020.[43] We also construct an updated Eurosystem portfolio path $\{f^{CB}_{t+s}(\tau), f^{CB*}_{t+s}(\tau)\}^{pre-PEPP}_{\tau\geq 0, s\geq 0}$ that includes the moderate expansion of the APP envelope (€120 billion) announced on May 12, 2020. Third, we update the anticipated portfolio again to include the initial €750 billion envelope of PEPP purchases, as announced on March 18, 2020, to define $\{f^{CB}_{t+s}(\tau), f^{CB*}_{t+s}(\tau)\}^{post-PEPP}_{\tau\geq 0, s\geq 0}$. We assume no additional fiscal news at the time of the PEPP announcement, setting $\{d_{t+s}, f_{t+s}(\tau), f^*_{t+s}(\tau)\}^{post-PEPP}_{\tau\geq 0, s\geq 0} = \{d_{t+s}, f_{t+s}(\tau), f^*_{t+s}(\tau)\}^{pre-PEPP}_{\tau\geq 0, s\geq 0}$.[44]

Preferred-habitat demand. The average sovereign debt of Italy and Germany over the ELB period 2013-2019, net of Eurosystem holdings, was 2,097 billion euros and 1,856 billion euros, respectively. To infer how much debt arbitrageurs must absorb, we next calibrate preferred-habitat demand. Eser et al. (2023), Table 1, report that the fraction of net debt of the big-four euro area economies held by preferred-habitat investors (excluding Eurosystem central banks) was 41.4% in 2014, and 47.0% in 2018.[45] We consider the mean of these two figures – 44.2% of each country's net debt – and calibrate the intercept terms $h(\tau)$ and $h^*(\tau)$ accordingly. That is, we scale the intercepts so that their sums across all maturities τ, $H \equiv \int_0^{\tau^{max}} h(\tau)d\tau = 927$ billion euros and $H^* \equiv \int_0^{\tau^{max}} h^*(\tau)d\tau = 820$ billion euros, equal 44.2% of Italy's and Germany's sovereign debt net of Eurosystem holdings in this period.

The impact of preferred-habitat investors also depends on how their demand is distributed across maturities. Lacking independent evidence on the distribution of preferred-habitat demand, we assume that each component of the demand functions $Z_t(\tau)$ and $Z^*_t(\tau)$ is proportional to $g(\tau)$. This assumption is not an unreasonable bench-

[43] To adequately capture expectations of future deficits and net bond supply in the early, pre-PEPP weeks of the pandemic crisis, we average across fiscal forecasts in the December, 2019 and June, 2020, ECB/Eurosystem projections. The June projections included an updated and quite pessimistic estimate of the impact of the pandemic, but were based partly on information that was not available to investors in mid-March. Thus, the average of the December and June fiscal projections provides a reasonable proxy of investors' expectations immediately ahead of the PEPP announcement.

[44] Fig. 8, in Sec. 5.4 below, illustrates how the anticipated paths of debt and other fiscal variables change with the pandemic outbreak and the PEPP announcement, and how these changes transmit to the default probability and yields.

[45] Eser et al. (2023) classify insurance companies and pension funds (ICPFs) and the Eurosystem central banks as preferred habitat investors.

mark, since governments have an incentive to issue more of any given class of debt, relative to others, if there is more demand for that class of debt. Thus, for $\tau \leq \tau^{max}$, we set the intercepts to $h^*(\tau) = H^* g(\tau)$ and $h(\tau) = Hg(\tau)$, with zero demand for higher maturities. Analogously, we scale $\varsigma^*(\tau)$, $\varsigma(\tau)$, $\alpha^*(\tau)$, and $\alpha(\tau)$ in proportion to $g(\tau)$ as well (see Sec. 4.4 below). Under these assumptions, we can use the market clearing equations (7) to calculate the amounts that must be held by arbitrageurs at all times, for each country and maturity.

4.3 Constructing a distance criterion

The model's remaining parameters are not directly observable. Therefore, we jointly calibrate them by minimizing a distance criterion that measures model fit. Our distance criterion assesses fit along two dimensions: (i) first and second moments of yields over the long run; and (ii) yield curve shifts in response to the PEPP announcement.

Long-run moments. For the first component of the distance criterion, we compare our full sample of yields (1999-2022) to the long-run distribution of yields in the model, when fiscal pressure is at its long-run value. Constant fiscal pressure implies that the default rate is also constant, $\psi_t = \underline{\psi}$, where $\underline{\psi}$ is a parameter to be included in the calibration. Using the analytical solution of the model's ergodic distribution, we calculate the sum of squared deviations between the model and the data for selected first and second moments:

- Mean yields on 1m, 1Y, 5Y, and 10Y DE bonds, and 1Y, 5Y, and 10Y IT bonds;
- The standard deviations of yields on 1m, 1Y, 5Y, and 10Y DE bonds, and 1Y, 5Y, and 10Y IT bonds;
- The correlations between 1Y and 10Y yields, for DE and IT bonds
- The cross-country correlation between 1Y yields, and the cross-country correlation between 10Y yields.

When calculating this sum of squared deviations, we express all yields and their standard deviations in annualized percentage points, and we express all correlations in percentage points. We abstract from 20-year bonds, and Italian 1-month bonds, since these are unavailable for the full sample; for German 1-month yields we use the spliced series of OIS and German rates described earlier.

Figure 3: Baseline PEPP purchase scenario

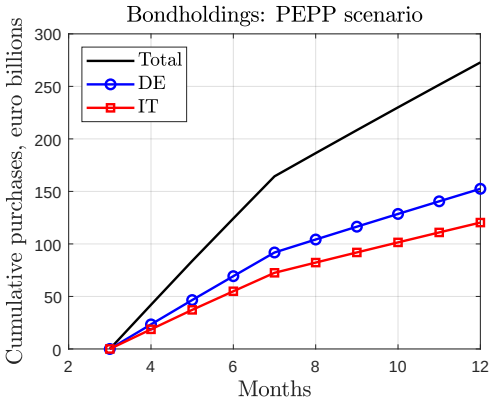

Note: Baseline model scenario for PEPP purchase expectations as of March 2020. Blue circles: DE; red squares: IT; black: aggregate face value. Effect on yields is shown in Figs. 6 and 7.

PEPP announcement. The second component of the distance criterion measures the model's fit to the shift in yield curves that was observed after the PEPP announcement, in the context of the time-varying fiscal conditions that were then foreseen. The PEPP was announced on March 18, 2020, with an initial purchase envelope of €750 bn.[46] Our calculations analyze the portion of this envelope that was dedicated to purchases of German and Italian sovereign bonds. The surprise nature of the announcement, in an emergency meeting of the ECB Governing Council, makes it easy to map this episode into our model.[47]

We model the impact of the PEPP announcement by comparing equilibrium yields, from March 2020 onwards, under the *pre-PEPP* and *post-PEPP* information sets described in Sec. 4.2. However, since the PEPP permitted a flexible path of purchases, in contrast to the earlier APP, we must also make some assumptions regarding arbitrageurs' expectations, in March 2020, about the eventual use of PEPP's margins of flexibility. Our scenario assumes that arbitrageurs anticipated PEPP purchases through

[46] The press release stated: "This new PEPP will have an overall envelope of €750 billion. Purchases will be conducted until the end of 2020 and will include all the asset categories eligible under the existing asset purchase programme (APP)." See https://www.ecb.europa.eu/press/pr/date/2020/html/ecb.pr200318_1~3949d6f266.en.html.

[47] We focus on the immediate effects of PEPP as it was originally announced in March, with an overall envelope of 750 billion euros to be spent over the course of 2020; these effects capture well the actual causal impact of the announcement, given its unexpected nature. Subsequent recalibrations of the PEPP purchase envelope (in June and December that year) were largely anticipated by the market, according to various surveys.

June 2020 with perfect foresight – implying some frontloading, and some excess purchases of Italian debt, compared with Italy's capital key.[48] We assume that from July to December, PEPP purchases were expected to accrue at a constant pace, up to the original PEPP envelope, while maintaining the deviations from capital key that were observed through June. Fig. 3 graphs total PEPP holdings, in the net purchases phase of 2020, under this scenario.[49] After the end of net purchases in December 2020, our scenario assumes that holdings decline naturally as the portfolio matures (not shown in the figure).

We compare the model-generated shift in yields when the *post-PEPP* scenario is substituted for the *pre-PEPP* scenario to the observed change in yields from 18 to 20 March, 2020, expressing all yields in annual percentage points. Then the final component of our distance criterion is the sum of squared deviations between the model and the data for the following statistics:

- The change in yields on 1m, 1Y, 5Y, 10Y, and 20Y DE and IT bonds from 18 to 20 March, 2020.

4.4 Minimizing the distance criterion

Functional forms. We now impose further functional form restrictions to reduce the number of free parameters we must estimate. First, we suppose that the distribution of the default cost, $\Phi(\chi)$, is uniform over an interval $[F_{min}, F^{max}]$ sufficiently wide to include all the fiscal scenarios we consider. Then, using equations (31)-(32), the default rate can be written as

$$\psi_t = \underline{\psi} + \theta \left(F_t - \underline{F} \right). \tag{36}$$

where $\theta \equiv \eta / \left(F^{max} - F_{min} \right)$ equals the arrival rate η of a rollover crisis times the density $1 / \left(F^{max} - F_{min} \right)$ of the uniform distribution Φ, and $\underline{\psi}$ is an intercept term associated with the long-run steady state fiscal pressure $\underline{F}$. Hence the default arrival rate has two parameters to estimate: its intercept, $\underline{\psi}$, and its slope, θ.

[48] In Online Appendix D, we show that this flexibility in the timing and allocation of purchases substantially enhanced the impact of the PEPP announcement.

[49] Note that our simulation scenarios treat the PEPP envelope as a limit on the total face value of purchases. In reality, it limited the total market value of purchases. Assuming a limit on the face value instead simplifies our calculations, since it allows us to avoid a fixed point loop in bond prices and therefore to obtain an affine solution for yields.

Second, we assume that the impact of preferred-habitat demand shocks across maturities τ is proportional both to $g(\tau)$, and to each country's long-run debt stock, setting $\varsigma^*(\tau) = \frac{H^*}{H^*+H} g(\tau)$ and $\varsigma(\tau) = \frac{H}{H^*+H} g(\tau)$. We assume the demand shocks have the same mean reversion coefficient κ_h in the two countries, but may differ in variance. We allow for correlation across the countries' bond demand shocks, but assume these are independent of the risk-free rate, defining the matrices K and Σ as follows:

$$K = \begin{bmatrix} \kappa & 0 & 0 \\ 0 & \kappa_h & 0 \\ 0 & 0 & \kappa_h \end{bmatrix}, \quad \Sigma = \begin{bmatrix} \sigma & 0 & 0 \\ 0 & \upsilon_h \sigma_h & \chi_h \upsilon_h \sigma_h \\ 0 & \chi_h \sigma_h & \sigma_h \end{bmatrix}.$$

Here σ_h scales the overall volatility of preferred-habitat demand, while υ_h scales the volatility of innovations to demand for Italian bonds relative to German bonds. The correlation between the Italian and German preferred-habitat demand innovations is controlled by $\chi_h \in [-1, 1]$.

Finally, regarding the slope of preferred-habitat demand with respect to yield, we assume that it is also proportional to $g(\tau)$ over $[\tau^{min}, \tau^{max}]$:

$$\tau\alpha(\tau) = \begin{cases} \alpha_h \varsigma(\tau), & \tau^{min} \leq \tau \leq \tau^{max}, \\ 0, & \tau > \tau^{max}, \end{cases} \tag{37}$$

where τ^{min} denotes one month, and τ^{max} is the maximum maturity of government debt, 20 years.[50] Likewise, for Core, we assume $\tau\alpha^*(\tau) = \alpha_h \varsigma^*(\tau)$ for $\tau^{min} \leq \tau \leq \tau^{max}$, and $\tau\alpha^*(\tau) = 0$ at higher maturities.[51]

Parameters. This specification leaves us with ten model parameters to estimate, by minimizing the distance criterion defined in the previous subsection. Clearly, our distance metric overidentifies the ten parameters, as the number of moments (28) is much larger. The estimated parameter values are displayed in Table 1.[52] The esti-

[50] For values of τ less than one month, we define $\alpha(\tau) \equiv \alpha_h / \tau^{min}$. This is irrelevant for our numerical results, since we perform no simulations with a time step finer than one month. For our analytical framework, it ensures that all integrals are bounded.

[51] Vayanos and Vila (2021) instead consider a specification where the slope with respect to yield is hump-shaped as a function of maturity: $\tau\alpha(\tau) = \tau\alpha \exp(-\delta_\alpha \tau)$, where α and δ_α are constants. Imposing this hump shape does not improve our model's fit to the data.

[52] Table 1 states the parameters in annualized terms. Table 6 in Online App. C.3 reports the parameters in the actual numerical model, which is programmed with a monthly time unit, but is

Table 1: Estimated parameters

Parameters	**Values**
γ: Risk aversion	0.0108
$\underline{\psi}$: Default rate intercept	86.2 bp
θ: Slope of default rate	2.05 bp / billion eur
$\hat{r}+\phi$: Discount rate in fiscal pressure	30.7%
κ_h: Mean reversion of PH shocks	0.00535
σ_h: Volatility of PH demand innovations	499 billion eur
υ_h: Relative volatility of IT PH demand	0.300
χ_h: Demand correlation parameter	-0.558
α_h: Slope parameter of PH demand	80.0 billion eur / p.p.
ζ: Remittance rule coefficient	1

mated value of risk aversion γ is 0.0108. The long-run default rate is 86.2 bp *per annum*. The slope of the default rate θ is 2.05 bp per billion euros of additional fiscal pressure compared to the steady state. The effective discount rate in the fiscal pressure integral equals 30.7% in annual terms.[53] The scale parameter on annual innovations to preferred-habitat (PH) demand is $\sigma_h = 499$ billion eur, with autoregressive coefficient $\kappa_h = 0.00535$ annually. Hence the standard deviation of annual innovations to PH demand for German bonds is $\sqrt{(1+\chi_h^2)}\sigma_h = 572$ billion eur implying that demand for German bonds is extremely volatile and persistent, almost Brownian motion. PH demand innovations are strongly negatively correlated between IT and DE, with parameter $\chi_h = -0.558$, implying a correlation coefficient of $\frac{2\chi_h}{1+\chi_h^2} = -0.84$, and the scale of fluctuations in Italian bond demand is only 30% of those in German demand, so the standard deviation of innovations to Italian PH demand is $\upsilon_h\sqrt{(1+\chi_h^2)}\sigma_h = 172$ billion eur. Since these fluctuations in Italian PH demand partially offset the shocks to German PH demand, they reduce the variance of the risk price λ_t, and thereby reduce the term premium. Since $\int(\varsigma(\tau)+\varsigma^*(\tau))d\tau = 1$ by construction, an interpretation of the PH demand coefficient α_h is that a 1pp across-the-board increase in yields causes an 80 billion euro rise in aggregate PH demand for IT and DE bonds. Finally, the remittance coefficient $\zeta \in [0,1]$ is estimated to be one, i.e., the distance minimization routine hits

quantitatively equivalent.

[53] This discount rate implies that our fiscal pressure measure (32) looks basically at a horizon of three to four years. This is plausible in our context, as it broadly coincides with the political cycle. Relatively high discount rates are not uncommon in the sovereign default literature; see for example Arellano (2008).

a corner solution at the upper bound we imposed on this parameter. Therefore, viewed through the lens of our model, Peripheral yield data suggest that markets expect rather generous dividend policies if a rollover crisis arrives.

5 Quantitative results

5.1 Long-run moments

Our estimated model achieves a good fit to many long-run patterns in the data, as Fig. 4 shows. The figure compares the model's ergodic distribution to sample first and second moments over our full sample period, 1999-2022.[54] The fit to the sample average yield curves is remarkably good for both countries. Furthermore, the standard deviation of yields in these long-run data is almost flat, independently of maturity. The calibrated model reproduces the volatility of short rates by construction, but also displays volatilities at long horizons that are similar to those at the short end, and are higher for German yields than Italian yields, as in the data.

Identifying risk aversion. The upper row of the figure also illustrates our yield decomposition. The upper left panel decomposes mean German yields $\mathbb{E}y_t^*(\tau)$ into the expectations component $\mathbb{E}y_t^{EX*}(\tau)$ and the term premium $\mathbb{E}y_t^{TP*}(\tau)$. Under the assumed short-term rate process, the ergodic mean of the expectations component is constant across maturities at the level $\mathbb{E}y_t^{EX*}(\tau) = \bar{r}$. The German term premium is simply the yield minus the expectations term, in this case $\mathbb{E}y_t^*(\tau) - \bar{r} = \mathbb{E}y_t^{TP*}(\tau)$. The model slightly overpredicts the long-run average of the ten-year German term premium, which is 1.25% in the sample, versus 1.42% in the simulation. Table 2 reports quantitative details of the yield decomposition – and Sharpe ratios, which are closely related – for ten-year bonds. Note that the long-run term premium can be written as

$$\mathbb{E}y_t^{TP*}(\tau) = \frac{1}{\tau}\int_0^\tau \left[A^*(s)^\top \mathbb{E}\lambda_t - \frac{1}{2}A^*(s)^\top \Sigma\Sigma^\top A^*(s)\right] ds, \tag{38}$$

where

$$\lambda_t = \gamma\Sigma\Sigma^\top \int_0^{\tau^{max}} \left(X_t\left(\tau\right) A(\tau) + X_t^*\left(\tau\right) A^*(\tau)\right) d\tau. \tag{39}$$

[54] The stars in Fig. 4 indicate the maturities that are included in the distance criterion to assess levels and standard deviations of yields.

Figure 4: German and Italian yields: long-run behavior

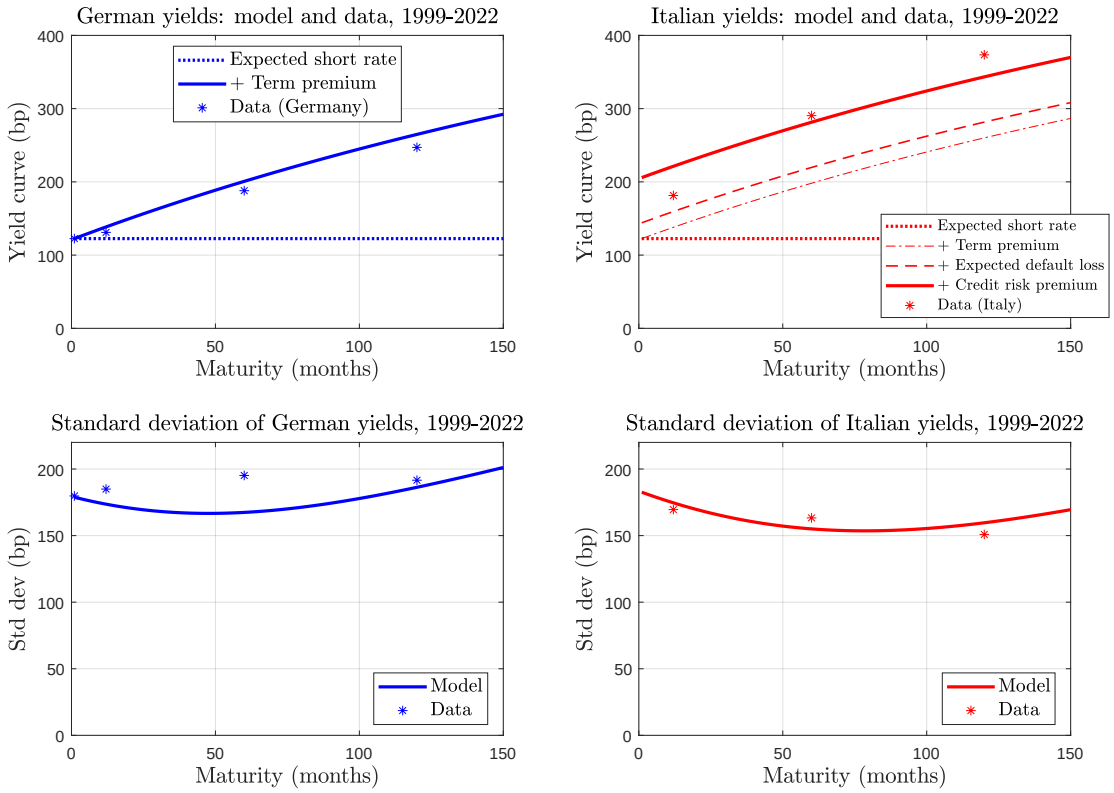

Data source: German and Italian yields (annualized, basis points) on zero-coupon 1m, 1Y, 5Y, and 10Y sovereign bonds from Datastream. German 1m yield is spliced to 1m OIS yield prior to 2011; Italian 1m yield unavailable.
Top row. *Stars*: average German (left) and Italian (right) sovereign yields, 1999-2022.
Lines: Decomposition of model-generated mean yields (solid), under the ergodic distribution, into expectations component (dotted) plus term premium (dash-dotted), plus expected default loss (dashed), plus credit risk premium.
Bottom row. *Stars*: standard deviations of German and Italian yields, 1999-2022.
Lines: model standard deviations of yields, under the ergodic distribution.

This says that the risk-price vector λ_t equals risk aversion γ times the variance matrix of the factor innovations, $\Sigma\Sigma^\top$, times arbitrageurs' portfolio weighted by the bond price factor loadings $A(\tau)$ and $A^*(\tau)$. Therefore, the term premium at a given maturity τ is an increasing function of γ.[55]

But γ cannot be inferred from the German term premium alone, which also depends on the variance of preferred habitat demand. Concretely, since the risk-free rate is in-

[55] While (38)-(39) may make the term premium appear linear in γ, this is not the case, because γ also enters the ODEs (73) and (75) that determine $A(\tau)$ and $A^*(\tau)$, introducing nonlinearities.

Table 2: Decomposing 10-year yields, spreads, and Sharpe ratios

	DE 10Y yield		IT-DE 10Y spread	
	variable	*value*	*variable*	*value*
Yield/Spread: data†	-	2.47%	-	1.26%
Yield/Spread: model†	$\mathbb{E}y_t^*$	2.65%	$\mathbb{E}y_t - \mathbb{E}y_t^*$	0.79%
Expected rates /default loss†	$\mathbb{E}y_t^{EX*} = \bar{r}$	1.23%	$\mathbb{E}y_t^{DL} = \delta\underline{\psi}$	0.22%
Term / credit premium†	$\mathbb{E}y_t^{TP*}$	1.42%	$\mathbb{E}y_t^{CR} = \mathbb{E}\underline{\xi}_t$	0.62%
Sharpe ratio: data 1999-2022	-	0.51	-	0.23
Sharpe ratio: model	$\mathbb{S}_t^*(\tau)$	0.57	$\mathbb{S}_t^{\Delta}(\tau)$	0.27
Numerator†	$A^{*\top}\mathbb{E}\lambda_t$	2.70%	$\mathbb{E}\xi_t$	0.62%
Denominator†	$\sqrt{A^{*\top}\Sigma\Sigma^\top A^*}$	4.72%	$\delta\sqrt{\underline{\psi}}$	2.32%

Note. The table reports the instantaneous Sharpe ratios $\mathbb{S}_t^*(\tau)$ and $\mathbb{S}_t^{\Delta}(\tau)$, interpreting the time unit as one year, for $\tau = 10$ years, and related yield components. Quantities with a dagger (†) are stated in annualized percentage points. Model notation is used to clarify the quantities shown, but the function argument (τ) is omitted for brevity.

dependent of the preferred habitat factors, λ_t can be broken into two pieces: a term $\gamma\sigma^2 \int_0^{\tau^{max}} \left(X_t(\tau) A^r(\tau) + X_t^*(\tau) A^{r,*}(\tau)\right) d\tau$ related to the short rate process, which is observed, and a term $\gamma\Sigma_h\Sigma_h^\top \int_0^{\tau^{max}} \left(X_t(\tau) A^h(\tau) + X_t^*(\tau) A^{h,*}(\tau)\right) d\tau$ related to the preferred habitat process, which must be estimated.[56] Either higher risk aversion or a more volatile preferred habitat process will increase the term premium, so to distinguish between the two we include the second moments of yields in our estimation criterion. At the short end, both the level and variability of German yields are tied down exactly by the short-rate process, since the model has the property that $\lim_{\tau\to 0} y_t^*(\tau) = r_t$. For longer bonds, matching the standard deviations of one-, five-, and ten-year German and Italian yields provides sufficient targets to identify the five free parameters (σ_h, κ_h, υ_h, χ_h, and α_h) of the preferred habitat demand block (the good fit is seen in the bottom row of Fig. 4).[57] In summary, jointly matching these second moments and the German term premia on longer bonds overidentifies both arbitrageurs' risk aversion and preferred habitat demand.

Identifying the long-run default probability. Next, matching Italian yields (or the IT-DE spread) also depends on the probability of default. As Sec. 4.3 discussed, long-run moments are calculated under the assumption that both fiscal pressure and

[56] Here Σ_h refers to the 2×2 diagonal block of Σ that relates to the preferred habitat process.

[57] In practice, σ_h is the most important of these parameters, because Σ_h is proportional to σ_h, so the second component of λ_t scales quadratically in σ_h.

hence the default rate equal their long-run values, $F_t = \underline{F}$ and $\psi_t = \underline{\psi}$. Both of the yield components that compensate for possible Italian default, $y_t^{DL}(\tau)$ and $y_t^{CR}(\tau)$, are increasing in the default rate, so $\underline{\psi}$ is overidentified by including mean one-, five-, and ten-year Italian yields in the distance criterion. Overall, the fit is quite good, but with just one free parameter to match these three targets, we see (top, right panel of Fig. 4) that the model underpredicts 10-year yields and overpredicts one-year yields. As long as $\underline{\psi}$ is small, Prop. 2 implies that the German and Italian term premia are approximately equal, as we can verify by comparing the top two panels of Fig. 4. Thus, fitting Italian yields is essentially the same problem as fitting IT-DE spreads, which are likewise underpredicted at the ten-year horizon but overpredicted for one-year bonds (see Fig. 5).

Importance of the credit risk premium. Having identified risk aversion and the long-run default rate, we can now break down the IT-DE spread into its components, as shown in Fig. 4 and Table 2. The long-run expected default loss is $\mathbb{E}y_t^{DL}(\tau) = \delta\underline{\psi} = 0.22\%$ for all τ (the distance between the dash-dot and dashed lines in the top, right panel of Fig. 4), based on an estimated long-run default probability of $\underline{\psi} = 0.86\%$ *per annum* and our calibrated haircut ($\delta = 0.25$). The long-run sovereign credit risk premium is $\mathbb{E}y_t^{CR}(\tau) = \mathbb{E}\xi_t = \gamma\underline{\psi}\delta^2 \int_0^{\tau^{max}} \mathbb{E}X_t(s)\,ds = 0.62\%$ (the distance between the dashed and solid lines). This formula is analogous to (39): it says that the credit risk premium equals risk aversion γ times the variance of the default loss, $\underline{\psi}\delta^2$, times arbitrageurs' holdings of Italian debt, $\int_0^{\tau^{max}} \mathbb{E}X_t(s)\,ds = 1058$ billion euros. Taking account of a five-basis point difference in the term premia on German and Italian bonds, we obtain an overall sovereign spread of 0.79% on ten-year IT bonds, as Table 2 shows. More than 3/4 of this spread is accounted for by the credit risk premium.

To better understand the size of the credit risk premium relative to the expected default loss, notice that their ratio is $\mathbb{E}y_t^{CR}(\tau)/\mathbb{E}y_t^{DL}(\tau) = \delta\gamma \int_0^{\tau^{max}} \mathbb{E}X_t(s)\,ds$. Interestingly, the finding that the credit risk premium greatly exceeds the expected default loss does not actually depend on the default rate $\underline{\psi}$, as both components are proportional to $\underline{\psi}$. On one hand, it depends on whether risk aversion γ is high in the context of the amount of defaultable debt that arbitrageurs must hold, $\int_0^{\tau^{max}} \mathbb{E}X_t(s)\,ds$. As we have already made clear, our risk aversion estimate is tied down independently by matching German term premia. On the other hand, a lower haircut δ would make default less risky, reducing the credit risk premium more than the expected default loss. But our calibration of δ is already conservatively low, considering international evidence.

Since risk aversion is inferred from term premia, it is also instructive to compare the credit risk premium to the term premium. Assuming that the default rate $\underline{\psi}$ is low, and using a first-order approximation at $\tau = 0$, we have[58]

$$\frac{\mathbb{E}y_t^{CR}(\tau)}{\mathbb{E}y_t^{TP*}(\tau)} \approx \frac{2\underline{\psi}\delta^2\mathbb{E}\int_0^{\tau^{max}} X_t(s)ds}{A(\tau)^\top\Sigma\Sigma^\top\mathbb{E}\int_0^{\tau^{max}}\left(X_t(s)+X_t^*(s)\right)A(s)ds}. \tag{40}$$

This formula points to two key ratios that link the inferred credit risk premium $\mathbb{E}y_t^{CR}(\tau)$ to the observed term premium $\mathbb{E}y_t^{TP*}(\tau)$: (i) the ratio of Poisson jump risk to diffusion risk, $\underline{\psi}\delta^2/A(\tau)^\top\Sigma\Sigma^\top A(\tau)$, and (ii) the ratio of arbitrageurs' defaultable to total bond-holdings, $\mathbb{E}\int_0^{\tau^{max}} X_t(s)ds \,/\, \mathbb{E}\int_0^{\tau^{max}}\left(X_t(s)+X_t^*(s)\right)ds$. While formula (40) cannot be explicitly factored into these two ratios (since they are convoluted together in the denominator), it helps explain why we conclude that $\mathbb{E}y_t^{CR}(\tau)$ is large. First, our model implies a larger credit risk premium when default risk is higher, compared with the riskiness of the return to a non-defaulted bond. Second, it implies a larger credit risk premium when defaultable bonds form a larger part of arbitrageurs' portfolio.

Sharpe ratios. Table 2 also documents the goodness of model fit by reporting Sharpe ratios on ten-year German bonds and on default risk for ten-year Italian bonds (see Online App. C.3.5 for details on computing these ratios in the data and in the model). The lower-left panel of the table reports the ten-year German Sharpe ratio in the ergodic distribution of our model (0.57) and in the data (0.51).[59] This Sharpe ratio can be computed as $\mathbb{S}_t^*(\tau) \equiv \frac{A^*(\tau)^\top\mathbb{E}\lambda_t}{\sqrt{A^*(\tau)^\top\Sigma\Sigma^\top A^*(\tau)}}$. While this ratio is not a targeted moment in our estimation routine, its numerator and denominator bear a close analytical relation to the term premium and to second moments. Concretely, the Sharpe numerator $A^*(\tau)^\top\mathbb{E}\lambda_t$ is the quantity that is averaged across maturities in the first term of the term premium formula (38). The Sharpe denominator is the standard deviation of innovations to the price of a bond with maturity τ. Hence the model's good fit to the term premium and to the standard deviation of yields helps explain why it achieves a good fit to this Sharpe ratio as well.

Next, Table 2 displays the Sharpe ratio of the Italian-German spread, given by

[58] To derive this formula, note that $A_t(0) = A_t^*(0) = \vec{0}$. Therefore, to a first-order approximation at $\tau = 0$, (18) implies $y_t^{TP*}(\tau) \approx \frac{1}{2}A_t^*(\tau)^\top\lambda_t$, as can be verified in Table 2. In a long-run situation with low $\underline{\psi}$, Prop. 2 applies, and therefore $\mathbb{E}\lambda_t \approx \gamma\Sigma\Sigma^\top\mathbb{E}\int_0^{\tau^{max}}\left(X_t(s)+X_t^*(s)\right)A(s)ds$.

[59] The Sharpe ratios reported in the table are scaled for consistency with a time unit of one year.

Figure 5: IT-DE spreads: long-run behavior

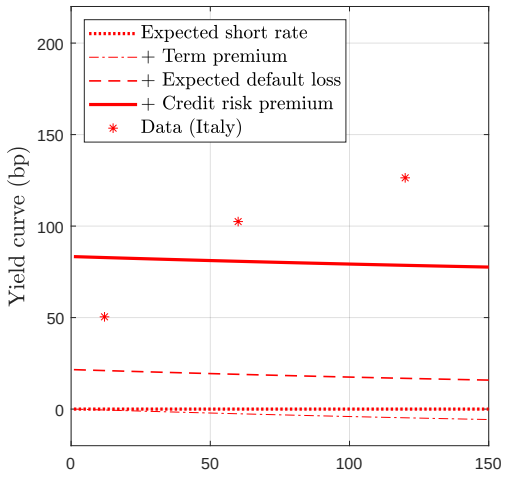

Data source: German and Italian yields (annualized, basis points) on zero-coupon 1Y, 5Y, and 10Y sovereign bonds from Datastream.
Stars: average Italian-German sovereign spreads, 1999-2022.
Lines: Decomposition of model-generated mean spreads (solid), under the ergodic distribution, into expectations component (dotted) plus term premium (dash-dotted), plus expected default loss (dashed), plus credit risk premium.

$\mathbb{S}_t^{\Delta}(\tau) \equiv \frac{\mathbb{E}\xi_t}{\delta\sqrt{\underline{\psi}}} = \gamma\delta\sqrt{\underline{\psi}}\mathbb{E}\int_0^{\tau^{max}} X_t(s)ds$. Again, this ratio is untargeted, so its good fit (0.27 in the model versus 0.23 in the data) provides additional support for our calibration of these parameters, related to the cost of bearing default risk. Note that the Sharpe numerator equals the credit risk premium, on average under the ergodic distribution: $\mathbb{E}y_t^{CR}(\tau) = \mathbb{E}\xi_t$. Therefore our conclusion that the credit risk premium is large is *not* driven by an unreasonably high Sharpe ratio for default risk – quite the contrary. The denominator of this Sharpe ratio is the standard deviation of the default loss per unit of bond holdings. The fact that default is a very costly event when it occurs (even though it occurs rarely) means that this denominator leads to a rather low Sharpe ratio, even though the numerator is quite large.

Term structure of the sovereign spread. While most aspects of Fig. 4 fit well, the IT-DE spread displays one key shortcoming of the model. By Prop. 3, the model implies that the long-run means $\mathbb{E}y_t^{DL}(\tau)$ and $\mathbb{E}y_t^{CR}(\tau)$ are both independent of maturity, but the sovereign spread increases with τ on average over the sample period. Fig. 5 zooms in on the spread to highlight this discrepancy, decomposing it into the four components of Prop. 1. A plausible explanation is that our analytical solution requires the default probability ψ_t to be a deterministic function of time, while in reality markets

Table 3: Variance decomposition of yields

	One-year yields		**Ten-year yields**	
	DE	IT	DE	IT
Standard deviation (data)	180	170	192	151
Standard deviation (model)	174	175	186	160
Short-rate contribution	99.3%	94.2%	46.4%	60.7%
PH demand contribution	0.7%	5.8%	53.6%	39.3%

Top two lines: long-run standard deviations of yields, in basis points at annualized rates, in the data (1999-2022) and in the model.
Bottom two lines: long-run variance decomposition of yields, showing contribution of risk-free rate shocks r_t and preferred-habitat demand shocks ε_t^h and ε_t^{h*}.

likely perceive ψ_t as a stochastic process. This could imply greater uncertainty about default in the distant future, making the credit risk premium increase with τ. Solving a model with a stochastic default probability is an interesting topic for future work, but we expect it will require a fully numerical solution.

Variance decomposition. Finally, Table 3 further dissects the model's behavior by presenting a variance decomposition for the ergodic distribution of yields. The first two rows report the standard deviations of the model and the data for one- and ten-year yields. As discussed above, the model matches the data well in this respect. In particular, it reproduces the lower volatility of long-term Italian yields, despite their defaultable nature. The model attributes this to the lower volatility of their PH demand shocks. The third and fourth rows of the table decompose the volatility into the contributions of the short rate and of PH demand. While short-term yields are basically driven by shocks to the short-term interest rate, long-term yields also fluctuate in response to PH demand shocks, especially in the case of Germany, where these shocks are estimated to be larger.

5.2 The PEPP announcement

The large long-run credit risk premium that we find on peripheral euro area bonds suggests that changes in net bond supply could be a powerful driver of yields. Thus, our model may have potential to explain the shifts in euro area yields associated with the anticipated fiscal response to the pandemic outbreak, and the subsequent PEPP announcement. In standard (no default) models of risk-averse arbitrage, these changes in net supply would steepen or flatten yields (respectively) *via* changes in term premia.

But here their impact is reinforced by several default-related channels. First, a reduction in the net supply of defaultable bonds $S_t(\tau)$ shrinks the credit risk premium $y_t^{CR}(\tau)$. This effect operates even if the default probability is exogenous. But with endogenous default, purchases also increase future redemptions of central bank-held Italian bonds, $f_{t+s}^{CB}(0)$, and hence reduce the default probability (both at t and at future times $t+s$). This lowers the expected default loss $y_t^{DL}(\tau)$ and also reinforces the fall in the credit risk premium.

Identifying the default probability function. The extent and time-profile of these effects in our model depends on how deficits and bond redemptions aggregate into fiscal pressure on the government, and how strongly this pressure affects its default probability. That is, they depend on several parameters related to default: the passthrough of revenue from bond redemptions, ζ, the government's discount rate in its repayment decision, $\hat{r}+\phi$, and the marginal impact of fiscal pressure on the default rate, θ. These parameters were not mentioned in Sec. 5.1, since the ergodic moments reported there assumed constant fiscal conditions, implying constant fiscal pressure and a constant default rate $\psi_t = \underline{\psi}$. These three parameters are identified by including in our estimation criterion the model's fit to the changes in German and Italian yields at the time of the PEPP announcement, at one-month and one-, five-, ten-, and twenty-year maturities.

Impacts on announcement. The results of our benchmark PEPP simulation are shown in Fig. 6, where stars in the top panels indicate the observed change in yields between March 18 (pre-announcement) and March 20, 2020 (post-announcement).[60] The blue stars in the top left panel show that the PEPP announcement had a small, non-monotonic impact on German yields, which rose for one-year bonds and fell at five- to twenty-year maturities. In contrast, Italian yields fell dramatically (top right panel, red stars), with a hump-shaped decline that had its largest impact, of 86 bp, on five-year bonds. Hence, across all maturities, the announcement was associated with a large decrease in average eurozone yields, and a sharp drop in the IT-DE spread.

This simulation is based on the parameter estimates in Table 1, and on the purchase scenario (*post-PEPP*) illustrated in Fig. 3. The overall scale of the shift in Italian yields is matched by construction, determining the elasticity θ, but the close fit to the shapes of the shifts of both countries' yields curves suggests that the model is consistent with

[60] We take the change from March 18 to 20 as our measure of the impact of the PEPP announcement, because yields were still volatile across Europe on the 19th, but settled down from the 20th onwards.

Figure 6: Effects of PEPP announcement: baseline scenario ($\zeta = 1$).

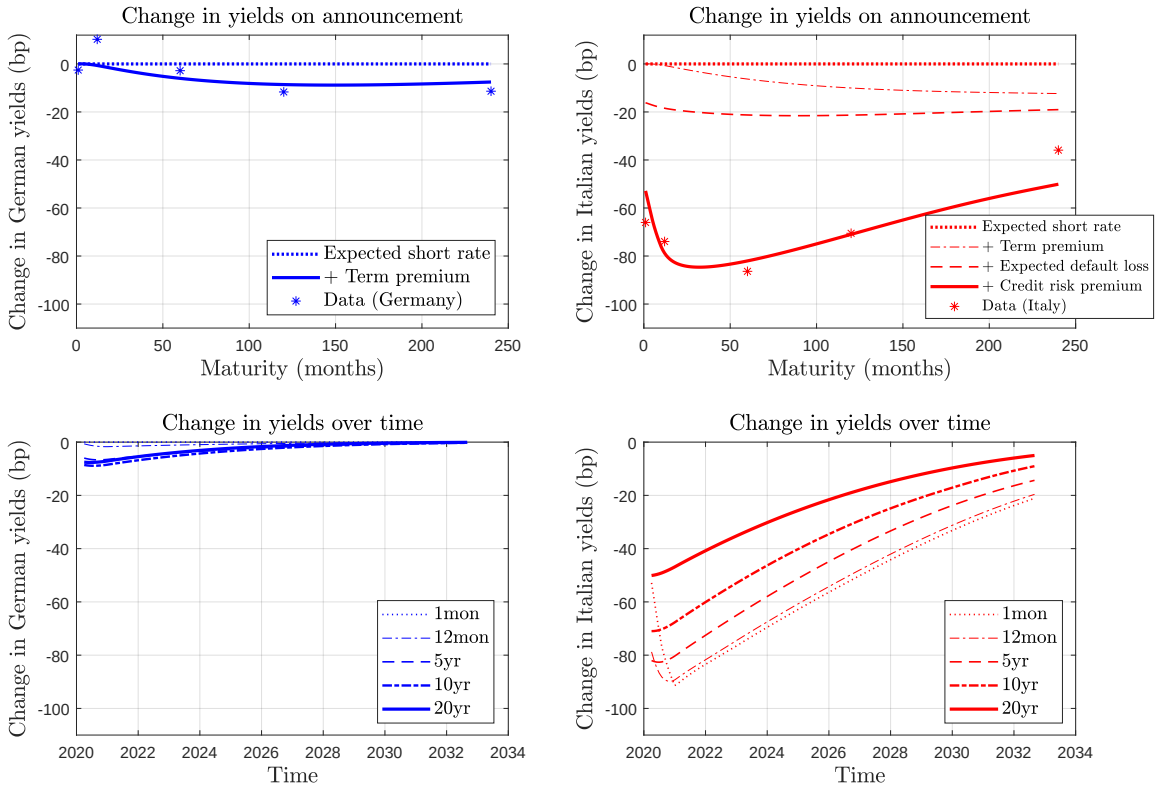

Data source: German and Italian yields (annualized, basis points) on zero-coupon 1m, 1Y, 5Y, 10Y, and 20Y sovereign bonds from Datastream.
Top row. *Stars*: Shift in German (left) and Italian (right) yields, 18 to 20 March, 2020.
Lines: Model-generated shift in yields upon PEPP announcement (solid), decomposed into expectations component (dotted) plus term premium (dash-dotted), plus expected default loss (dashed), plus credit risk premium.
Bottom row. Model-generated impulse response of 1m, 1Y, 5Y, 10Y and 20Y yields in response to PEPP announcement.

the underlying mechanisms at work. The estimated model allows us to decompose the mechanisms behind these shifts. The model predicts a small decline in the German term premium in response to the PEPP announcement, of roughly 10 bp for ten-year bonds and 11 bp for 20-year bonds.[61] Consistently with Prop. 2, the inferred effect on the Italian term premium is similar. However, the Italian sovereign spread declines sharply (e.g., by 62 bp at a ten-year horizon), first of all because the increased absorption of

[61] Since the model treats the riskless short rate as an exogenous factor, changing the path of purchases has no impact on the expectations component $y_t^{EX}(\tau)$.

credit risk makes the market more willing to hold part of this risk. Moreover, the PEPP announcement reduces the default probability substantially, as the expected default loss component reveals, with a maximum impact of 17 bp on Italian bonds of two years' maturity or less. The reduction in the default probability in turn reinforces the compression in credit risk premia. Thus, the model suggests that the extraction of defaultable bonds from the market, together with the resulting reduction in their default risk, jointly caused a large decrease in the credit risk premium $y_t^{CR}(\tau)$. At a ten-year horizon, the 50 bp decline in $y_t^{CR}(\tau)$ accounts for 81% of the model-predicted decline in the sovereign spread.

Italian yields decline at the time of the announcement across all maturities, but the reduction is strongest for bonds of intermediate duration, which will be maturing when cumulative net purchases are still large. In contrast, one-month bonds mature before many purchases have taken place. Thus, the large shift in one-month yields might seem surprising, but it reflects the forward-looking nature of the default decision: anticipated purchases lower expected fiscal pressure over many future periods, reducing the government's default incentives immediately. This is reflected even at the shortest end of the yield curve. At the opposite extreme, for 20-year bonds, most net redemptions will have occurred, and hence yields will be normalized again, by the time the bonds mature. Hence forward-looking behavior reduces the shift in longer yields: the anticipated future return to normality limits the change in the longest yields on impact.

Persistent effects of PEPP. Beyond its powerful effect at announcement, the model also predicts that PEPP's impact should persist over time. The bottom panels of Fig. 6 illustrate the impulse responses of yields to the announcement, for selected maturities, assuming that the purchase program unfolds as expected under our baseline scenario. The small decrease in German yields (left panel) mostly affects long bonds, and decays smoothly. The much larger reduction in Italian yields (right panel) is very persistent, but differs across durations. The shortest yields fall steadily over the course of 2020, because the quantity of short bonds held increases over that period, accumulating new purchases with bonds purchased earlier at slightly greater maturity. The maximal impact on short yields, of over 90 basis points, occurs just as gross purchases cease. From this time onwards, the whole portfolio gradually matures, causing the declines in 20- and 10-year yields to fade away smoothly over time. The decrease in 20-year yields from 2021 onwards (i.e., after the end of the net purchase phase envisioned in the March 2020 announcement) is due only to arbitrage across durations, not

Figure 7: Effects of PEPP announcement: low-remittances scenario ($\zeta = 0$).

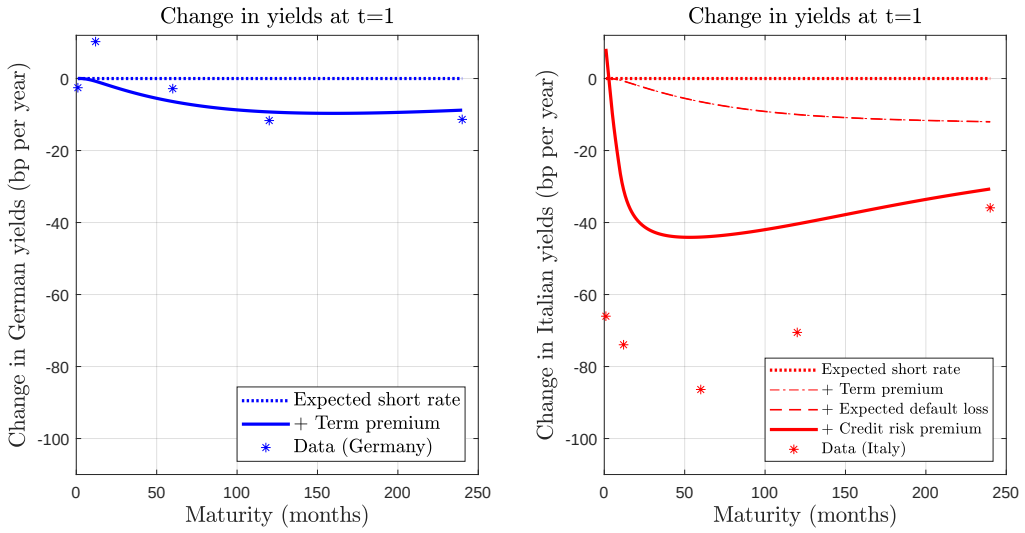

Data source: German and Italian yields (annualized, basis points) on zero-coupon 1m, 1Y, 5Y, 10Y, and 20Y sovereign bonds from Datastream.
Stars: Shift in German (left) and Italian (right) yields, 18 to 20 March, 2020.
Lines: Model-generated shift in yields upon PEPP announcement (solid), decomposed into expectations component (dotted) plus term premium (dash-dotted), plus expected default loss (dashed), plus credit risk premium.

because the program still holds any bonds with a 20-year residual maturity. As the average maturity of the PEPP portfolio shortens, its impact on long yields fades away, followed by its impact on short yields. The final effects of the program disappear as the last bonds mature, 240 months after the end of gross purchases.

The low-remittances scenario. Our baseline calibration includes an estimated coefficient $\zeta = 1$ in the remittance rule (30). While the yield data strongly favor that parameterization, it is instructive to consider alternative values of ζ, which governs the impact of asset purchases on the Peripheral default probability. For clarity we consider the simple, polar-opposite case $\zeta = 0$, representing a scenario in which the central bank would *not* provide any income support during a rollover crisis (over and above net transfers in the amount $-\bar{\Gamma}$). This case is also interesting since it shuts down any impact of asset purchases on default risk, thereby quantifying the importance of the endogenous default channel in our benchmark results.

Fig. 7 displays the results in this case. The fit to the Italian yield curve movement worsens relative to the baseline calibration, as the expected default loss does not change

and the impact on the credit risk premium is reduced. Nonetheless, the overall response is still large, and qualitatively similar to the benchmark specification, except at the very shortest end. The near-zero impact of the announcement at the short end helps explain why our estimation strongly rejects the $\zeta = 0$ specification (or any low ζ). As it seems unlikely that central banks would fail to provide any income support to their treasuries during a rollover crisis, we can view this scenario as a lower bound on the impact of large-scale asset purchases in the euro area. It shows that credit risk extraction remains a relevant driver of yields on defaultable bonds even if purchases have no effect on the default probability itself.

5.3 Robustness

Our results indicate that the overall compensation for peripheral default risk in the euro area context is driven primarily by a credit risk premium which is substantially larger than the expected loss due to default, and also reacts more to Eurosystem asset purchases. Table 4 explores the robustness of this conclusion to alternative parameterizations. The third column reports the credit risk premium as a fraction of the total compensation for default risk, $\mathbb{E}y_t^{CR}(\tau) / \mathbb{E}\left(y_t^{CR}(\tau) + y_t^{DL}(\tau)\right)$, for bonds of maturity τ equal to 10 years, under the ergodic distribution. The fourth column reports the contribution of the credit risk premium to the *change* in the compensation for default risk induced by the announcement of PEPP, $\Delta y_t^{CR}(\tau) / \left(\Delta y_t^{CR}(\tau) + \Delta y_t^{DL}(\tau)\right)$, in our model's time-varying solution conditional on the fiscal conditions of March 2020.

The main message from the table is that our key result is remarkably robust. Under most parameterizations considered, the credit risk premium accounts for roughly three-quarters of the total compensation for default risk, in levels, in the model's ergodic distribution. The credit risk premium is even more important for the effects of the PEPP announcement, with a contribution over 80% in those same parameterizations. Note also that if PEPP has no endogenous impact on the default probability (the $\zeta = 0$ case), then the contribution of the credit risk premium is 100%, by construction.

The table also identifies extreme calibrations for which our main result disappears, in the sense that the contribution of the credit risk premium decreases relative to that of the expected default loss until the two are roughly balanced. Reducing the risk aversion coefficient γ to 1/3 of its baseline value implies a balanced (50%) contribution of the credit risk premium in the long run, and reducing it to 1/6 of its baseline cali-

Table 4: Robustness

Calibration	Model fit[a]	Credit risk prem. contribution[b]		Mean yields[c]		Standard deviation[c]		Sharpe ratio		PEPP impact[c]
		Long-run	PEPP	DE	IT	DE	IT	DE	IT-DE	IT
Data	-	-	-	247	373	192	151	0.51	0.23	-71
Benchmark*	0.548	0.74	0.81	265	343	186	160	0.57	0.27	-71
Parameters calibrated directly from observables										
$\kappa \times 1.25$	1.063	0.74	0.81	252	331	164	137	0.54	0.27	-70
$\sigma \times 1.25$	3.306	0.74	0.81	336	411	256	222	0.69	0.26	-73
$\delta = 0.1$	2.854	0.54	0.68	268	286	184	179	0.59	0.11	-24
$\delta = 0.05$	3.817	0.37	0.52	268	275	184	183	0.59	0.054	-16
Parameters estimated by minimizing the distance criterion										
$\gamma \times 1.25$	1.201	0.78	0.84	299	389	213	173	0.70	0.33	-83
$\gamma \div 3$	5.448	0.50	0.63	170	213	139	135	0.20	0.092	-35
$\gamma \div 6$	8.356	0.33	0.47	145	177	134	133	0.10	0.046	-23
$\underline{\psi} \times 1.25$	0.663	0.74	0.82	264	362	187	156	0.57	0.30	-71
$\overline{\theta} \times 1.25$	0.633	0.74	0.81	265	343	186	160	0.57	0.27	-84
$(\hat{r} + \phi) \times 1.25$	0.593	0.74	0.82	265	343	186	160	0.57	0.27	-62
$\sigma_h \times 1.25$	0.724	0.74	0.81	268	345	217	178	0.58	0.27	-73
$\upsilon_h \times 1.5$	0.651	0.74	0.81	263	343	172	154	0.57	0.27	-77
$\kappa_h \times 1.5$	0.603	0.74	0.81	265	343	168	148	0.57	0.27	-71
$\chi_h \times 1.5$	0.576	0.74	0.81	265	342	192	149	0.57	0.27	-72
$\alpha_h \times 1.5$	0.653	0.73	0.80	253	328	180	152	0.53	0.25	-64
$\zeta = 0$	1.516	0.74	1.00	265	343	186	160	0.57	0.27	-40

Notes. *The benchmark calibration is described in Table 1. The following rows each describe the effect of changing one parameter by the stated amount, relative to its benchmark value.
[a]"Model fit" refers to the sum of squared deviations of the statistics, expressed in percentage points, listed in the bullet points in Sec. 4.3.
[b]"Credit risk contribution" means the credit risk premium as a fraction of the total compensation for default risk at 10-year maturity, either in the long run or (in differences) in the effects of the PEPP announcement.
[c]Annual yields on 10-year bonds, expressed in basis points.

bration implies that the two components of default risk compensation respond roughly equally to the PEPP announcement. Intuitively, it takes an extremely low degree of risk aversion to make the credit risk premium as small as the expected default loss.

Likewise, haircuts δ as low as 0.1 and 0.05 reduce the contribution of the credit risk premium to slightly more than one-half in the long run, and in the impact of the PEPP announcement, respectively. This reflects the fact that, as shown in Sec. 2, expected default losses and credit risk premia are proportional to δ and δ^2, respectively,

so reducing the haircut lowers the latter more quickly than it does the former.

However, these low-risk-aversion and low-haircut calibrations are empirically implausible, notably worsening model fit (see the second column of the table). By shrinking the credit risk premium, low γ and low δ both decrease the level of Italian yields and their responsiveness to PEPP; in addition, low γ shrinks the term premium, reducing the slope of the yield curve. Hence, in the fifth and sixth columns of the table, we see that the low-γ and low-δ calibrations imply much lower average yields than in the data, especially on Italian bonds (from 177 to 286 bp, vs 373 bp in the data, at a ten-year horizon). They also predict a far smaller reaction of Italian 10-year yields to the PEPP announcement (from 16 to 35 bp) than the observed one (71 bp –see last column). In sum, while some parameter configurations can make the credit risk premium less relevant, such calibrations considerably worsen the model's ability to explain the level, slope, and responsiveness of yields, both over the full sample and in the PEPP episode.

5.4 Understanding the effects of net bond supply

Next, we look in more detail at how policies that shift net bond demand transmit to the default probability and yields. It is helpful here to delve deeper by comparing the effects of the PEPP announcement to those of the pandemic outbreak. The transmission of the two shocks is similar but not identical, since a change in deficits affects fiscal pressure directly, while a change in purchases affects fiscal pressure only through remittances of central bank profits.

Transmission channels of fiscal pressure. Fig. 8 illustrates how the fiscal conditions associated with the pandemic, and the purchases announced under the PEPP, feed through to fiscal pressure and the default rate and hence to yields. The impact of the pandemic outbreak – that is, the change in model quantities when the *pre-pandemic* forecasts are replaced by the *post-pandemic, pre-PEPP* forecasts – is shown by the green dashed lines. The solid black line shows the joint impact of the pandemic and the PEPP announcement, meaning the change in model quantities when the *pre-pandemic* forecasts are replaced by the *post-PEPP* forecasts. The first two panels show the changes in the net supply of IT sovereign debt (gross supply minus purchases) and in the fiscal deficit d_t. These are simply differences in model inputs between the *pre-pandemic*, *pre-PEPP*, and *post-PEPP* forecasts. The third panel shows the monthly bond redemptions $f_t(0)$ implied by the maturation of the simulated portfolio, net of

Figure 8: Changes in fiscal variables and default rate following pandemic and PEPP

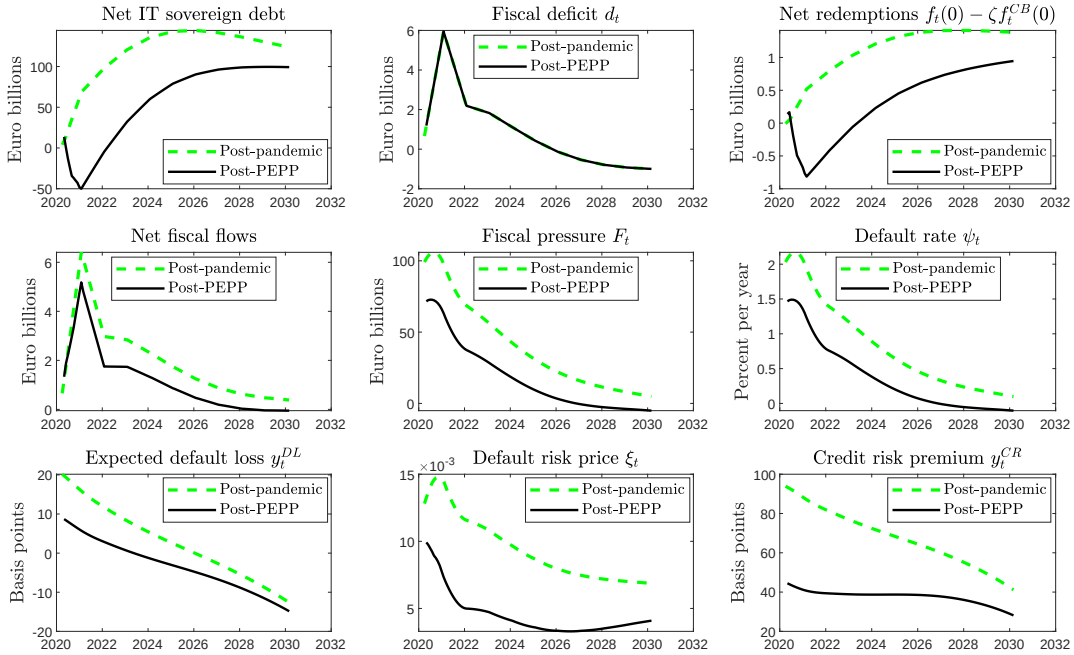

Green dashed lines: Changes in anticipated monthly paths of Italian fiscal variables and default probability in response to pandemic outbreak. *Black solid lines*: changes in anticipated monthly paths due to cumulative effect of pandemic and PEPP announcement.
Top row: Changes in (i) sovereign debt, net of Eurosystem purchases; (ii) monthly fiscal deficits d_t; (iii) monthly bond redemptions, net of remittances from the Eurosystem to the government.
Middle row: Changes in (i) net fiscal flows; (ii) fiscal pressure F_t; (iii) Annual default rate ψ_t.
Bottom row: Changes in (i) 10-year expected default loss $y_t^{DL}(\tau)$; (ii) default risk price ξ_t; (iii) 10-year credit risk premium $y_t^{CR}(\tau)$.

the remittances $\zeta f_t^{CB}(0)$ to be paid conditional on a rollover crisis arriving. For this variable, the green dashed line shows increased payments by the government to redeem the pandemic-related debt, while the black line shows that in the first few years after the PEPP announcement (roughly 2020-2023), increased central bank remittances outweigh the costs of increased debt redemptions.

The second row of Fig. 8 shows the change in the net monthly fiscal flows $d_t + f_t(0) - \zeta f_t^{CB}(0)$, and the changes in fiscal pressure F_t and the default probability ψ_t. Note that since fiscal pressure is a forward-looking integral of net fiscal flows, it jumps up immediately when the pandemic arrives, and then shifts partway down again when PEPP is announced. Since the default probability is linearly related to fiscal pressure, the shifts in ψ_t are proportional to those in F_t. The lower-left panel shows the changes

Table 5: Model-implied Sharpe ratios, conditional on events of Feb.-Mar. 2020

	DE 10Y yield	**IT-DE 10Y spread**
Sharpe ratio		
Pre-pandemic	0.399	0.362
Pre-PEPP	0.394	0.521
Post-PEPP	0.407	0.489
Sharpe numerator†	$A_t^*(\tau)^\top \lambda_t$	ξ_t
Pre-pandemic	1.93%	1.22%
Pre-PEPP	1.90%	2.58%
Post-PEPP	1.96%	2.21%
Sharpe denominator†	$\sqrt{A_t^*(\tau)^\top \Sigma \Sigma^\top A_t^*(\tau)}$	$\delta\sqrt{\psi_t}$
Pre-pandemic	4.82%	3.37%
Pre-PEPP	4.83%	4.96%
Post-PEPP	4.83%	4.53%

Note. The table reports the model-implied instantaneous Sharpe ratios $\mathbb{S}_t^*(\tau)$ and $\mathbb{S}_t^\Delta(\tau)$, interpreting the time unit as one year, for t = March 2020 and τ = 10 years, conditional on the *pre-pandemic*, *pre-PEPP*, and *post-PEPP* information sets. Quantities with a dagger (†) are stated in annualized percentage points. Model notation is used to clarify the quantities shown.

in the expected default loss $y_t^{DL}(\tau)$ on 10-year bonds. Since $y_t^{DL}(\tau)$ is a forward-looking integral over ψ_t (in this case, looking forward over the next ten years), it also jumps up on impact but is even smoother and more forward-looking than F_t.[62]

The last two panels in Fig 8 show the changes in the default risk price ξ_t, and the credit risk premium on 10-year bonds, $y_t^{CR}(\tau)$. The time profile of ξ_t resembles that of ψ_t, to which it is closely related, by (13). It also increases with arbitrageurs' holdings of IT bonds, which rise gradually following the pandemic outbreak (not shown), but are then partially reversed by the PEPP announcement. Since $y_t^{CR}(\tau)$ is a forward-looking integral over ξ_t, the shift in $y_t^{CR}(\tau)$ resembles the shift in $y_t^{DL}(\tau)$, but is substantially larger, given the level of risk aversion that we infer from German term premia.

Sharpe ratios. These large variations in the default probability and its risk premium make it interesting to ask how Sharpe ratios changed with the pandemic outbreak and the PEPP announcement. Table 5 documents the model-implied Sharpe numer-

[62] The forecasts we have used as model inputs predict lower Italian deficits after 2026 in the *pre-PEPP* forecast than in the *pre-pandemic* forecast. This eventually feeds into a reduced Italian default rate in the decade of the 2030s. This explains why the expected default loss $y_t^{DL}(\tau)$ on 10-year bonds declines from 2027 onwards under the post-outbreak forecast ($y_t^{DL}(\tau)$ is proportional to the 10-year forward average of the default rate). In contrast, the credit risk premium $y_t^{CR}(\tau)$ does not decrease over the years shown in Fig. 8, since it also depends on arbitrageurs' holdings, which increase persistently.

Figure 9: Impact of the pandemic outbreak: German and Italian yields, Feb.-Mar. 2020

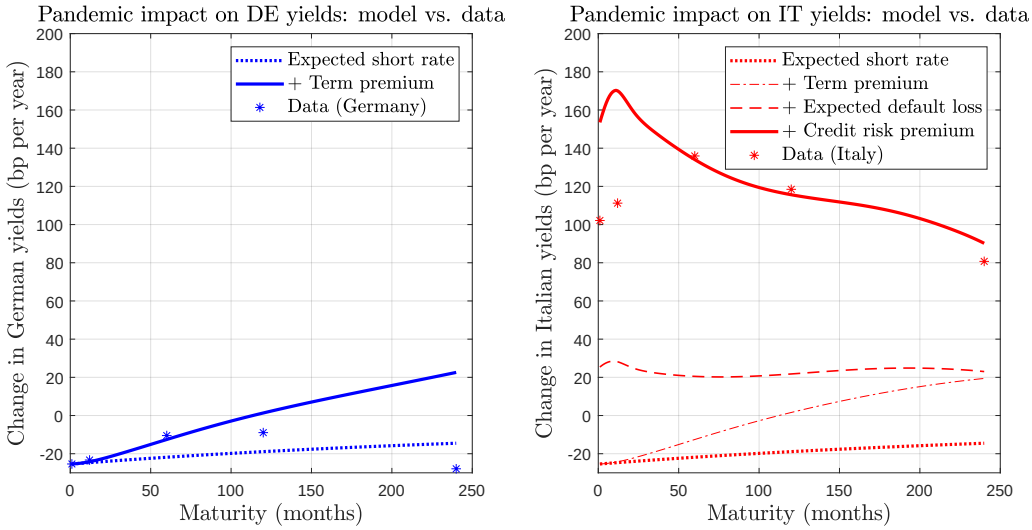

Data source: German and Italian yields (annualized, basis points) on zero-coupon 1m, 1Y, 5Y, 10Y, and 20Y sovereign bonds from Datastream.
Stars: Shift in weekly average German yields (left) and Italian yields (right) from week of 13-19 February 2020 to week of 12-18 March 2020.
Lines: Model-generated change in yields in response to revised fiscal expectations associated with the pandemic (solid), decomposed into expectations component (dotted), plus term premium (dash-dotted), plus expected default loss (dashed), plus credit risk premium.

ators, denominators, and ratios immediately before the pandemic, after the outbreak but before PEPP, and immediately after the PEPP announcement. Already, before the pandemic, the Italian default rate had climbed from its long-run value of $\underline{\psi} = 0.86\%$ annually to $\psi_t \approx 2\%$, leading to a Sharpe ratio of 0.362 on default risk. The rise in debt and deficits due to the pandemic immediately doubled the default rate to roughly $\psi_t \approx 4\%$, which was partially offset by the PEPP announcement, which brought the rate back down to $\psi_t = 3.7\%$. This is reflected in the strong increase in the corresponding Sharpe ratio, to 0.521, which then fell back to 0.489 after the PEPP announcement, as seen in Table 5. While these movements in the annual Sharpe ratio are large, they never reach implausible levels.[63]

Impact of the pandemic outbreak. Finally, Fig. 9 illustrates the model's fit to the yield curve movements following the pandemic outbreak. The figure compares the model-generated shift in yields to the difference between the average yields observed

[63]For comparison, using data on the S&P 500 index for 1960-2022 we calculate a Sharpe ratio of 0.49. See https://shillerdata.com.

over the week of 13-19 February 2020, and the average over the week of 12-18 March 2020 (which is exactly four weeks later, and precedes the announcement of the PEPP). As these observations are *not* used in the estimation, this exercise serves as a useful out-of-sample test. In the model, the pandemic outbreak is represented by the shift in expectations from the *pre-pandemic* to the *pre-PEPP* forecasts. Hence it incorporates the increase in debt and deficits due to the pandemic, partially offset by the €120 billion expansion of the APP envelope announced on March 12, 2020. In addition, it incorporates a 22 bp decrease in the short rate factor r_t, which is the observed change in German one-month yields between 13-19 February and 12-18 March, 2020.

The right panel of the figure shows that the pandemic shock generates a large upward shift in Italian yields in our model (red curves), of the same order of magnitude as the shift observed in bond markets from February to March 2020 (red stars). The model somewhat overpredicts the market reaction for the shortest Italian bonds, and the longest German bonds. The 20 bp shift in the expected default loss component and the 100 bp shift in the credit risk premium, for ten-year Italian bonds, correspond to the jumps in these components that are shown as green dashed lines in the bottom row of Fig. 8. The key conclusion from the figure is that our model generates an upward shift across all maturities of Italian yields, a movement that cannot be explained by a standard model without default. As Fig. 8 makes clear, the forward-looking nature of the endogenous default decision is crucial for this finding. This upward shift reflects an increase in the expected default loss due to the deteriorating fiscal scenario, but its main driver is the substantially larger increase in the credit risk premium.

6 Conclusions

This paper proposes a micro-founded model of the term structure of sovereign interest rates in a heterogeneous monetary union. We extend the Vayanos and Vila (2021) affine term structure model to a two-country monetary union where one of the two sovereign issuers (Periphery) faces default risk, due to the possibility of rollover crises. In addition to the familiar *duration risk extraction channel* of asset purchase programs, our model features a novel *default risk extraction channel*, whereby announcements of central bank asset purchases reduce both the expected amount of defaultable bonds the market must absorb and the sovereign default probability itself, thus reducing the compensation risk-averse investors require to absorb default risk.

Arbitrage across issuers in this multicountry structure helps us identify model parameters. We calibrate the model to data on German and Italian yields. Assuming that German default risk is negligible, arbitrageurs' risk aversion can be identified by fitting the model to the German yield curve. Given risk aversion, fitting the sovereign spread identifies the long-run probability of default. We can then decompose the sovereign spread into the part that represents the expected loss due to Italian default (under the physical measure), and the part that represents a risk premium on sovereign credit risk. Under our inferred parameters, and given the implied amount of Italian sovereign bonds absorbed by arbitrageurs, we find that the credit risk premium accounts for roughly three-quarters of the long-run sovereign spread.

This large credit risk premium implies that there is substantial scope for asset purchases to reduce the mean and the variability of the sovereign spread through the default risk extraction channel. We show that our model can explain the large shift in Italian yields – across all maturities, including short ones – that occurred in response to the PEPP announcement. At a ten-year maturity, roughly four-fifths of the resulting reduction in the sovereign spread is attributable to a decline in the credit risk premium. Moreover, as we show in an appendix, the flexibility in the timing and cross-country allocation of purchases permitted by the PEPP substantially enhanced its impact, compared to the inflexible design of the earlier APP. Our model could be fruitfully applied to further analyze different designs for balance sheet expansions and reductions in the context of a monetary union.

References

Aguiar, M., M. Amador, E. Farhi, and G. Gopinath (2015). Coordination and crisis in monetary unions. *Quarterly Journal of Economics 130*(4), 1727–1779. 10

Altavilla, C., G. Carboni, and R. Motto (2021). Asset purchase programs and financial markets: Lessons from the euro area. *International Journal of Central Banking 17*(4), 1–48. 1

Ang, A. and M. Piazzesi (2003). A no-arbitrage vector autoregression of term structure dynamics with macroeconomic and latent variables. *Journal of Monetary Economics 50*, 745–787. 1

Arellano, C. (2008). Default risk and income fluctuations in emerging economies. *American Economic Review 98*(3), 690–712. 53

Arellano, C., Y. Bai, and G. P. Mihalache (2020). Monetary policy and sovereign risk in emerging economies (NK-default). NBER Working Paper 26671. 10

Arellano, C., X. Mateos-Planas, and V. Ríos-Rull (2023). Partial default. *Journal of Political Economy 131*(6), 1385–1439. 14, 3

Bacchetta, P., E. Perazzi, and E. van Wincoop (2018). Self-fulfilling debt crises: Can monetary policy really help? *Journal of International Economics 110*, 119–134. 10

Bianchi, J. and J. Mondragon (2022). Monetary independence and rollover crises. *Quarterly Journal of Economics 137*(1), 435–491. 10

Borgy, V., T. Laubach, J.-S. Mésonnier, and J.-P. Renne (2012). Fiscal sustainability, default risk, and euro area sovereign bond spreads. Banque de France DT350. 1

Broeders, D., L. de Haan, and J. W. van den End (2023). How QE changes the nature of sovereign risk. *Journal of International Money and Finance 137*(102881). 1

Burriel, P., I. Kataryniuk, and J. J. Perez (2022). Computing the EU SURE interest savings using an extended debt sustainability assessment tool. Occasional Papers 2210, Bank of Spain. 39

Calvo, G. (1988). Servicing the public debt: The role of expectations. *American Economic Review 78*(4), 647–661. 1, 10, 3

Camous, A. and R. Cooper (2019). "Whatever it takes" is all you need: Monetary policy and debt fragility. *American Economic Journal: Macroeconomics 11*(4), 38–81. 10

Cole, H. L. and T. J. Kehoe (2000). Self-fulfilling debt crises. *Review of Economic Studies 67*(1), 91–116. 1, 10, 3

Corradin, S. and B. Schwaab (2023). Euro area sovereign bond risk premia during the Covid-19 pandemic. *European Economic Review 153*(104402). 6

Corsetti, G. and L. Dedola (2016). The mystery of the printing press: Monetary policy and self-fulfilling debt crises. *Journal of the European Economic Assocation 14*(6), 1329–1371. 2, 1, 10, 3

Costain, J., G. Nuño, and C. Thomas (2022). The term structure of interest rates in a heterogeneous monetary union. Banco de España Working Paper 2223. 35

Cruces, J. and C. Trebesch (2013). Sovereign defaults: The price of haircuts. *American Economic Journal: Macroeconomics 5*, 85–117. 42

De Grauwe, P. and Y. Ji (2013). Self-fulfilling crises in the eurozone: An empirical test. *Journal of International Money and Finance 34*, 15–36. 1

Del Negro, M. and C. Sims (2015). When does a central bank's balance sheet require fiscal support? *Journal of Monetary Economics 73*, 1–19. 29, A

Demir, I., B. Eroglu, and S. Yildirim-Karaman (2021). Heterogeneous effects of unconventional monetary policy on the bond yields across the euro area. *Journal Money, Credit and Banking 54*(5), 1425–1457. 6

Duffie, D. and R. Kan (1996). A yield-factor model of interest rates. *Mathematical Finance 6*(4), 379–406. 1

Duffie, D. and K. Singleton (1999). Modeling term structures of defaultable bonds. *Review of Financial Studies 12*(4), 687–720. 1, 2, 15, 3

Emmer, S. and C. Kluppelberg (2004, January). Optimal portfolios when stock prices follow an exponential Lévy process. *Finance and Stochastics 8*(1), 17–44. 13

Eser, F., W. Lemke, K. Nyholm, S. Radde, and A. Vladu (2023). Tracing the impact of the ECB's asset purchase programme on the yield curve. *International Journal of Central Banking 19*(3), 359–422. 4, 1, 4.2, 45

Gilchrist, S., B. Wei, V. Yue, and E. Zakrajšek (2024). The Fed takes on corporate credit risk: An analysis of the efficacy of the SMCCF. *Journal of Monetary Economics* (Forthcoming). 1

Gourinchas, P.-O., W. Ray, and D. Vayanos (2022). A preferred-habitat model of term premia, exchange rates, and monetary policy spillovers. NBER Working Paper 29875. 1, 2

Greenwood, R., S. Hanson, J. Stein, and A. Sunderam (2023). A quantity-driven theory of term premia and exchange rates. *Quarterly Journal of Economics 138*(4), 2327–2389. 1

Greenwood, R., S. Hanson, and D. Vayanos (2024). Supply and demand and the term structure of interest rates. *Annual Review of Financial Economics* (Forthcoming). 8

Greenwood, R. and D. Vayanos (2014). Bond supply and excess bond returns. *Review of Financial Studies 27*(3), 663–713. 1, 1

Hamilton, J. and J. C. Wu (2012). The effectiveness of alternative monetary policy tools in a zero lower bound environment. *Journal of Money, Credit and Banking 44*(Supplement), 1–46. 1, 1, C.3, 72

Hayashi, F. (2018). Computing equilibrium bond prices in the Vayanos-Vila model. *Research in Economics 72*(2), 181–195. 4.1

He, Z., S. Nagel, and Z. Song (2023). Treasury inconvenience yields during the Covid-19 crisis. *Journal of Financial Economics 143*(1), 57–79. 1

Jappelli, R., L. Pellizon, and M. Subrahmanyam (2023). Quantitative easing, the repo market, and the term structure of interest rates. SAFE Working Paper 395, Goethe University. 1

Kallsen, J. (2000, August). Optimal portfolios for exponential Lévy processes. *Mathematical Methods of Operations Research 51*(3), 357–374. 13

King, T. B. (2019). Expectation and duration at the zero lower bound. *Journal of Financial Economics 134*(3), 736–760. 1

Krishnamurthy, A. (2022). Quantitative easing: What have we learned? Seminar presentation, Princeton Univ., 24 March. 1

Krishnamurthy, A., S. Nagel, and A. Vissing-Jorgensen (2018). ECB policies involving government bond purchases: Impact and channels. *Review of Finance 22*(1), 1–44. 6

Li, C. and M. Wei (2013). Term structure modeling with supply factors and the Federal Reserve's large-scale asset purchase programs. *International Journal of Central Banking 9*(1), 375–402. 1

Na, S., S. Schmitt-Grohe, M. Uribe, and V. Yue (2018). The twin Ds: Optimal default and devaluation. *American Economic Review 108*(7), 1773–1819. 10

Nuño, G., S. Hurtado, and C. Thomas (2023). Monetary policy and sovereign debt sustainability. *Journal of the European Economic Association 21*(1), 293–325. 10

Ortobelli, S., I. Huber, S. Rachev, and E. Schwartz (2003). Portfolio choice theory with non-gaussian distributed returns. In: Handbook of Heavy Tailed Distributions in Finance (S. T. Rachev, ed.). 13

Rachev, S. and S. Han (2000, April). Portfolio management with stable distributions. *Mathematical Methods of Operations Research 51*(2), 341–352. 13

Ray, W. (2019). Monetary policy and the limits to arbitrage: Insights from a New Keynesian preferred habitat model. Manuscript, UC Berkeley. 1

Reis, R. (2013). The mystique surrounding the central bank's balance sheet, applied to the european crisis. *American Economic Review 103*(3), 135–140. 10, A

Vayanos, D. and J.-L. Vila (2021). A preferred habitat model of the term structure of interest rates. *Econometrica 89*(1), 77–112. 1, 2, 2, 12, 16, 2.1, 20, 2.1, 4.1, 51, 6, 69

Internet Appendix

A Appendix: Central bank accounting

The main text focuses on bond market equilibrium, without spelling out the broader financial context, notably including the role of the central bank. Here, we provide more context. Most importantly, we derive expressions for central bank profits and use them to explain why a remittance rule based on profits would render our affine solution method inapplicable.

Besides the arbitrageurs and preferred-habitat investors, financial market participants include commercial banks that can hold short-term riskless bonds and central bank reserves (indeed, some arbitrageurs may be commercial banks). Arbitrage then ensures that the short-term riskless rate (r_t) equals the interest rate on reserves.

The balance sheet of the common central bank consists of sovereign bonds on the assets side and bank reserves and capital on the liabilities side. We assume that the central bank maintains separate accounts associated with each national government in the monetary union, and determines seignorage transfers in relation to its holdings of each country's bonds. This roughly corresponds to the case of the Eurosystem, in which most bonds are held by the national central banks (NCBs) of the countries that issued them, with only a small fraction of holdings subject to "risk sharing" across the NCBs.

In our model, the central bank's balance sheet affects bond market equilibrium in two ways. First, central bank bond holdings reduce the net supply of bonds to be absorbed by the private sector, $(S_t(\tau), S_t^*(\tau))$. Second, under our assumed remittance rule (30), redemptions of central bank-held bonds affect dividend payments to the government and therefore the default probability, by (28). As an alternative to our redemptions-based rule, one could consider a remittance rule based on central bank profits, which would be more consistent with actual practice. However, as the main text mentioned, this would prevent us from obtaining an affine solution for bond yields, which is central toour analysis. To understand this issue, we next show how to compute central bank profits in our framework. We pay particular attention to ECB/Eurosystem accounting principles for valuing securities held for monetary policy purposes (the only central bank asset in our model), but we also show how one can simplify the algebra by relaxing such principles.

Central bank profits: some additional notation. For each bond in the central bank's portfolio at time t, let $\tilde{t} \in [t - \tau^{max}, t]$ denote the time when it was purchased and $\tilde{\tau}$ its residual maturity at the time of purchase. Residual maturity in the present is $\tau = \tilde{\tau} - (t - \tilde{t})$, i.e. residual maturity at the purchase date minus the time elapsed since then. Let $P_{\tilde{t}}(\tilde{\tau})$ denote the purchase price. For a zero-coupon bond, the yield-to-maturity at the time of purchase, $y_{\tilde{t}}(\tilde{\tau})$, is determined by

$$P_{\tilde{t}}(\tilde{\tau}) = e^{-y_{\tilde{t}}(\tilde{\tau})\tilde{\tau}}. \tag{41}$$

Amortised cost accounting. All Eurosystem members (the ECB and the national central banks) are required to value their monetary policy portfolios *at amortised cost*. The value at amortised cost at time t of bond $(\tilde{\tau}, \tilde{t})$ is given by

$$V_t(\tilde{\tau}, \tilde{t}) = P_{\tilde{t}}(\tilde{\tau}) e^{y_{\tilde{t}}(\tilde{\tau})(t-\tilde{t})}. \tag{42}$$

Therefore, the initial value of the bond equals its purchase price: $V_{\tilde{t}}(\tilde{\tau}, \tilde{t}) = P_{\tilde{t}}(\tilde{\tau})$. Thereafter, its value grows at the same rate as the bond's IRR, $y_{\tilde{t}}(\tilde{\tau})$, converging to its face value at maturity: $V_{\tilde{t}+\tilde{\tau}}(\tilde{\tau}, \tilde{t}) = P_{\tilde{t}}(\tilde{\tau}) e^{y_{\tilde{t}}(\tilde{\tau})\tilde{\tau}} = 1$, where the second equality follows from (41). In turn, the *interest income* from the bond at t is given by

$$I_t(\tilde{\tau}, \tilde{t}) = V_t(\tilde{\tau}, \tilde{t}) y_{\tilde{t}}(\tilde{\tau}), \tag{43}$$

i.e. the bond's current value (at amortized cost) times its yield at the time of purchase. Since the bond's value $V_t(\cdot)$ increases over time, its interest income does too.

Equation (43) shows how amortised cost accounting *periodifies* the bond's total income over the period in which it is held (to maturity) by the central bank. To see this, and to simplify the algebra, without loss of generality, normalize the purchase time to $\tilde{t} = 0$, and let $P_0(\tilde{\tau}) \equiv P(\tilde{\tau})$, $y_0(\tilde{\tau}) \equiv y(\tilde{\tau})$, $V_t(\tilde{\tau}, 0) = P(\tilde{\tau}) e^{y(\tilde{\tau})t} \equiv V_t(\tilde{\tau})$, and $I_t(\tilde{\tau}, 0) = V_t(\tilde{\tau}) y(\tilde{\tau}) \equiv I_t(\tilde{\tau})$. Then, integrating (43) over the holding period yields

$$\int_0^{\tilde{\tau}} I_t(\tilde{\tau}) dt = y(\tilde{\tau}) P(\tilde{\tau}) \int_0^{\tilde{\tau}} e^{y(\tilde{\tau})t} dt = y(\tilde{\tau}) P(\tilde{\tau}) \left[\frac{1}{y(\tilde{\tau})} e^{y(\tilde{\tau})t} \right]_0^{\tilde{\tau}} = P(\tilde{\tau}) \left[e^{y(\tilde{\tau})\tilde{\tau}} - 1 \right] = 1 - P(\tilde{\tau}),$$

where the last equality uses the fact that $P(\tilde{\tau}) e^{y(\tilde{\tau})\tilde{\tau}} = 1$. The last expression in the above equation is precisely the total income on a zero-coupon bond: its face value (which we normalize to one) minus its purchase price.

Central bank profits. Let $f_t^{CB}(\tilde{\tau}, \tilde{t})$ denote the central bank's holdings at time t of bonds that were purchased at time $\tilde{t}$ with residual maturity $\tilde{\tau}$.[64] Then the total interest income from the bond portfolio at time t is

$$I_t^{tot} = \int_{t-\tau^{max}}^{t} \int_0^{\tau^{max}} I_t(\tilde{\tau}, \tilde{t}) f_t^{CB}(\tilde{\tau}, \tilde{t}) d\tilde{\tau} d\tilde{t}. \tag{44}$$

The central bank's profit flow at time t is its total interest income minus interest payments on reserves,

$$\Pi_t^{cb} = I_t^{tot} - r_t D_t, \tag{45}$$

where D_t are central bank reserves and r_t is the interest rate on reserves. Finally, the law of motion of reserves is given by

$$\dot{D}_t = r_t D_t + \int_0^{\tau^{max}} P_t(\tau) \iota_t^{CB}(\tau) d\tau + \Gamma_t - f_t^{CB}(0), \tag{46}$$

i.e. reserves increase with interest payments on reserves, bond purchases ($\int P_t(\tau)\iota_t^{CB}(\tau)d\tau$) and dividend payments (Γ_t), and decrease with bond redemptions ($f_t^{CB}(0)$).

Profit-based remittance rules. As the main text discusses, remittance rules based on central bank profits are incompatible with our affine solution method. As (28) in the paper shows, the default rate at any time t depends on the future streams of government primary deficits and total bond redemptions, which are both assumed to be deterministic,[65] and on the future stream of dividends paid to the Treasury, $\{\Gamma_{t+s}\}_{s\geq 0}$. Under profit-based dividend rules, this last term would depend on past and future bond prices, thus making our affine solution inapplicable.

To see this in the simplest way possible, suppose the central bank pays off its entire accounting profit at all times: $\Gamma_{t+s} = \Pi_{t+s}^{cb} = I_{t+s}^{tot} - r_{t+s} D_{t+s}$ for all $s \geq 0$.[66] The default probability would then depend on the future streams of interest income and interest

[64] We do not need to include the *current* (time-t) residual maturity as an argument of the portfolio distribution, as it is implied by the other arguments: $\tau = \tilde{\tau} - (t - \tilde{t})$.

[65] As explained in the paper, we assume that the central bank commits to a certain path of future bond purchases in *face value* terms (as opposed to market value terms), precisely so that we obtain an affine solution for yields. Under this assumption, the future stream of central bank-held bond redemptions is indeed deterministic and therefore does not depend on bond prices.

[66] In reality, Eurosystem NCBs do not typically pay all their accounting profits to their national treasuries, and instead retain some income to accumulate capital buffers. How much is retained varies across NCBs, depending on the risks in their balance sheets and their risk provisioning methodologies.

payments on reserves, which both depend on past and future (from the point of view of time t) bond prices. Indeed, by (42)-(44), total interest income I_t^{tot} equals

$$I_t^{tot} = \int_{t-\tau^{max}}^{t} \int_0^{\tau^{max}} P_{\tilde{t}}(\tilde{\tau}) e^{y_{\tilde{t}}(\tilde{\tau})(t-\tilde{t})} y_{\tilde{t}}(\tilde{\tau}) f_t^{CB}(\tilde{\tau}, \tilde{t}) d\tilde{\tau} d\tilde{t}, \tag{47}$$

where yields depend on prices through $y_{\tilde{t}}(\tilde{\tau}) = -\log(P_{\tilde{t}}(\tilde{\tau}))/\tilde{\tau}$. Therefore, at any future time $t+s > t$, interest income I_{t+s}^{tot} would depend on the prices paid by the central bank on all bonds held in its portfolio at that time. Regarding interest payments on reserves, from equation (46) the stock of reserves at any future time $t+s$ is

$$D_{t+s} = e^{\int_0^s r_{t+j} dj} D_t + \int_0^s e^{\int_u^s r_{t+j} dj} \left(\int_0^{\tau^{max}} P_{t+u}(\tau) \iota_{t+u}^{CB}(\tau) d\tau + \Gamma_{t+u} - f_{t+u}^{CB}(0) \right) du,$$

Therefore, future reserves D_{t+s} and the interest payments on them, $r_{t+s} D_{t+s}$, depend on future bond prices, both through prices paid in future purchases ($\int_0^{\tau^{max}} P_{t+u}(\tau) \iota_{t+u}^{CB}(\tau) d\tau$) and through the profit-based dividend rule itself ($\Gamma_{t+u} = \Pi_{t+u}^{cb}$).

Simplifying the algebra of central bank profits. As mentioned before, the total income earned on a zero-coupon bond, from purchase to redemption, is

$$1 - P_{\tilde{t}}(\tilde{\tau}), \tag{48}$$

i.e. its face value minus the purchase price. While amortised cost accounting periodifies this income over the entire holding period, one could consider a simpler accounting framework that only recognizes the bond's income upon redemption. One could then aggregate (48) across all bonds maturing at t (those with residual maturity $\tau = 0$) to obtain a simpler expression for total bond income:

$$\hat{I}_t^{tot} = \int_0^{\tau^{max}} (1 - P_{\tilde{t}}(\tilde{\tau})) \tilde{f}_t^{CB}(0, \tilde{t}) d\tilde{t} = f_t^{CB}(0) - \int_0^{\tau^{max}} P_{\tilde{t}}(\tilde{\tau}) \tilde{f}_t^{CB}(0, \tilde{t}) d\tilde{t}, \tag{49}$$

where $\tilde{f}_t^{CB}(0, \tilde{t})$ is the mass of central bank-held bonds maturing at time t that were purchased at $\tilde{t}$ (with residual maturity $\tilde{\tau} = t - \tilde{t}$) and $f_t^{CB}(0) = \int_0^{\tau^{max}} \tilde{f}_t^{CB}(0, \tilde{t}) d\tilde{t}$ is total redemptions at t of central bank-held bonds. While far simpler than the expression (44) for income under amortised-cost accounting, expression (49) still depends on bond prices. Therefore, simplifying the accounting conventions for central bank profits would not eliminate the dependence of profits on bond prices, which prevents us from obtaining

an affine solution.

Central bank capital in a rollover crisis. As mentioned in the main text, our assumed remittance rule implies that the central bank may, under some circumstances, face a reduction in its capital. To see this formally, we can use equations (30) and (46) to obtain the law of motion of central bank reserves in a rollover crisis:

$$\dot{D}_t = r_t D_t + \int P_t(\tau)\, \iota_t^{CB}(\tau)\, d\tau - \bar{\Gamma} - (1-\zeta)\, f_t^{CB}(0)\,. \tag{50}$$

We can define the national central bank's capital as

$$K_t \equiv \int_{t-\tau^{max}}^{t} \int_0^{\tau^{max}} V_t(\tilde{\tau},\tilde{t}) f_t^{CB}(\tilde{\tau},\tilde{t}) d\tilde{\tau} d\tilde{t} - D_t,$$

Capital then evolves as follows,

$$\begin{aligned}
\dot{K}_t &= \int_0^{\tau^{max}} \left[V_t(\tilde{\tau},\tilde{t}) f_t^{CB}(\tilde{\tau},\tilde{t}) - V_{t-\tau^{max}}(\tilde{\tau},\tilde{t}) f_{t-\tau^{max}}^{CB}(\tilde{\tau},\tilde{t})\right] d\tilde{\tau} d\tilde{t} \\
&+ \int_{t-\tau^{max}}^{t} \int_0^{\tau^{max}} \int \left(\frac{\partial V_t(\tilde{\tau},\tilde{t})}{\partial t} f_t^{CB}(\tilde{\tau},\tilde{t}) + V_t(\tilde{\tau},\tilde{t}) \frac{\partial f_t^{CB}(\tilde{\tau},\tilde{t})}{\partial t} \right) d\tilde{\tau} d\tilde{t} - \dot{D}_t.
\end{aligned}$$

During a rollover crisis, equation (50) implies

$$\begin{aligned}
\dot{K}_t &= \int_0^{\tau^{max}} \left[V_t(\tilde{\tau},\tilde{t}) f_t^{CB}(\tilde{\tau},\tilde{t}) - V_{t-\tau^{max}}(\tilde{\tau},\tilde{t}) f_{t-\tau^{max}}^{CB}(\tilde{\tau},\tilde{t})\right] d\tilde{\tau} d\tilde{t} \\
&+ \int_{t-\tau^{max}}^{t} \int_0^{\tau^{max}} \int \left(\frac{\partial V_t(\tilde{\tau},\tilde{t})}{\partial t} f_t^{CB}(\tilde{\tau},\tilde{t}) + V_t(\tilde{\tau},\tilde{t}) \frac{\partial f_t^{CB}(\tilde{\tau},\tilde{t})}{\partial t} \right) d\tilde{\tau} d\tilde{t} \\
&- r_t D_t - \int_0^{\tau^{max}} P_t(\tau) \iota_t^{CB}(\tau) d\tau + \bar{\Gamma} + (1-\zeta)\, f_t^{CB}(0)\,.
\end{aligned}$$

Thus, capital maydecrease during a crisis, potentially falling below zero. This will depend on the maturity structure of central bank assets, the path of interest payments on reserves, and the constant $\bar{\Gamma}$. In particular, a sufficiently large capital retention term $\bar{\Gamma}$ can make the probability of a negative capital event arbitrarily small. In any case, as Del Negro and Sims (2015) and Reis (2013) discuss, a central bank can operate with low or even negative capital (within limits). Hence the small probability that the central bank may at some time face negative capital is inessential for our analysis.

B Model solution

B.1 Solving the one-factor model

For the one-factor model, we conjecture that there exist two pairs of deterministic functions $(A_t(\tau), C_t(\tau))$ and $(A_t^*(\tau), C_t^*(\tau))$ such that the price of bonds can be expressed in log-affine form:

$$P_t(\tau) = e^{-[A_t(\tau) r_t + C_t(\tau)]},\ P_t^*(\tau) = e^{-[A_t^*(\tau) r_t + C_t^*(\tau)]}. \tag{51}$$

Applying Itô's lemma, the time-t instantaneous return on an undefaulted bond of maturity τ is

$$\frac{dP_t(\tau)}{P_t(\tau)} = \mu_t(\tau)\, dt - \sigma A_t(\tau)\, dB_t,\ \frac{dP_t^*(\tau)}{P_t^*(\tau)} = \mu_t^*(\tau)\, dt - \sigma A_t^*(\tau)\, dB_t, \tag{52}$$

where[67]

$$\mu_t(\tau) = \left(\frac{\partial A_t}{\partial \tau} - \frac{\partial A_t}{\partial t}\right) r_t + \left(\frac{\partial C_t}{\partial \tau} - \frac{\partial C_t}{\partial t}\right) - A_t(\tau)\,\kappa(\bar{r} - r_t) + \frac{1}{2}\sigma^2 [A_t(\tau)]^2, \tag{53}$$

and

$$\mu_t^*(\tau) = \left(\frac{\partial A_t^*}{\partial \tau} - \frac{\partial A_t^*}{\partial t}\right) r_t + \left(\frac{\partial C_t^*}{\partial \tau} - \frac{\partial C_t^*}{\partial t}\right) - A_t^*(\tau)\,\kappa(\bar{r} - r_t) + \frac{1}{2}\sigma^2 [A_t^*(\tau)]^2. \tag{54}$$

If we substitute bond returns (52) into the law of motion of wealth (6), we obtain

$$\begin{aligned} dW_t &= \left[W_t r_t + \int_0^\infty \left(X_t(\tau)\left(\mu_t(\tau) - r_t\right) + X_t^*(\tau)\left(\mu_t^*(\tau) - r_t\right)\right) d\tau\right] dt \\ &- \left[\int_0^\infty \left(X_t(\tau) A_t(\tau) + X_t^*(\tau) A_t^*(\tau)\right) d\tau\right] \sigma dB_t \\ &- \left[\int_0^\infty X_t(\tau)\, d\tau\right] \delta dN_t. \end{aligned} \tag{55}$$

Using (55) to evaluate the expectation and variance of dW_t in (5), the arbitrageur´s problem can be expressed as (9), with first-order conditions (10)-(11).

Since preferred habitat demand is assumed to be affine in yields, equations (14)-(15)

[67] Note that τ is a state with dynamics $d\tau = -dt$, so Itô's lemma yields derivatives in τ as well as t.

imply that the risk prices λ_t and ξ_t that appear in the first-order conditions must be affine too. Hence, a solution requires $\lambda_t = \Lambda_t r_t + \bar{\lambda}_t$ and $\xi_t = \Xi_t r_t + \bar{\xi}_t$, where

$$\begin{aligned}
\Lambda_t &\equiv -\gamma\sigma^2 \int_0^\infty \left(\alpha(\tau)\left[A_t(\tau)\right]^2 + \alpha^*(\tau)\left[A_t^*(\tau)\right]^2\right) d\tau, \\
\bar{\lambda}_t &\equiv \gamma\sigma^2 \int_0^\infty \left[\left(S_t(\tau) - h_t(\tau) - \alpha(\tau) C_t(\tau) + \tau\alpha(\tau)\hat{\delta}\psi_t\right) A_t(\tau) + \left(S_t^*(\tau) - h_t^*(\tau) - \alpha^*(\tau) C_t^*(\tau)\right) A_t^*(\tau)\right] d\tau, \\
\Xi_t &\equiv -\gamma\psi_t\delta^2 \int_0^\infty \alpha(\tau) A_t(\tau)\, d\tau, \\
\bar{\xi}_t &\equiv \gamma\psi_t\delta^2 \int_0^\infty \left(S_t(\tau) - h_t(\tau) - \alpha(\tau) C_t(\tau) + \tau\alpha(\tau)\hat{\delta}\psi_t\right) d\tau.
\end{aligned}$$

With this notation, if we substitute $\mu_t(\tau)$ and $\mu_t^*(\tau)$ from (53)-(54) into (10)-(11), the first-order conditions on the arbitrageurs' portfolio weights are:

$$\begin{aligned}
0 &= -\left(\frac{\partial A_t}{\partial \tau} - \frac{\partial A_t}{\partial t}\right) r_t - \left(\frac{\partial C_t}{\partial \tau} - \frac{\partial C_t}{\partial t}\right) + A_t(\tau)\kappa(\bar{r} - r_t) - \frac{1}{2}\sigma^2\left[A_t(\tau)\right]^2 + r_t \\
&+ A_t(\tau)\left(\Lambda_t r_t + \bar{\lambda}_t\right) + \psi_t\delta + \left(\Xi_t r_t + \bar{\xi}_t\right),
\end{aligned}$$

and

$$\begin{aligned}
0 &= -\left(\frac{\partial A_t^*}{\partial \tau} - \frac{\partial A_t^*}{\partial t}\right) r_t - \left(\frac{\partial C_t^*}{\partial \tau} - \frac{\partial C_t^*}{\partial t}\right) + A_t^*(\tau)\kappa(\bar{r} - r_t) - \frac{1}{2}\sigma^2\left[A_t^*(\tau)\right]^2 + r_t \\
&+ A_t^*(\tau)\left(\Lambda_t r_t + \bar{\lambda}_t\right).
\end{aligned}$$

Separating the terms with and without r, we must have

$$0 = -\frac{\partial A_t}{\partial \tau} + \frac{\partial A_t}{\partial t} - A_t(\tau)\kappa + 1 + \Lambda_t A_t(\tau) + \Xi_t, \tag{56}$$

$$0 = -\frac{\partial C_t}{\partial \tau} + \frac{\partial C_t}{\partial t} + A_t(\tau)\kappa\bar{r} - \frac{1}{2}\sigma^2\left[A_t(\tau)\right]^2 + \bar{\lambda}_t A_t(\tau) + \psi_t\delta + \bar{\xi}_t, \tag{57}$$

$$0 = -\frac{\partial A_t^*}{\partial \tau} + \frac{\partial A_t^*}{\partial t} - A_t^*(\tau)\kappa + 1 + \Lambda_t A_t^*(\tau), \tag{58}$$

$$0 = -\frac{\partial C_t^*}{\partial \tau} + \frac{\partial C_t^*}{\partial t} + A_t^*(\tau)\kappa\bar{r} - \frac{1}{2}\sigma^2\left[A_t^*(\tau)\right]^2 + \bar{\lambda}_t A_t^*(\tau). \tag{59}$$

This provides a system of PDEs to determine functions $(A_t(\tau), C_t(\tau))$ and $(A_t^*(\tau), C_t^*(\tau))$, verifying our guess that the bond price is an affine function of r_t.

B.2 Derivation of analytical results from Sec. 2.1

B.2.1 Proof of Prop. 1

We want to prove the decomposition: (1)

$$\begin{aligned} y_t(\tau) &= \underbrace{\frac{1}{\tau}\mathbb{E}_t\int_0^\tau r_{t+s}ds}_{\text{Expected rates } y_t^{EX}(\tau)} + \underbrace{\frac{1}{\tau}\mathbb{E}_t\int_0^\tau\left[A_{t+s}(\tau-s)\lambda_{t+s}-\frac{\sigma^2}{2}\left[A_{t+s}(\tau-s)\right]^2\right]ds}_{\text{Term premium } y_t^{TP}(\tau)} \\ &+ \underbrace{\frac{1}{\tau}\mathbb{E}_t\int_0^\tau\delta\psi_{t+s}ds}_{\text{Expected default loss } y_t^{DL}(\tau)} + \underbrace{\frac{1}{\tau}\mathbb{E}_t\int_0^\tau\xi_{t+s}ds}_{\text{Credit risk premium } y_t^{CR}(\tau)}. \end{aligned}$$

We can compute each of the terms of the decomposition recursively. We illustrate it in the case of the last term, the credit risk premium, but the proof is similar for the others. Note that we can express the credit risk premium as

$$\tau y_t^{CR}(\tau) = \mathbb{E}_t\int_0^{\hat\tau}\xi_{t+s}ds + \mathbb{E}_t\int_{\hat\tau}^{\tau}\xi_{t+s}ds = \mathbb{E}_t\int_0^{\hat\tau}\xi_{t+s}ds + (\tau-\hat\tau)\mathbb{E}_t\left[y_{t+\hat\tau}^{CR}(\tau-\hat\tau)\right].$$

This uses the fact that

$$\mathbb{E}_t\int_{\hat\tau}^{\tau}\xi_{t+s}ds = \mathbb{E}_t\left(\mathbb{E}_{t+\hat\tau}\int_0^{\tau-\hat\tau}\xi_{t+\hat\tau+s}ds\right) = (\tau-\hat\tau)\mathbb{E}_t\left[y_{t+\hat\tau}^{CR}(\tau-\hat\tau)\right].$$

Then, using the affine representation $\tau y_t^{CR}(\tau) = \left[A_t^{CR}(\tau)r_t + C_t^{CR}(\tau)\right]$, we can write

$$A_t^{CR}(\tau)r_t + C_t^{CR}(\tau) = \mathbb{E}_t\int_0^{\hat\tau}\xi_{t+s}ds + \mathbb{E}_t\left[A_{t+\hat\tau}^{CR}(\tau-\hat\tau)r_{t+\hat\tau} + C_{t+\hat\tau}^{CR}(\tau-\hat\tau)\right].$$

If we take the derivative with respect to $\hat\tau$, we get

$$0 = \xi_{t+\hat\tau} + \mathbb{E}_t\left[-\left(\frac{\partial A_{t+\hat\tau}^{CR}}{\partial\tau}-\frac{\partial A_{t+\hat\tau}^{CR}}{\partial t}\right)r_{t+\hat\tau} + A_{t+\hat\tau}^{CR}(\tau-\hat\tau)\kappa(\bar r - r_{t+\hat\tau}) - \left(\frac{\partial C_{t+\hat\tau}^{CR}}{\partial\tau}-\frac{\partial C_{t+\hat\tau}^{CR}}{\partial t}\right)\right],$$

so we can then take the limit as $\hat\tau\to 0$ and separate terms:

$$\begin{aligned} 0 &= -\frac{\partial A_t^{CR}}{\partial\tau} + \frac{\partial A_t^{CR}}{\partial t} - \kappa A_t^{CR}(\tau) + \Xi_t, \\ 0 &= -\frac{\partial C_t^{CR}}{\partial\tau} + \frac{\partial C_t^{CR}}{\partial t} + A_t^{CR}(\tau)^\top\kappa\bar r + \bar\xi_{t+\hat\tau}. \end{aligned}$$

We can derive similar recursive representations for the other components. The expected future rates:

$$\begin{aligned} 0 &= -\frac{\partial A_t^{EX}}{\partial \tau} + \frac{\partial A_t^{EX}}{\partial t} - \kappa A_t^{EX}(\tau) + 1, \\ 0 &= -\frac{\partial C_t^{EX}}{\partial \tau} + \frac{\partial C_t^{EX}}{\partial t} + A_t^{EX}(\tau)^\top \kappa \bar{r}. \end{aligned}$$

The term premium:

$$\begin{aligned} 0 &= -\frac{\partial A_t^{TP}}{\partial \tau} + \frac{\partial A_t^{TP}}{\partial t} - \kappa A_t^{TP}(\tau) + \Lambda_t A_t(\tau), \\ 0 &= -\frac{\partial C_t^{TP}}{\partial \tau} + \frac{\partial C_t^{TP}}{\partial t} + A_t^{TP}(\tau)\kappa \bar{r} - \frac{\sigma^2}{2}\left[A_t(\tau)\right]^2 + A_t(\tau)\bar{\lambda}_t. \end{aligned}$$

And the expected default loss:

$$\begin{aligned} 0 &= -\frac{\partial A_t^{DL}}{\partial \tau} + \frac{\partial A_t^{DL}}{\partial t} - \kappa A_t^{DL}(\tau), \\ 0 &= -\frac{\partial C_t^{DL}}{\partial \tau} + \frac{\partial C_t^{DL}}{\partial t} + A_t^{DL}(\tau)^\top \kappa \bar{r} + \psi_t \delta. \end{aligned}$$

Defining $A_t(\tau) \equiv A_t^{CR}(\tau) + A_t^{EX}(\tau) + A_t^{TP}(\tau) + A_t^{DL}(\tau)$, and $C_t(\tau) \equiv C_t^{CR}(\tau) + C_t^{EX}(\tau) + C_t^{TP}(\tau) + C_t^{DL}(\tau)$, it is straightforward to verify these four pairs of equations sum up to the equations (56)-(57) that govern $A_t(\tau)$ and $C_t(\tau)$. Therefore solutions for (56)-(57) sum up to a solution for $A_t(\tau)$ and $C_t(\tau)$.

B.2.2 Details of Props. 2-4

To derive the formulas on which Props. 2, 3, and 4 are based, we start with equations (56)-(59) from App. B.1. In steady state, the system simplifies to

$$0 = -\frac{\partial A}{\partial \tau} - A(\tau)\kappa + 1 + \Lambda A(\tau) + \Xi. \tag{60}$$

$$0 = -\frac{\partial C}{\partial \tau} + A(\tau)\kappa \bar{r} - \frac{1}{2}\sigma^2\left[A(\tau)\right]^2 + \bar{\lambda} A(\tau) + \psi\delta + \bar{\xi}. \tag{61}$$

$$0 = -\frac{\partial A^*}{\partial \tau} - A^*(\tau)\kappa + 1 + \Lambda A^*(\tau) \tag{62}$$

$$0 = -\frac{\partial C^*}{\partial \tau} + A^*(\tau)\kappa \bar{r} - \frac{1}{2}\sigma^2\left[A^*(\tau)\right]^2 + \bar{\lambda} A^*(\tau), \tag{63}$$

where we have suppressed the time index as functions are time-invariant. Differential equations (60) and (62) can be solved as

$$A^{*}(\tau) = \frac{1-e^{-\hat{\kappa}\tau}}{\hat{\kappa}},\ A(\tau) = \frac{(1+\Xi)\left(1-e^{-\hat{\kappa}\tau}\right)}{\hat{\kappa}}, \tag{64}$$

where

$$\hat{\kappa} = \kappa - \Lambda = \kappa + \gamma\sigma^{2}\int_{0}^{\infty}\left(\alpha(\tau)\left(\frac{(1+\Xi)\left(1-e^{-\hat{\kappa}\tau}\right)}{\hat{\kappa}}\right)^{2} + \alpha^{*}(\tau)\left(\frac{1-e^{-\hat{\kappa}\tau}}{\hat{\kappa}}\right)^{2}\right)d\tau.$$

Then, integrating equations (61) and (63), we get

$$\begin{aligned} C^{*}(\tau) &= \int_{0}^{\tau}\left[A^{*}(u)\left(\kappa\bar{r}+\bar{\lambda}\right) - \frac{1}{2}\sigma^{2}\left[A^{*}(u)\right]^{2}\right]du, \\ C(\tau) &= \left(\psi\delta+\bar{\xi}\right)\tau + \int_{0}^{\tau}\left[A(u)\left(\kappa\bar{r}+\bar{\lambda}\right) - \frac{1}{2}\sigma^{2}\left[A(u)\right]^{2}\right]du. \end{aligned}$$

Next, we analyze the limit as maturity converges to zero:

$$\begin{aligned} \lim_{\tau\to 0} y_{t}(\tau) &= \left(\psi\delta+\bar{\xi}\right) + \lim_{\tau\to 0}\left[\frac{(1+\Xi)\left(1-e^{-\hat{\kappa}\tau}\right)}{\hat{\kappa}}r_{t} + A(\tau)\left(\kappa\bar{r}+\bar{\lambda}\right) - \frac{1}{2}\sigma^{2}\left[A(\tau)\right]^{2}\right] \\ &= (1+\Xi)\,r_{t} + \left(\psi\delta+\bar{\xi}\right). \end{aligned}$$

Here we have used L'Hôpital's rule to obtain

$$\lim_{\tau\to 0}\frac{(1+\Xi)\left(1-e^{-\hat{\kappa}\tau}\right)}{\hat{\kappa}\tau} = \lim_{\tau\to 0}\frac{(1+\Xi)\,\hat{\kappa}e^{-\hat{\kappa}\tau}}{\hat{\kappa}} = (1+\Xi),$$

and the fact that $A(0)=0$ to derive

$$\lim_{\tau\to 0}\frac{\int_{0}^{\tau}\left[A(u)\left(\kappa\bar{r}+\bar{\lambda}\right) - \frac{1}{2}\sigma^{2}\left[A(u)\right]^{2}\right]du}{\tau} = \lim_{\tau\to 0}A(\tau)\left(\kappa\bar{r}+\bar{\lambda}\right) - \tfrac{1}{2}\sigma^{2}\left[A(\tau)\right]^{2} = 0.$$

B.3 Solving the model with demand risk

For the model extension with demand risk factors, we again conjecture deterministic functions $(A_{t}(\tau), C_{t}(\tau))$ and $(A_{t}^{*}(\tau), C_{t}^{*}(\tau))$, where $A_{t}(\tau) = \left(A_{t}^{r}(\tau), A_{t}^{h}(\tau), A_{t}^{h*}(\tau)\right)^{\top}$ and $A_{t}^{*}(\tau) = \left(A_{t}^{*r}(\tau), A_{t}^{*h}(\tau), A_{t}^{*h*}(\tau)\right)^{\top}$, such that bond prices can be expressed in

log-affine form:

$$P_t(\tau) = e^{-\left[A_t(\tau)^\top q_t + C_t(\tau)\right]},\ P_t^*(\tau) = e^{-\left[A_t^*(\tau)^\top q_t + C_t^*(\tau)\right]}. \tag{65}$$

Applying Itô's lemma, the time-t instantaneous return on an undefaulted bond of maturity τ is

$$\frac{dP_t(\tau)}{P_t(\tau)} = \mu_t(\tau)\,dt - A_t(\tau)^\top \Sigma dB_t,\ \frac{dP_t^*(\tau)}{P_t^*(\tau)} = \mu_t^*(\tau)\,dt - A_t^*(\tau)^\top \Sigma dB_t, \tag{66}$$

where[68]

$$\mu_t(\tau) = \left(\frac{\partial A_t}{\partial \tau} - \frac{\partial A_t}{\partial t}\right)^\top q_t + \left(\frac{\partial C_t}{\partial \tau} - \frac{\partial C_t}{\partial t}\right) - A_t(\tau)^\top K(\bar{r}\mathcal{E}_1 - q_t) + \frac{1}{2}A_t(\tau)^\top \Sigma\Sigma^\top A(\tau), \tag{67}$$

and

$$\mu_t^*(\tau) = \left(\frac{\partial A_t^*}{\partial \tau} - \frac{\partial A_t^*}{\partial t}\right)^\top q_t + \left(\frac{\partial C_t^*}{\partial \tau} - \frac{\partial C_t^*}{\partial t}\right) - A_t^*(\tau)^\top K(\bar{r}\mathcal{E}_1 - q_t) + \frac{1}{2}A_t^*(\tau)^\top \Sigma\Sigma^\top A^*(\tau). \tag{68}$$

The first-order conditions on the arbitrageurs' portfolio weights are

$$\mu_t(\tau) = r_t + A_t(\tau)^\top \lambda_t + \psi_t\delta + \xi_t, \tag{69}$$

$$\mu_t^*(\tau) = r_t + A_t^*(\tau)^\top \lambda_t, \tag{70}$$

where

$$\lambda_t = \gamma\Sigma\Sigma^\top \int_0^\infty \left(X_t(\tau)\,A_t(\tau) + X_t^*(\tau)\,A_t^*(\tau)\right)d\tau \tag{71}$$

and

$$\xi_t = \gamma\psi_t\delta^2 \int_0^\infty X_t(\tau)\,d\tau, \tag{72}$$

where λ_t is a 3x1 vector and ξ_t is a scalar.

Since preferred habitat demand is assumed to be affine in q_t, plugging the market clearing conditions into (71)-(72) implies that $\lambda_t = \Lambda_t^\top q_t + \bar{\lambda}_t$ and $\xi_t = \Xi_t^\top q_t + \bar{\xi}_t$ must

[68] Note that τ is a state with dynamics $d\tau = -dt$, so Itô's lemma yields derivatives in τ as well as t.

also be affine functions, with the following coefficients:

$$\begin{aligned}
\Lambda_t^\top &\equiv \gamma\Sigma\Sigma^\top \int_0^\infty \left(\varsigma(\tau) A_t(\tau)\mathcal{E}_2^\top - \alpha(\tau) A_t(\tau) A_t(\tau)^\top + \varsigma^*(\tau) A_t^*(\tau)\mathcal{E}_3^\top - \alpha^*(\tau) A_t^*(\tau) A_t^*(\tau)^\top\right) d\tau, \\
\bar{\lambda}_t &\equiv \gamma\Sigma\Sigma^\top \int_0^\infty \left[\left(S_t(\tau) - h_t(\tau) - \alpha(\tau) C_t(\tau) + \tau\alpha(\tau)\hat{\delta}\psi_t\right) A_t(\tau) + \left(S_t^*(\tau) - h_t^*(\tau) - \alpha^*(\tau) C_t^*(\tau)\right) A_t^*(\tau)\right] d\tau, \\
\Xi_t^\top &\equiv \gamma\psi_t\delta^2 \int_0^\infty \left[\varsigma(\tau)\mathcal{E}_2^\top - \alpha(\tau) A_t(\tau)^\top\right] d\tau, \\
\bar{\xi}_t &\equiv \gamma\psi_t\delta^2 \int_0^\infty \left(S_t(\tau) - h_t(\tau) - \alpha(\tau) C_t(\tau) + \tau\alpha(\tau)\hat{\delta}\psi_t\right) d\tau,
\end{aligned}$$

where $\mathcal{E}_2 = (0,1,0)^\top$ and $\mathcal{E}_3 = (0,0,1)^\top$. Notice that Λ_t is a 3x3 matrix, $\bar{\lambda}_t$ and Ξ_t are 3x1 vectors, and $\bar{\xi}_t$ is a scalar. Using this notation, the first-order conditions become:

$$\begin{aligned}
0 &= -\left(\frac{\partial A_t}{\partial\tau} - \frac{\partial A_t}{\partial t}\right)^\top q_t - \left(\frac{\partial C_t}{\partial\tau} - \frac{\partial C_t}{\partial t}\right) + A(\tau)^\top K(\bar{r}\mathcal{E}_1 - q_t) - \frac{1}{2} A_t(\tau)^\top \Sigma\Sigma^\top A_t(\tau) \\
&+ \mathcal{E}_1^\top q_t + A_t(\tau)^\top\left(\Lambda_t^\top q_t + \bar{\lambda}_t\right) + \psi_t\delta + \left(\Xi_t^\top q_t + \bar{\xi}_t\right),
\end{aligned}$$

and

$$\begin{aligned}
0 &= -\left(\frac{\partial A_t^*}{\partial\tau} - \frac{\partial A_t^*}{\partial t}\right)^\top q_t - \left(\frac{\partial C_t^*}{\partial\tau} - \frac{\partial C_t^*}{\partial t}\right) + A_t^*(\tau)^\top K(\bar{r}\mathcal{E}_1 - q_t) - \frac{1}{2} A_t^*(\tau)^\top \Sigma\Sigma^\top A_t^*(\tau) \\
&+ \mathcal{E}_1^\top q_t + A_t^*(\tau)^\top\left(\Lambda_t^\top q_t + \bar{\lambda}_t\right).
\end{aligned}$$

Transposing these equations and separating the terms with and without q, we must have

$$0 = -\frac{\partial A_t}{\partial\tau} + \frac{\partial A_t}{\partial t} - K^\top A_t(\tau) + \Lambda_t A_t(\tau) + \mathcal{E}_1 + \Xi_t. \tag{73}$$

$$0 = -\frac{\partial C_t}{\partial\tau} + \frac{\partial C_t}{\partial t} + A_t(\tau)^\top K\mathcal{E}_1\bar{r} + A_t(\tau)^\top\bar{\lambda}_t - \frac{1}{2} A_t(\tau)^\top\Sigma\Sigma^\top A_t(\tau) + \psi_t\delta + \bar{\xi}_t. \tag{74}$$

$$0 = -\frac{\partial A_t^*}{\partial\tau} + \frac{\partial A_t^*}{\partial t} - K^\top A_t^*(\tau) + \Lambda_t A_t^*(\tau) + \mathcal{E}_1 \tag{75}$$

$$0 = -\frac{\partial C_t^*}{\partial\tau} + \frac{\partial C_t^*}{\partial t} + A_t^*(\tau)^\top K\mathcal{E}_1\bar{r} + A_t^*(\tau)^\top\bar{\lambda}_t - \frac{1}{2} A_t^*(\tau)^\top\Sigma\Sigma^\top A_t^*(\tau). \tag{76}$$

This system of PDEs suffices to determine the functions $(A_t(\tau), C_t(\tau))$ and $(A_t^*(\tau), C_t^*(\tau))$, verifying our guess that the bond price is an affine function of q_t.[69]

[69] Equations (73) and (75) correspond to equation (36) of Vayanos and Vila (2021), while equations (74) and (76) correspond to their (38).

B.4 Model-generated moments

The yields for maturity τ in the periphery and core are

$$y_t(\tau) = \tau^{-1}\left(A_t^r(\tau) r_t + A_t^h(\tau)\varepsilon_t^h + A_t^{h*}(\tau)\varepsilon_t^{h*} + C_t(\tau)\right),$$

$$y_t^*(\tau) = \tau^{-1}\left(A_t^{*r}(\tau) r_t + A_t^{*h}(\tau)\varepsilon_t^h + A_t^{*h*}(\tau)\varepsilon_t^{h*} + C_t^*(\tau)\right).$$

Assuming that the demand risk factors are independent from the short-term rate, the volatility of yields in the ergodic distribution is

$$\sqrt{\mathbb{V}\text{ar}\left(y_t(\tau)\right)} = \frac{\sqrt{A^r(\tau)^2 \frac{\sigma_r^2}{2\kappa_r} + A^h(\tau)^2 \frac{\sigma_\varepsilon^2}{2\kappa_\varepsilon} + A^{h*}(\tau)^2 \frac{\sigma_{\varepsilon*}^2}{2\kappa_{\varepsilon*}} + 2A^h(\tau) A^{h*}(\tau)\mathbb{C}\text{ov}\left(\varepsilon_t^h, \varepsilon_t^{h*}\right)}}{\tau},$$

$$\sqrt{\mathbb{V}\text{ar}\left(y_t^*(\tau)\right)} = \frac{\sqrt{A^{*r}(\tau)^2 \frac{\sigma_r^2}{2\kappa_r} + A^{*h}(\tau)^2 \frac{\sigma_\varepsilon^2}{2\kappa_\varepsilon} + A^{*h*}(\tau)^2 \frac{\sigma_{\varepsilon*}^2}{2\kappa_{\varepsilon*}} + 2A^{*h}(\tau) A^{*h*}(\tau)\mathbb{C}\text{ov}\left(\varepsilon_t^h, \varepsilon_t^{h*}\right)}}{\tau}.$$

C Appendix: Computing the solution

C.1 Parameters

The parameters of our numerical model are reported in Table 6. The model is programmed with a monthly time unit (the units have been converted to annualized terms, for clarity, in Table 1 of the main text). The monthly time unit is convenient because it allows us to verify our results by running either a continuous-time method (App. C.2) or a discrete-time method (App. C.3.2), without any parameter transformations; the calibration stated in Table 6 applies to both algorithms.

C.2 Numerical algorithm: continuous time

C.2.1 Finite-difference computation of the long-run solution

The long-run solution of our model must satisfy the system of ODEs (60)-(63). These can be solved by a finite difference method.[70] To do so, we consider a grid of maturities

[70] We have defined and computed both continuous-time and discrete-time versions of the model. The discrete time version is described in the next section. Numerical simulations of both versions give the same results.

Table 6: Calibration

Parameters*	**Values**
Parameters calibrated directly from observables	
$\bar{r}$: Mean of monthly risk-free rate r_t	0.00102
κ: Monthly mean reversion of r_t	0.0052
σ : Standard deviation of monthly innovations to r_t	0.000153
Parameters estimated by minimizing the distance criterion	
γ: Risk aversion	0.0108
$\underline{\psi}$: Default probability intercept	0.000718
θ: Slope of default rate	1.71×10^{-5}
$\hat{r} + \phi$: Discount rate in fiscal pressure aggregate	0.0305
κ_h: Monthly mean reversion of PH shocks	0.000447
σ_h: Volatility of monthly PH innovations	144.2
υ_h: Relative volatility of IT PH demand	0.300
χ_h: Demand correlation parameter	-0.558
α_h: Slope parameter of PH demand	9.60×10^4
ζ: Remittance rule coefficient	1

* Parameters are expressed in terms of a monthly time unit. The unit of value is billions of euros.

$(\tau_1, .., \tau_I)$ with $\tau_0 = 0$ and constant step size $\Delta\tau$, so that $\tau_i \equiv \tau(i) = i\Delta\tau$. Define

$$\begin{aligned} A_i &= A(\tau_i), A_i^* = A^*(\tau_i), C_i = C(\tau_i), C_i^* = C^*(\tau_i), \\ S_i &= S(\tau_i), S_i^* = S^*(\tau_i), \alpha_i = \alpha(\tau_i), \alpha_i^* = \alpha^*(\tau_i), \\ h &= h(\tau_i), h_i^* = h^*(\tau_i). \end{aligned}$$

The boundary conditions are $A_0 = A(0) = 0$ and $C_0 = C(0) = 0$ because an instantaneous bond trades at par. We begin with a guess of A_i^n, A_i^{n*}, with $n = 0$. For instance, we can begin with $A_i^n = A_i^{n*} = \tau_i$ and $C_i^n = C_i^{n*} = 0$. Then, considering a backward finite-difference approximation $\frac{\partial A^{n+1}(\tau(i))}{\partial \tau} \approx \frac{A_i^{n+1} - A_{i-1}^{n+1}}{\Delta\tau}$, and likewise for the other unknown functions, we approximate the ODEs as:

$$\frac{A_i^{n+1} - A_{i-1}^{n+1}}{\Delta\tau} = A_i^{n+1}(\Lambda^n - \kappa) + 1 + \Xi^n,$$

$$\frac{C_i^{n+1} - C_{i-1}^{n+1}}{\Delta\tau} = A_i^{n+1}\left(\bar{\lambda}^n + \kappa\bar{r}\right) - \frac{1}{2}\sigma^2\left[A_i^{n+1}\right]^2 + \underline{\psi}\delta + \bar{\xi}^n,$$

$$\frac{A_i^{(n+1)*} - A_{i-1}^{(n+1)*}}{\Delta\tau} = A_i^{(n+1)*}(\Lambda^n - \kappa) + 1,$$

$$\frac{C_i^{(n+1)*} - C_{i-1}^{(n+1)*}}{\Delta\tau} = A_i^{(n+1)*}\left(\bar{\lambda}^n + \kappa\bar{r}\right) - \frac{1}{2}\sigma^2\left[A_i^{(n+1)*}\right]^2,$$

where

$$\begin{aligned}
\Lambda^n &= -\gamma\sigma^2\sum_{i=1}^{I}\left(\alpha_i\left[A_i^n\right]^2 + \alpha_i^*\left[A_i^{n*}\right]^2\right)\Delta\tau, \\
\bar{\lambda}^n &= \gamma\sigma^2\sum_{i=1}^{I}\left[\left(S_i - h_i - \alpha_i C_i^n + i\alpha_i\hat{\delta}\underline{\psi}\right)A_i^n + \left(S_i^* - h_i^* - \alpha_i^* C_i^{n*}\right)A_i^{n*}\right]\Delta\tau, \\
\Xi^n &= -\gamma\underline{\psi}\delta^2\sum_{i=1}^{I}\alpha_i A_i^n\Delta\tau. \\
\xi^n &= \gamma\underline{\psi}\delta^2\sum_{i=1}^{I}\left[\left(S_i - h_i - \alpha_i C_i^n + i\alpha_i\hat{\delta}\underline{\psi}\right)\right]\Delta\tau.
\end{aligned}$$

In matrix form, this amounts to

$$\overbrace{\begin{bmatrix}
\frac{1}{\Delta\tau} - \Lambda^n + \kappa & 0 & 0 & \cdots & 0 \\
-\frac{1}{\Delta\tau} & \frac{1}{\Delta\tau} - \Lambda^n + \kappa & 0 & \cdots & 0 \\
\vdots & -\frac{1}{\Delta\tau} & \frac{1}{\Delta\tau} - \Lambda^n + \kappa & \cdots & \vdots \\
0 & 0 & \cdots & \ddots & 0 \\
0 & 0 & \cdots & -\frac{1}{\Delta\tau} & \frac{1}{\Delta\tau} - \Lambda^n + \kappa
\end{bmatrix}}^{\mathbf{F^n}}
\overbrace{\begin{bmatrix} A_1^{n+1} \\ A_2^{n+1} \\ \vdots \\ A_{I-1}^{n+1} \\ A_I^{n+1} \end{bmatrix}}^{\mathbf{A^{n+1}}}
= \overbrace{\begin{bmatrix} 1+\Xi^n \\ 1+\Xi^n \\ \vdots \\ 1+\Xi^n \\ 1+\Xi^n \end{bmatrix}}^{\mathbf{f^n}}, \tag{77}$$

$$\begin{bmatrix}
\frac{1}{\Delta\tau} - \Lambda^n + \kappa & 0 & 0 & \cdots & 0 \\
-\frac{1}{\Delta\tau} & \frac{1}{\Delta\tau} - \Lambda^n + \kappa & 0 & \cdots & 0 \\
\vdots & -\frac{1}{\Delta\tau} & \frac{1}{\Delta\tau} - \Lambda^n + \kappa & \cdots & \vdots \\
0 & 0 & \cdots & \ddots & 0 \\
0 & 0 & \cdots & -\frac{1}{\Delta\tau} & \frac{1}{\Delta\tau} - \Lambda^n + \kappa
\end{bmatrix}
\overbrace{\begin{bmatrix} A_1^{(n+1)*} \\ A_2^{(n+1)*} \\ \vdots \\ A_{I-1}^{(n+1)*} \\ A_I^{(n+1)*} \end{bmatrix}}^{\mathbf{A^{(n+1)*}}}
= \overbrace{\begin{bmatrix} 1 \\ 1 \\ \vdots \\ 1 \\ 1 \end{bmatrix}}^{\mathbf{f^*}}, \tag{78}$$

$$\overbrace{\begin{bmatrix} \frac{1}{\Delta\tau} & 0 & 0 & \cdots & 0 \\ -\frac{1}{\Delta\tau} & \frac{1}{\Delta\tau} & 0 & \cdots & 0 \\ \vdots & -\frac{1}{\Delta\tau} & \frac{1}{\Delta\tau} & \cdots & \vdots \\ 0 & 0 & \cdots & \ddots & 0 \\ 0 & 0 & \cdots & -\frac{1}{\Delta\tau} & \frac{1}{\Delta\tau} \end{bmatrix}}^{\mathbf{G}} \overbrace{\begin{bmatrix} C_1^{n+1} \\ C_2^{n+1} \\ \vdots \\ C_{I-1}^{n+1} \\ C_I^{n+1} \end{bmatrix}}^{\mathbf{C^{n+1}}} = \overbrace{\begin{bmatrix} A_1^{n+1}\left(\bar{\lambda}^n + \kappa\bar{r}\right) - \frac{1}{2}\sigma^2\left[A_1^{n+1}\right]^2 + \underline{\psi}\delta + \bar{\xi}^n \\ A_2^{n+1}\left(\bar{\lambda}^n + \kappa\bar{r}\right) - \frac{1}{2}\sigma^2\left[A_2^{n+1}\right]^2 + \underline{\psi}\delta + \bar{\xi}^n \\ \vdots \\ A_{I-1}^{n+1}\left(\bar{\lambda}^n + \kappa\bar{r}\right) - \frac{1}{2}\sigma^2\left[A_{I-1}^{n+1}\right]^2 + \underline{\psi}\delta + \bar{\xi}^n \\ A_I^{n+1}\left(\bar{\lambda}^n + \kappa\bar{r}\right) - \frac{1}{2}\sigma^2\left[A_I^{n+1}\right]^2 + \underline{\psi}\delta + \bar{\xi}^n \end{bmatrix}}^{\mathbf{g^{n+1}}}, \tag{79}$$

$$\begin{bmatrix} \frac{1}{\Delta\tau} & 0 & 0 & \cdots & 0 \\ -\frac{1}{\Delta\tau} & \frac{1}{\Delta\tau} & 0 & \cdots & 0 \\ \vdots & -\frac{1}{\Delta\tau} & \frac{1}{\Delta\tau} & \cdots & \vdots \\ 0 & 0 & \cdots & \ddots & 0 \\ 0 & 0 & \cdots & -\frac{1}{\Delta\tau} & \frac{1}{\Delta\tau} \end{bmatrix} \overbrace{\begin{bmatrix} C_1^{(n+1)*} \\ C_2^{(n+1)*} \\ \vdots \\ C_{I-1}^{(n+1)*} \\ C_I^{(n+1)*} \end{bmatrix}}^{\mathbf{C^{(n+1)*}}} = \overbrace{\begin{bmatrix} A_1^{(n+1)*}\left(\bar{\lambda}^n + \kappa\bar{r}\right) - \frac{1}{2}\sigma^2\left[A_1^{(n+1)*}\right]^2 \\ A_2^{(n+1)*}\left(\bar{\lambda}^n + \kappa\bar{r}\right) - \frac{1}{2}\sigma^2\left[A_2^{(n+1)*}\right]^2 \\ \vdots \\ A_{I-1}^{(n+1)*}\left(\bar{\lambda}^n + \kappa\bar{r}\right) - \frac{1}{2}\sigma^2\left[A_{I-1}^{(n+1)*}\right]^2 \\ A_I^{(n+1)*}\left(\bar{\lambda}^n + \kappa\bar{r}\right) - \frac{1}{2}\sigma^2\left[A_I^{(n+1)*}\right]^2 \end{bmatrix}}^{\mathbf{g^{(n+1)*}}}, \tag{80}$$

where we have already applied the boundary conditions.

The idea is to solve equations (77) and (78) iteratively from the initial guess, updating Λ^n and Ξ^n and at each step, and then calculate $\bar{\lambda}^n$ and $\bar{\xi}^n$ in order to solve (79) and (80) in a single step.

C.2.2 Finite-difference computation: long-run, multifactor case

The long-run solution of our model must satisfy the system of ODEs (73)-(76). The boundary conditions are $A_0 = A(0) = (0,0,0)^\top$ and $C_0 = C(0) = 0$ because an instantaneous bond trades at par. We begin by guessing the 3x1 vectors A_i^n, A_i^{n*} and the scalars C_i^n, C_i^{n*} at iteration step $n = 0$. Then, using the backward finite-difference approximation $\frac{\partial A^{n+1}(\tau(i))}{\partial\tau} \approx \frac{A_i^{n+1} - A_{i-1}^{n+1}}{\Delta\tau}$, and likewise for the other unknown functions, we approximate the ODEs as:

$$\frac{A_i^{n+1} - A_{i-1}^{n+1}}{\Delta\tau} = \left(\Lambda^n - K^\top\right) A_i^{n+1} + \mathcal{E}_1 + \Xi^n,$$

$$\frac{C_i^{n+1} - C_{i-1}^{n+1}}{\Delta\tau} = \left(A_i^{n+1}\right)^\top \left(\bar{\lambda}^n + K\mathcal{E}_1\bar{r}\right) - \frac{1}{2}\left(A_i^{n+1}\right)^\top \Sigma\Sigma^\top A_i^{n+1} + \underline{\psi}\delta + \bar{\xi}^n,$$

$$\frac{A_i^{(n+1)*} - A_{i-1}^{(n+1)*}}{\Delta\tau} = \left(\Lambda^n - K^\top\right) A_i^{(n+1)*} + \mathcal{E}_1,$$

$$\frac{C_i^{(n+1)*} - C_{i-1}^{(n+1)*}}{\Delta\tau} = \left(A_i^{(n+1)*}\right)^\top \left(\bar{\lambda}^n + K\mathcal{E}_1\bar{r}\right) - \frac{1}{2}\left(A_i^{(n+1)*}\right)^\top \Sigma\Sigma^\top A_i^{(n+1)*},$$

where

$$\begin{aligned}
\Lambda^n &= \gamma \sum_{i=1}^{I} \left(\varsigma_i \mathcal{E}_2 \left(A_i^n\right)^\top - \alpha_i A_i^n \left(A_i^n\right)^\top + \varsigma_i^* \mathcal{E}_3 \left(A_i^{n*}\right)^\top - \alpha_i^* A_i^{n*} \left(A_i^{n*}\right)^\top\right) \Sigma\Sigma^\top \Delta\tau, \\
\bar{\lambda}^n &= \gamma\Sigma\Sigma^\top \sum_{i=1}^{I} \left[\left(S_i - h_i - \alpha_i C_i^n + i\alpha_i \hat{\delta}\underline{\psi}\right) A_i^n + \left(S_i^* - h_i^* - \alpha_i^* C^{n*}\right) A_i^{n*}\right] \Delta\tau, \\
\Xi^n &= \gamma\underline{\psi}\delta^2 \sum_{i=1}^{I} \left(\varsigma_i \mathcal{E}_2 - \alpha_i \left(A_i^n\right)\right) \Delta\tau. \\
\xi^n &= \gamma\underline{\psi}\delta^2 \sum_{i=1}^{I} \left[\left(S_i - h_i - \alpha_i C_i^n + i\alpha_i \hat{\delta}\underline{\psi}\right)\right] \Delta\tau.
\end{aligned}$$

In matrix form, using I_3 to indicate the 3x3 identity matrix, this amounts to

$$\overbrace{\begin{bmatrix}
\frac{1}{\Delta\tau} I_3 - \Lambda^n + K^\top & 0 & 0 & \cdots & 0 \\
-\frac{1}{\Delta\tau} I_3 & \frac{1}{\Delta\tau} I_3 - \Lambda^n + K^\top & 0 & \cdots & 0 \\
\vdots & -\frac{1}{\Delta\tau} I_3 & \frac{1}{\Delta\tau} I_3 - \Lambda^n + K^\top & \cdots & \vdots \\
0 & 0 & \cdots & \ddots & 0 \\
0 & 0 & \cdots & -\frac{1}{\Delta\tau} I_3 & \frac{1}{\Delta\tau} I_3 - \Lambda^n + K^\top
\end{bmatrix}}^{\mathbf{F^n}}
\overbrace{\begin{bmatrix} A_1^{n+1} \\ A_2^{n+1} \\ \vdots \\ A_{I-1}^{n+1} \\ A_I^{n+1} \end{bmatrix}}^{\mathbf{A^{n+1}}}
= \overbrace{\begin{bmatrix} \mathcal{E}_1 + \Xi^n \\ \mathcal{E}_1 + \Xi^n \\ \vdots \\ \mathcal{E}_1 + \Xi^n \\ \mathcal{E}_1 + \Xi^n \end{bmatrix}}^{\mathbf{f^n}}, \tag{81}$$

$$\overbrace{\begin{bmatrix}
\frac{1}{\Delta\tau} I_3 - \Lambda^n + K^\top & 0 & 0 & \cdots & 0 \\
-\frac{1}{\Delta\tau} I_3 & \frac{1}{\Delta\tau} I_3 - \Lambda^n + K^\top & 0 & \cdots & 0 \\
\vdots & -\frac{1}{\Delta\tau} I_3 & \frac{1}{\Delta\tau} I_3 - \Lambda^n + K^\top & \cdots & \vdots \\
0 & 0 & \cdots & \ddots & 0 \\
0 & 0 & \cdots & -\frac{1}{\Delta\tau} I_3 & \frac{1}{\Delta\tau} I_3 - \Lambda^n + \kappa
\end{bmatrix}}^{}
\overbrace{\begin{bmatrix} A_1^{(n+1)*} \\ A_2^{(n+1)*} \\ \vdots \\ A_{I-1}^{(n+1)*} \\ A_I^{(n+1)*} \end{bmatrix}}^{\mathbf{A^{(n+1)*}}}
= \overbrace{\begin{bmatrix} \mathcal{E}_1 \\ \mathcal{E}_1 \\ \vdots \\ \mathcal{E}_1 \\ \mathcal{E}_1 \end{bmatrix}}^{\mathbf{f^*}}, \tag{82}$$

$$\overbrace{\begin{bmatrix} \frac{1}{\Delta\tau} & 0 & 0 & \cdots & 0 \\ -\frac{1}{\Delta\tau} & \frac{1}{\Delta\tau} & 0 & \cdots & 0 \\ \vdots & -\frac{1}{\Delta\tau} & \frac{1}{\Delta\tau} & \cdots & \vdots \\ 0 & 0 & \cdots & \ddots & 0 \\ 0 & 0 & \cdots & -\frac{1}{\Delta\tau} & \frac{1}{\Delta\tau} \end{bmatrix}}^{\mathbf{G}} \overbrace{\begin{bmatrix} C_1^{n+1} \\ C_2^{n+1} \\ \vdots \\ C_{I-1}^{n+1} \\ C_I^{n+1} \end{bmatrix}}^{\mathbf{C^{n+1}}} = \overbrace{\begin{bmatrix} \left(A_1^{n+1}\right)^\top \left(\bar{\lambda}^n + K\mathcal{E}_1\bar{r}\right) - \frac{1}{2}\left(A_1^{n+1}\right)^\top \Sigma\Sigma^\top A_1^{n+1} + \underline{\psi}\delta + \bar{\xi}^n \\ \left(A_2^{n+1}\right)^\top \left(\bar{\lambda}^n + K\mathcal{E}_1\bar{r}\right) - \frac{1}{2}\left(A_2^{n+1}\right)^\top \Sigma\Sigma^\top A_2^{n+1} + \underline{\psi}\delta + \bar{\xi}^n \\ \vdots \\ \left(A_{I-1}^{n+1}\right)^\top \left(\bar{\lambda}^n + K\mathcal{E}_1\bar{r}\right) - \frac{1}{2}\left(A_{I-1}^{n+1}\right)^\top \Sigma\Sigma^\top A_{I-1}^{n+1} + \underline{\psi}\delta + \bar{\xi}^n \\ \left(A_I^{n+1}\right)^\top \left(\bar{\lambda}^n + K\mathcal{E}_1\bar{r}\right) - \frac{1}{2}\left(A_I^{n+1}\right)^\top \Sigma\Sigma^\top A_I^{n+1} + \underline{\psi}\delta + \bar{\xi}^n \end{bmatrix}}^{\mathbf{g^{n+1}}}, \tag{83}$$

$$\begin{bmatrix} \frac{1}{\Delta\tau} & 0 & 0 & \cdots & 0 \\ -\frac{1}{\Delta\tau} & \frac{1}{\Delta\tau} & 0 & \cdots & 0 \\ \vdots & -\frac{1}{\Delta\tau} & \frac{1}{\Delta\tau} & \cdots & \vdots \\ 0 & 0 & \cdots & \ddots & 0 \\ 0 & 0 & \cdots & -\frac{1}{\Delta\tau} & \frac{1}{\Delta\tau} \end{bmatrix} \overbrace{\begin{bmatrix} C_1^{(n+1)*} \\ C_2^{(n+1)*} \\ \vdots \\ C_{I-1}^{(n+1)*} \\ C_I^{(n+1)*} \end{bmatrix}}^{\mathbf{C^{(n+1)*}}} = \overbrace{\begin{bmatrix} \left(A_1^{(n+1)*}\right)^\top \left(\bar{\lambda}^n + K\mathcal{E}_1\bar{r}\right) - \frac{1}{2}\left(A_1^{(n+1)*}\right)^\top \Sigma\Sigma^\top A_1^{(n+1)*} \\ \left(A_2^{(n+1)*}\right)^\top \left(\bar{\lambda}^n + K\mathcal{E}_1\bar{r}\right) - \frac{1}{2}\left(A_2^{(n+1)*}\right)^\top \Sigma\Sigma^\top A_2^{(n+1)*} \\ \vdots \\ \left(A_{I-1}^{(n+1)*}\right)^\top \left(\bar{\lambda}^n + K\mathcal{E}_1\bar{r}\right) - \frac{1}{2}\left(A_{I-1}^{(n+1)*}\right)^\top \Sigma\Sigma^\top A_{I-1}^{(n+1)*} \\ \left(A_I^{(n+1)*}\right)^\top \left(\bar{\lambda}^n + K\mathcal{E}_1\bar{r}\right) - \frac{1}{2}\left(A_I^{(n+1)*}\right)^\top \Sigma\Sigma^\top A_I^{(n+1)*} \end{bmatrix}}^{\mathbf{g^{(n+1)*}}}, \tag{84}$$

where we have already applied the boundary conditions. In these equations, $\mathbf{A^{n+1}}$ and $\mathbf{A^{(n+1)*}}$ are vectors of length $3I$, while $\mathbf{C^{n+1}}$ and $\mathbf{C^{(n+1)*}}$ are vectors of length I, while $\mathbf{F^n}$ and $\mathbf{G}$ are matrices of size $3I \times 3I$ and $I \times I$, respectively.

The idea is to solve equations (81) and (82) iteratively from the initial guess, updating Λ^n and Ξ^n and at each step, and then calculate $\bar{\lambda}^n$ and $\bar{\xi}^n$ in order to solve (83) and (84) in a single step.

C.2.3 Computing the dynamics

To compute the dynamics, consider a distant terminal time T at which the model has converged to the long-run solution. We solve the PDEs (56)-(59) backwards from time T with time steps of size $\Delta t \equiv \Delta\tau$, so that backwards induction step n refers to calendar time $t(n) \equiv T - n\Delta\tau$. Using the fact that $A_i^{n+1} - A_i^n \approx -\frac{\partial A^n(\tau(i))}{\partial t}\Delta\tau$, the PDEs can be discretized as follows::

$$\begin{aligned} \frac{\mathbf{A^{n+1}} - \mathbf{A^n}}{\Delta\tau} + \mathbf{F^n}\mathbf{A^n} &= \mathbf{f^n}, \\ \frac{\mathbf{A^{(n+1)*}} - \mathbf{A^{n*}}}{\Delta\tau} + \mathbf{F^n}\mathbf{A^{n*}} &= \mathbf{f^*}, \\ \frac{\mathbf{C^{n+1}} - \mathbf{C^n}}{\Delta\tau} + \mathbf{G}\mathbf{C^n} &= \mathbf{g^n}, \\ \frac{\mathbf{C^{(n+1)*}} - \mathbf{C^{n*}}}{\Delta\tau} + \mathbf{G}\mathbf{C^{n*}} &= \mathbf{g^{n*}}. \end{aligned}$$

Matrices $\mathbf{F}^{\mathrm{n}}$, $\mathbf{G}$, $\mathbf{f}^{\mathrm{n}}$, $\mathbf{f}^{*}$, $\mathbf{g}^{\mathrm{n}}$, and $\mathbf{g}^{\mathrm{n}*}$ are defined as before, except that we calculate Λ_t, Ξ_t, $\bar{\lambda}_t$, and $\bar{\xi}_t$ under time-varying conditions. In particular, we evaluate them conditional on the net bond supply $S_t(\tau)$ and default rate ψ_t at time $t = t(n)$.[71]

C.3 Discrete time representation

Here we present the discrete-time counterpart of the model, along the lines of Hamilton and Wu (2012) .

C.3.1 Single-factor case

It is straightforward to derive and compute a discrete-time framework equivalent to our continuous-time model. In discrete time, we write the price of a bond with a maturity of i periods, issued by jurisdiction $j \in \{P, C\}$ ("Periphery" or "Core"), as $P_{i,t}^{j} = \exp\left(p_{i,t}^{j}\right) = \exp\left(-A_{i,t}^{j} r_t - C_{i,t}^{j}\right)$. Let the rate on reserves follow $r_{t+1} = \rho r_t + (1-\rho)\bar{r} + \sigma\varepsilon_{t+1}$, where $\varepsilon_{t+1} \sim N(0,1)$. If arbitrageurs maximize a mean-variance utility function over the increase of their wealth, then if the time period is sufficiently short, their optimization problem can be approximated as follows:[72]

$$\begin{aligned}
\max_{\{X_{i,t}^{j}\}} \quad & \left(W_t - \textstyle\sum_{i=1}^{I}\sum_{j\in\{P,C\}} X_{i,t}^{j}\right) r_t \\
+ \quad & \textstyle\sum_{i=1}^{I}\sum_{j\in\{P,C\}} X_{i,t}^{j}\left(-C_{i-1,t+1}^{j} - A_{i-1,t+1}^{j}\left((1-\rho)\bar{r} + \rho r_t\right) + C_{i,t}^{j} + A_{i,t}^{j} r_t + \frac{\sigma^2}{2}\left(A_{i-1,t+1}^{j}\right)^2 - \delta\psi_t^{j}\right) \\
- \quad & \frac{\gamma\sigma^2}{2}\left[\textstyle\sum_{i=2}^{I}\sum_{j\in\{P,C\}} X_{i,t}^{j} A_{i-1,t+1}^{j}\right]^2 - \frac{\gamma\psi_t^{P}}{2}\delta^2\left[\textstyle\sum_{i=1}^{I} X_{i,t}^{P}\right]^2 .
\end{aligned}$$

where $\psi_t^{C} = 0$ denotes the Core default probability, and $\psi_t^{P} = \psi_t$ is the Peripheral default probability, given by (31). Hence, the first-order condition on the investment $X_{i,t}^{j}$ in bonds of maturity i from jurisdiction j is

$$r_t = -\left(C_{i-1,t+1}^{j} + A_{i-1,t+1}^{j}\left((1-\rho)\bar{r} + \rho r_t\right)\right) + \left(C_{i,t}^{j} + A_{i,t}^{j} r_t\right) + \frac{\sigma^2}{2}\left(A_{i-1,t+1}^{j}\right)^2 - \delta\psi_t^{j} - A_{i-1,t+1}^{j}\lambda_t - \xi_t^{j},$$

[71] Inspecting the definitions of the matrices in (77)-(80), we see that this algorithm calculates equilibrium objects at time $t(n) - \Delta\tau$ using the risk prices $\lambda_{t(n)}$ and $\xi_{t(n)}$ from time $t(n)$. It would therefore be incorrect to apply this algorithm with a large time step $\Delta\tau$, but in the limit as $\Delta\tau \to 0$, it gives the correct solution of the continuous-time PDE.

[72] See Hamilton and Wu (2012) for details.

where

$$\lambda_t = \gamma\sigma^2 \sum_{i=2}^{I} \sum_{j\in\{P,C\}} X_{i,t}^j A_{i-1,t+1}^j,$$

$$\xi_t^j = \gamma\psi_t^j\delta^2 \sum_{i=1}^{I} X_{i,t}^j \ .$$

Note that since $A_{0,t}^j = C_{0,t}^j = 0$, the first-order conditions for holdings of one-period bonds are simply

$$r_t = y_{1,t}^C = C_{1,t}^C + A_{1,t}^C r_t \ , \ r_t = C_{1,t}^P + A_{1,t}^P r_t - \delta\psi_t - \xi_t \ ,$$

which implies $A_{1,t}^C = 1$, $A_{1,t}^P = 1 + \Xi_t^j$, $C_{1,t}^C = 0$, and $C_{1,t}^P = \delta\psi_t + \bar{\xi}_t$. The FOC for longer bonds can be interpreted as

$$p_{i,t}^j \ = \ -r_t + E_t p_{i-1,t+1}^j + \frac{1}{2} Var_t p_{i-1,t+1}^j - A_{i-1,t+1}^j \lambda_t - \delta\psi_t^j - \xi_t^j,$$

or equivalently

$$P_{i,t}^j \ = \ \exp\left(-r_t - A_{i-1,t+1}^j \lambda_t - \delta\psi_t^j - \xi_t^j\right) E_t P_{i-1,t+1}^j.$$

Now apply the market clearing condition $X_{i,t}^j = S_{i,t}^j - Z_{i,t}^j$, where preferred-habitat demand is $Z_{i,t}^j = h_{i,t}^j + i\alpha_i^j \left(y_{i,t}^j - \hat{\delta}\psi_t^j\right)$, and write the risk compensation terms in affine form as $\lambda_t = \Lambda_t r_t + \bar{\lambda}_t$ and $\xi_t^P = \Xi_t^P r_t + \bar{\xi}_t^P$, with $\xi_t^C = \Xi_t^C = \bar{\xi}_t^C = 0$. Then, the first-order conditions imply the following restrictions on the affine coefficients:

$$A_{i,t}^j \ = \ 1 + A_{i-1,t+1}^j \left(\rho + \Lambda_t\right) + \Xi_t^j, \tag{85}$$

$$C_{i,t}^j \ = \ C_{i-1,t+1}^j - \frac{1}{2}\left(\sigma A_{i-1,t+1}^j\right)^2 + A_{i-1,t+1}^j \left((1-\rho)\,\bar{r} + \bar{\lambda}_t\right) + \delta\psi_t^j + \bar{\xi}_t^j, \tag{86}$$

where

$$\Lambda_t = -\gamma\sigma^2 \sum_{i=2}^{I} \sum_{j\in\{P,C\}} A_{i-1,t+1}^j \left(\alpha_i^j A_{i,t}^j\right), \tag{87}$$

$$\bar{\lambda}_t = \gamma\sigma^2 \sum_{i=2}^{I} \sum_{j\in\{P,C\}} A_{i-1,t+1}^j \left(S_{i,t}^j - h_{i,t}^j - \alpha_i^j C_{i,t}^j + i\alpha_i^j \hat{\delta}\psi_t^j\right), \tag{88}$$

$$\Xi_t^P = -\gamma\delta^2\psi_t^P \sum_{i=1}^{I} \left(\alpha_i^P A_{i,t}^P\right), \tag{89}$$

$$\bar{\xi}_t^P = \gamma\delta^2\psi_t^P \sum_{i=1}^{I} \left(S_{i,t}^P - h_{i,t}^P - \alpha_i^P C_{i,t}^P + i\alpha_i^P \hat{\delta}\psi_t^P\right). \tag{90}$$

These difference equations can be solved by backwards induction, starting from a distant time T at which we assume that the pricing functions are known, bearing in mind that $A_{0,t}^j = C_{0,t}^j = 0$ for all j and t. To ensure a correct solution of the discrete-time model, we can apply a fixed-point calculation at each time step:

1. Guess $A_{i,t}^j = A_{i,t+1}^j$ and $C_{i,t}^j = C_{i,t+1}^j$.
2. Calculate Λ_t, Ξ_t^P, $\bar{\lambda}_t$, and $\bar{\xi}_t^P$ from (87)-(90).
3. Update $A_{i,t}^j = A_{i,t+1}^j$ and $C_{i,t}^j = C_{i,t+1}^j$ using (85)-(86).
4. Iterate to convergence.

Once the time t equilibrium has been calculated, we can step backwards to calculate the time $t-1$ equilibrium by the same method.

C.3.2 Discrete time representation: multi-factor case

For the discrete-time, multi-factor case, we write the price of a bond with maturity i, issued by jurisdiction $j \in \{P, C\}$, as $P_{i,t}^j = \exp\left(p_{i,t}^j\right) = \exp\left(-\left(A_{i,t}^j\right)^\top q_t - C_{i,t}^j\right)$. Let the factors follow $q_{t+1} = (I_3 - K)q_t + K\mathcal{E}_1\bar{r} + \Sigma\varepsilon_{t+1}$, where $\varepsilon_{t+1} \sim N(0, I_3)$. If arbitrageurs maximize a mean-variance utility function over the increase of their wealth, then if the time period is sufficiently short, their optimization problem can be approximated as follows:

$$\begin{aligned}
\max_{\{X_{i,t}^j\}} \quad & \left(W_t - \textstyle\sum_{i=1}^{I}\sum_{j\in\{P,C\}} X_{i,t}^j\right) r_t + \sum_{i=1}^{I}\sum_{j\in\{P,C\}} X_{i,t}^j \left(-C_{i-1,t+1}^j - \left(A_{i-1,t+1}^j\right)^\top \left(K\mathcal{E}_1\bar{r} + (I_3 - K)q_t\right)\right) \\
+ \quad & \sum_{i=1}^{I}\sum_{j\in\{P,C\}} X_{i,t}^j \left(C_{i,t}^j + \left(A_{i,t}^j\right)^\top q_t + \tfrac{1}{2}\left(A_{i-1,t+1}^j\right)^\top \Sigma\Sigma^\top A_{i-1,t+1}^j - \delta\psi_t^j\right) \\
- \quad & \tfrac{\gamma}{2}\sum_{i,k=2}^{I}\sum_{j,l\in\{P,C\}} X_{i,t}^j X_{k,t}^l \left(A_{i-1,t+1}^j\right)^\top \Sigma\Sigma^\top A_{k-1,t+1}^l - \tfrac{\gamma\psi_t^P}{2}\delta^2\left[\textstyle\sum_{i=1}^{I} X_{i,t}^P\right]^2.
\end{aligned}$$

where $\psi_t^C = 0$ denotes the Core default probability, and $\psi_t^P = \psi_t$ is the Peripheral default probability, given by (31). Here we have used the fact that the variance of the

portfolio value, conditional on no default, is

$$\mathbb{V}\mathrm{ar}_t \sum_{i=2}^{I} \sum_{j\in\{P,C\}} X_{i,t}^j P_{i-1,t+1}^j = E_t \left[\sum_{i=2}^{I} \sum_{j\in\{P,C\}} X_{i,t}^j \left(A_{i-1,t+1}^j\right)^\top \Sigma\varepsilon_{t+1} \right]^2 = \sum_{i,k=2}^{I} \sum_{j,l\in\{P,C\}} X_{i,t}^j X_{k,t}^l \left(A_{i-1,t+1}^j\right)^\top \Sigma\Sigma^\top A_{k-1,t+1}^l$$

Hence, the first-order condition on the investment $X_{i,t}^j$ in bonds of maturity i from jurisdiction j is

$$\begin{aligned} r_t \;=\; \mathcal{E}_1^\top q_t \;&=\; -\left(C_{i-1,t+1}^j + \left(A_{i-1,t+1}^j\right)^\top (K\mathcal{E}_1\bar{r} + (I_3 - K)q_t)\right) + \left(C_{i,t}^j + \left(A_{i,t}^j\right)^\top q_t\right) \\ &+\; \frac{1}{2}\left(A_{i-1,t+1}^j\right)^\top \Sigma\Sigma^\top A_{i-1,t+1}^j - \delta\psi_t^j - \left(A_{i-1,t+1}^j\right)^\top \lambda_t - \xi_t^j, \end{aligned}$$

where

$$\lambda_t = \gamma\Sigma\Sigma^\top \sum_{i=2}^{I} \sum_{j\in\{P,C\}} X_{i,t}^j A_{i-1,t+1}^j,$$

$$\xi_t^j = \gamma\psi_t^j\delta^2 \sum_{i=1}^{I} X_{i,t}^j \ .$$

Note that since $A_{0,t}^j = C_{0,t}^j = 0$, the first-order conditions for holdings of one-period bonds are simply

$$r_t = y_{1,t}^C = C_{1,t}^C + \left(A_{1,t}^C\right)^\top q_t \ , \ r_t = C_{1,t}^P + \left(A_{1,t}^P\right)^\top q_t - \delta\psi_t - \xi_t \ ,$$

which implies $A_{1,t}^C = \mathcal{E}_1$, $A_{1,t}^P = \mathcal{E}_1 + \Xi_t$, $C_{1,t}^C = 0$, and $C_{1,t}^P = \delta\psi_t + \bar{\xi}_t$. The FOC for longer bonds can be interpreted as

$$p_{i,t}^j \;=\; -r_t + E_t p_{i-1,t+1}^j + \frac{1}{2} Var_t p_{i-1,t+1}^j - \left(A_{i-1,t+1}^j\right)^\top \lambda_t - \delta\psi_t^j - \xi_t^j,$$

or equivalently

$$P_{i,t}^j \;=\; \exp\left(-r_t - \left(A_{i-1,t+1}^j\right)^\top \lambda_t - \delta\psi_t^j - \xi_t^j\right) E_t P_{i-1,t+1}^j.$$

Now apply the market clearing condition $X_{i,t}^j = S_{i,t}^j - Z_{i,t}^j$, where preferred-habitat demand is $Z_{i,t}^j = h_{i,t}^j - \varsigma_{i,}^j\varepsilon_{i,t}^j + i\alpha_i^j\left(y_{i,t}^j - \hat{\delta}\psi_t^j\right)$, and write the risk compensation terms in affine form as $\lambda_t = \Lambda_t^\top q_t + \bar{\lambda}_t$ and $\xi_t^P = \left(\Xi_t^P\right)^\top q_t + \bar{\xi}_t^P$, with $\xi_t^C = \Xi_t^C = \bar{\xi}_t^C = 0$.

Then, the first-order conditions imply the following restrictions:

$$A_{i,t}^{j} = \mathcal{E}_1 + \left(\Lambda_t + \left(I_3 - K^\top\right)\right) A_{i-1,t+1}^{j} + \Xi_t^j, \tag{91}$$

$$C_{i,t}^{j} = C_{i-1,t+1}^{j} - \frac{1}{2}\left(A_{i-1,t+1}^{j}\right)^\top \Sigma\Sigma^\top A_{i-1,t+1}^{j} + \left(A_{i-1,t+1}^{j}\right)^\top \left(K\mathcal{E}_1\bar{r} + \bar{\lambda}_t\right) + \delta\psi_t^j + \bar{\xi}_t^j, \tag{92}$$

where

$$\Lambda_t^\top = \gamma\Sigma\Sigma^\top \sum_{i=2}^{I} \left[A_{i-1,t+1}^{P}\left(\varsigma_i^P \mathcal{E}_2^\top - \alpha_i^P \left(A_{i,t}^{P}\right)^\top\right) + A_{i-1,t+1}^{C}\left(\varsigma_i^C \mathcal{E}_3^\top - \alpha_i^C \left(A_{i,t}^{C}\right)^\top\right)\right], \tag{93}$$

$$\bar{\lambda}_t = \gamma\Sigma\Sigma^\top \sum_{i=2}^{I} \sum_{j\in\{P,C\}} A_{i-1,t+1}^{j}\left(S_{i,t}^{j} - h_{i,t}^{j} - \alpha_i^j C_{i,t}^{j} + i\alpha_i^j \hat{\delta}\psi_t^j\right), \tag{94}$$

$$\left(\Xi_t^P\right)^\top = \gamma\delta^2\psi_t^P \sum_{i=1}^{I}\left(\varsigma_i^P \mathcal{E}_2^\top - \alpha_i^P \left(A_{i,t}^{P}\right)^\top\right), \tag{95}$$

$$\bar{\xi}_t^P = \gamma\delta^2\psi_t^P \sum_{i=1}^{I}\left(S_{i,t}^{P} - h_{i,t}^{P} - \alpha_i^P C_{i,t}^{P} + i\alpha_i^P \hat{\delta}\psi_t^P\right). \tag{96}$$

These difference equations can be solved by backwards induction, starting from a distant time T at which we assume that the pricing functions are known, bearing in mind that $A_{0,t}^{j} = C_{0,t}^{j} = 0$ for all j and t. To ensure a correct solution of the discrete-time model, we can apply a fixed-point calculation at each time step:

1. Guess $A_{i,t}^{j} = A_{i,t+1}^{j}$ and $C_{i,t}^{j} = C_{i,t+1}^{j}$.
2. Calculate Λ_t, Ξ_t^P, $\bar{\lambda}_t$, and $\bar{\xi}_t^P$ from (93)-(96).
3. Update $A_{i,t}^{j} = A_{i,t+1}^{j}$ and $C_{i,t}^{j} = C_{i,t+1}^{j}$ using (91)-(92).
4. Iterate to convergence.

Once the time t equilibrium has been calculated, we can step backwards to calculate the time $t-1$ equilibrium by the same method.

C.3.3 Decomposing prices and yields

The decomposition of the discrete-time version of the model can be computed by a method analogous to the one spelled out in App. B.2.1 for the continuous-time model.

The overall yield can be decomposed into four affine terms:

$$\begin{aligned}\tau y_{i,t}^{j}(q) &= \left(A_{i,t}^{j}\right)^{\top} q + C_{i,t}^{j} \\ &= \left(A_{i,t}^{j,EX}\right)^{\top} q + C_{i,t}^{j,EX} + \left(A_{i,t}^{j,DL}\right)^{\top} q + C_{i,t}^{j,DL} + \left(A_{i,t}^{j,TP}\right)^{\top} q + C_{i,t}^{j,TP} + \left(A_{i,t}^{j,CR}\right)^{\top} q + C_{i,t}^{j,CR}.\end{aligned}$$

The individual components can each be computed recursively:

$$A_{i,t}^{j,EX} = \mathcal{E}_1 + \left(I_3 - K_t^{\top}\right) A_{i-1,t+1}^{j,EX}, \tag{97}$$

$$C_{i,t}^{j,EX} = C_{i-1,t+1}^{j,EX} + \left(A_{i-1,t+1}^{j,EX}\right)^{\top} K_t \mathcal{E}_1 \bar{r}_t. \tag{98}$$

$$A_{i,t}^{j,DL} = \left(I_3 - K_t^{\top}\right) A_{i-1,t+1}^{j,DL}, \tag{99}$$

$$C_{i,t}^{j,DL} = C_{i-1,t+1}^{j,DL} + \left(A_{i-1,t+1}^{j,DL}\right)^{\top} K_t \mathcal{E}_1 \bar{r}_t + \delta\psi_t^{j}. \tag{100}$$

$$A_{i,t}^{j,CR} = \left(I_3 - K_t^{\top}\right) A_{i-1,t+1}^{j,CR} + \Xi_t^{j}, \tag{101}$$

$$C_{i,t}^{j,CR} = C_{i-1,t+1}^{j,CR} + \left(A_{i-1,t+1}^{j,CR}\right)^{\top} K_t \mathcal{E}_1 \bar{r}_t + \bar{\xi}_t^{j}. \tag{102}$$

$$A_{i,t}^{j,TP} = \left(I_3 - K_t^{\top}\right) A_{i-1,t+1}^{j,TP} + \Lambda_t A_{i-1,t+1}^{j}, \tag{103}$$

$$C_{i,t}^{j,TP} = C_{i-1,t+1}^{j,TP} + \left(A_{i-1,t+1}^{j,TP}\right)^{\top} K_t \mathcal{E}_1 \bar{r}_t - \frac{1}{2}\left(A_{i-1,t+1}^{j}\right)^{\top} \Sigma_t \Sigma_t^{\top} A_{i-1,t+1}^{j} + \left(A_{i-1,t+1}^{j}\right)^{\top} \bar{\lambda}_t. \tag{104}$$

These equations can all be solved backwards from the terminal conditions $A_{0,t}^{j,k} = \overrightarrow{0}$, and $C_{0,t}^{j,k} = 0$, for $k \in \{EX, DL, CR, TP\}$. We can see that the default loss and credit risk components are zero for Core, and in addition $A_{i,t}^{P,DL} = 0$ for Periphery.

It is straightforward to verify that equations (97)-(104) sum up to the equations (91)-(92) that govern $A_{i,t}^{j}$ and $C_{i,t}^{j}$. Therefore solutions to (97)-(104) sum up to a solution for $A_{i,t}^{j}$ and $C_{i,t}^{j}$.

C.3.4 Model generated moments

The one-period innovation to the factors is

$$q_{t+1} - E_t q_{t+1} \overset{iid}{\sim} N\left(0, \Sigma\Sigma^{\top}\right),$$

and the n-period innovation to the factors is

$$q_{t+n} - E_t q_{t+n} = \sum_{s=1}^{n} (I_3 - K)^{n-s} \Sigma \varepsilon_{t+s}.$$

Therefore, we can calculate the unconditional variance of q_t as follows:

$$\mathbb{V}\text{ar}\left(q_t\right) = \sum_{s=0}^{\infty} (I_3 - K)^s \Sigma \Sigma^\top (I_3 - K)^s.$$

The shock to the yield $y_{i,t+1}^j$ is a linear transformation of the shock to q_{t+1}:

$$y_{i,t+1}^j - E_t y_{i,t+1}^j = \frac{1}{i} \left(A_{i,t+1}^j\right)^\top \left(q_{t+1} - E_t q_{t+1}\right).$$

Therefore, considering a stationary situation in which the factor loadings A are independent of time, the unconditional covariance of the yield $y_{i,t}^j$ with the yield $y_{i,t}^k$ is

$$\mathbb{C}\text{ov}\left(y_{i,t}^j, y_{i,t}^k\right) = \frac{1}{i^2} \left(A_i^j\right)^\top \mathbb{V}\text{ar}\left(q_t\right) A_i^k.$$

C.3.5 Computing Sharpe ratios

To define Sharpe ratios in our context, note that excess returns are affected both by variations in bond prices and by default events. Therefore, the instantaneous Sharpe ratios for Core and Periphery in the continuous-time model can be defined as $\mathbb{S}_t^*(\tau)$ and $\mathbb{S}_t(\tau)$ below, which take both these risks into account:

$$\mathbb{S}_t^*(\tau) dt^{1/2} \equiv \mathbb{E}_t \left(\frac{dP_t^*(\tau)}{P_t^*(\tau)} - r_t dt \right) / \left(\mathbb{V}ar_t \left(\frac{dP_t^*(\tau)}{P_t^*(\tau)} \right) \right)^{1/2}, \tag{105}$$

$$\mathbb{S}_t(\tau) dt^{1/2} \equiv \mathbb{E}_t \left(\frac{dP_t(\tau)}{P_t(\tau)} - \delta dN_t - r_t dt \right) / \left(\mathbb{V}ar_t \left(\frac{dP_t(\tau)}{P_t(\tau)} - \delta dN_t \right) \right)^{1/2}. \tag{106}$$

To isolate the excess return and risk embodied in the sovereign spread, we can also calculate the following Sharpe ratio on default risk:

$$\mathbb{S}_t^\Delta(\tau) dt^{1/2} \equiv \mathbb{E}_t \left(\frac{dP_t(\tau)}{P_t(\tau)} - \delta dN_t - \frac{dP_t^*(\tau)}{P_t^*(\tau)} \right) / \left(\mathbb{V}ar_t \left(\frac{dP_t(\tau)}{P_t(\tau)} - \delta dN_t - \frac{dP_t^*(\tau)}{P_t^*(\tau)} \right) \right)^{1/2}. \tag{107}$$

We report empirical and model counterparts to $\mathbb{S}_t^*(\tau)$ and $\mathbb{S}_t^\Delta(\tau)$ in Tables 2, 4, and 5, scaled for consistency with an annual time unit.

We compute the empirical Sharpe ratios from monthly yield series in Datastream for 1999-2022, as follows. We divide the monthly series of zero-coupon yields, in percentage points, by 1200 to construct samples of monthly logarithmic yields $\hat{y}_{i,t}^j$ for $j =$ DE or IT, and for $i =$ 12, 24, 60, 108 or 120 months. We interpolate yields on 119-month bonds linearly using 9-year German yields and 5-year Italian yields together with 10-year yields, and we extrapolate yields on 11-month bonds linearly using 2-year and 1-year yields. We then construct samples of monthly excess returns:

$$\hat{rx}_{i,t+1}^j = i\hat{y}_{i,t}^j - (i-1)\hat{y}_{i-1,t+1}^j - \hat{r}_t, \tag{108}$$

where $\hat{r}_t$ is the risk-free rate, and the monthly return spread:

$$\hat{rx}_{i,t+1}^\Delta = i\hat{y}_{i,t}^{IT} - (i-1)\hat{y}_{i-1,t+1}^{IT} - i\hat{y}_{i,t}^{DE} + (i-1)\hat{y}_{i-1,t+1}^{DE}. \tag{109}$$

To calculate excess returns, we use the same spliced series of German 1-month yields and 1-month OIS that we used for the model calibration, dividing by 1200 to express it as a monthly logarithmic yield (also from Datastream; see Sec. 4.2).

We can then compute a monthly sample Sharpe ratio $\hat{S}_i^j$ as follows:

$$\hat{S}_i^j = \frac{\hat{\mathbb{E}}\left(\hat{rx}_{i,t+1}^j\right) + \frac{1}{2}\hat{\mathbb{V}ar}\left(\hat{rx}_{i,t+1}^j\right)}{\left(\hat{\mathbb{V}ar}\left(\hat{rx}_{i,t+1}^j\right)\right)^{1/2}}, \tag{110}$$

for $j =$ DE or IT or Δ, where $\hat{\mathbb{E}}$ and $\hat{\mathbb{V}ar}$ denote the sample mean and variance. Since the numerator of this ratio scales in proportion to the time period, while the denominator scales in proportion to the square root of the time period, we multiply by $\sqrt{12}$ to produce the annualized empirical Sharpe ratios that are reported in the tables.

To compute the model counterparts of (105)-(107), the numerators are

$$\mathbb{E}_t\left(\frac{dP_t^*(\tau)}{P_t^*(\tau)} - r_t dt\right) \;=\; \left(\mu_t^*(\tau) - r_t\right) dt \;=\; A_t^*(\tau)^\top \lambda_t dt, \tag{111}$$

$$\mathbb{E}_t\left(\frac{dP_t(\tau)}{P_t(\tau)} - \delta dN_t - r_t dt\right) \;=\; \left(\mu_t(\tau) - \psi_t\delta - r_t\right) dt \;=\; \left(A_t(\tau)^\top \lambda_t + \xi_t\right) dt, \tag{112}$$

$$\mathbb{E}_t\left(\frac{dP_t(\tau)}{P_t(\tau)} - \delta dN_t - \frac{dP_t^*(\tau)}{P_t^*(\tau)}\right) = \left(\left(A_t(\tau)^\top - A_t^*(\tau)^\top\right)\lambda_t + \xi_t\right)dt = \xi_t dt. \quad (113)$$

The variances in the denominators can be calculated as

$$\mathbb{V}ar_t\left(\frac{dP_t^*(\tau)}{P_t^*(\tau)}\right) = A_t^*(\tau)^\top \Sigma\Sigma^\top A_t^*(\tau)dt, \quad (114)$$

$$\mathbb{V}ar_t\left(\frac{dP_t(\tau)}{P_t(\tau)} - \delta dN_t\right) = \left(A_t(\tau)^\top \Sigma\Sigma^\top A_t(\tau) + \psi_t\delta^2\right)dt, \quad (115)$$

$$\mathbb{V}ar_t\left(\frac{dP_t(\tau)}{P_t(\tau)} - \delta dN_t - \frac{dP_t^*(\tau)}{P_t^*(\tau)}\right) = \psi_t\delta^2 dt. \quad (116)$$

Equations (113) and (116) follow from Prop. 2. We evaluate these formulas using the objects constructed in the finite difference approximation to the long-run solution of the continuous-time model, as described in Sec. C.2.2.[73] Since the model is computed with a monthly time unit, we then scale the numerator by 12, and the denominator by $\sqrt{12}$, to produce the annualized numerators and denominators reported in the tables. Hence the annualized Sharpe ratio is effectively multiplied by $\sqrt{12}$.

D Purchase program design: the value of flexibility

Since our results suggest that the impact of PEPP was mainly attributable to the way it shrank credit risk premia in peripheral euro area countries, it is interesting to ask how the PEPP's flexible design altered its impact. Here, we compare our PEPP scenario to a counterfactual alternative based on the design principles of the APP, which tightly constrained the allocation of purchases over time and across jurisdictions. Fig. 10 illustrates the two scenarios we compare, showing cumulative purchases at face value, in billions of euro, over months 3-12 (indicating March-December, 2020). The figure shows German and Italian purchases as blue lines with circles, and red lines with squares, respectively; their sum is shown in black.

The solid lines show the baseline scenario that we used in Sec. 5.2 as a stand-in for expectations about the PEPP upon its announcement. The path of purchases up to the end of June represents actual PEPP purchases, which accumulated almost linearly over time, at a pace that, if continued, would have exhausted the envelope before the

[73] Alternatively, we can evaluate the formulas using the discrete time solution. The only difference is that factor loadings of maturity i, A_i^j, are replaced by the maturity $i-1$ loadings, A_{i-1}^j.

Figure 10: Comparing baseline purchase scenario and inflexible alternative.

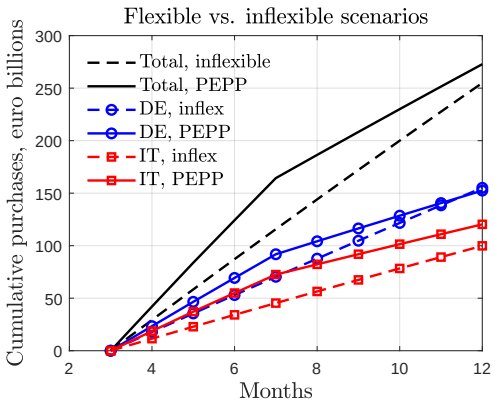

Notes: Comparing baseline PEPP scenario (solid lines) vs. inflexible "APP-style" scenario with a constant pace of purchases and allocations equal to capital keys (dashed lines).
Blue circles: DE; red squares: IT; black: aggregate face value. Effect on yields is shown in Fig. 11.

end of the year. As a fraction of the monthly total, Italian purchases exceeded Italy's capital key, while purchases of German bonds were close to capital key (purchases of French bonds were substantially below capital key). Since our scenario aims to model the effects of the initial announcement, we abstract from the actual path of purchases after June (when a recalibration of the PEPP envelope was announced), and instead suppose that purchases from July onwards were expected to use up the initial PEPP envelope at a constant pace, while maintaining the initial deviations in capital key.

APP-style purchases. We compare this PEPP scenario to a counterfactual alternative based on the inflexible design of the longer-standing Asset Purchase Programme (APP). That program imposed a constant pace of purchases over a pre-specified period of time, and allocated purchases according to each euro area member state's capital key. Following these principles, we design a hypothetical "APP-style" purchase announcement whereby the ECB would have committed to the same overall envelope, but would have distributed purchases linearly over time, allocating them in proportion to the German (26.4%) and Italian (17.0%) capital keys.[74] Fig. 10 compares the two scenarios. Dashed lines represent the APP-style scenario, while solid lines show our benchmark PEPP scenario (the color coding is the same as in Fig. 3). Clearly, the

[74] While the total PEPP envelope was 750 billion euros, we only analyze the part that was dedicated to sovereign bonds (608 billion), abstracting from private-sector and supranational purchases.

Figure 11: Comparing impact of PEPP scenario with "inflexible" alternative

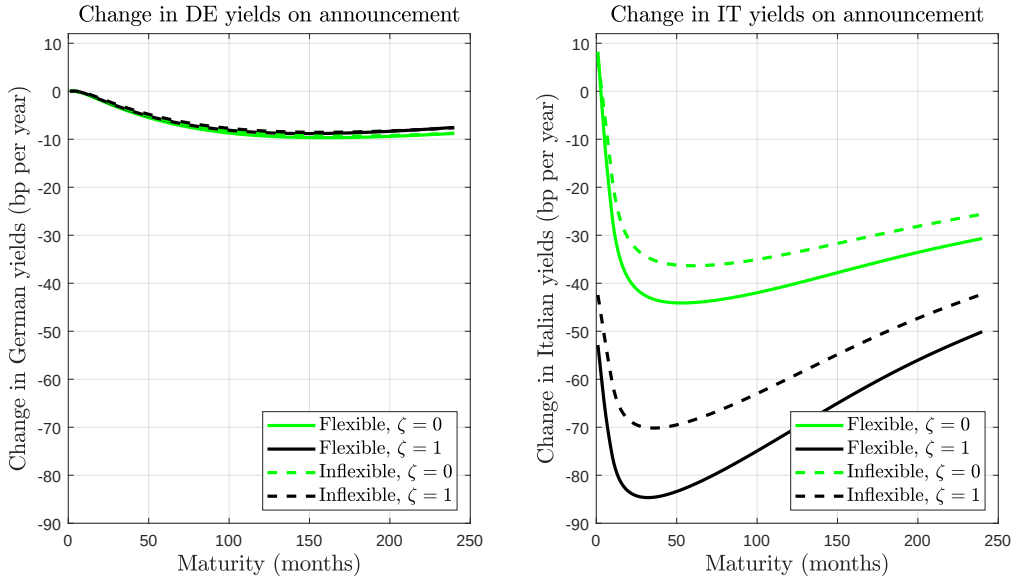

Left panel: model simulations of Germany. *Right panel*: model simulations of Italy.
Panels show the model-generated impact of the PEPP announcement (solid lines) and an "APP-style" scenario (dashed lines) that imposes a constant pace of purchases and allocations equal to capital keys, as illustrated in Fig. 10.
Black lines: full pass-through of bond redemption income ($\zeta = 1$) to the Italian treasury. *Green lines*: zero pass-through ($\zeta = 0$).

PEPP scenario imposes frontloading, with an initial pace of purchases faster than the APP design would permit. Simultaneously, the PEPP scenario allocates more purchases to Italy than the APP design would, while total purchases of German debt in the PEPP scenario are similar to those in the APP scenario (close to capital key).[75]

Fig. 11 compares the effects of the purchases under the PEPP and APP designs, showing that the former reduces yields more than the latter, in both countries and at all maturities. The left panel refers to Germany, while the right panel refers to Italy. The PEPP design causes a tiny extra reduction in German yields, by 1 bp at longer maturities, compared to the APP-style program. The reduction in yields is much more significant in the Italian case, where PEPP shifts the yield curve by as much as 14 additional basis points, exceeding 10 bp at most maturities, compared with the APP

[75]Hence total PEPP purchases (black solid line) end up slightly above the intended envelope (black dashed line) since our two-country simulation abstracts from the jurisdictions where purchases were lowest, relative to capital key.

design. Most of the difference between the PEPP and APP designs is attributable to a decline in the credit risk pre mium (decomposition not shown). The figure also shows a counterfactual low-remittances scenario ($\zeta = 0$, shown in green). In the low-remittances case, the difference in impact across program designs is reduced, but is still significant.